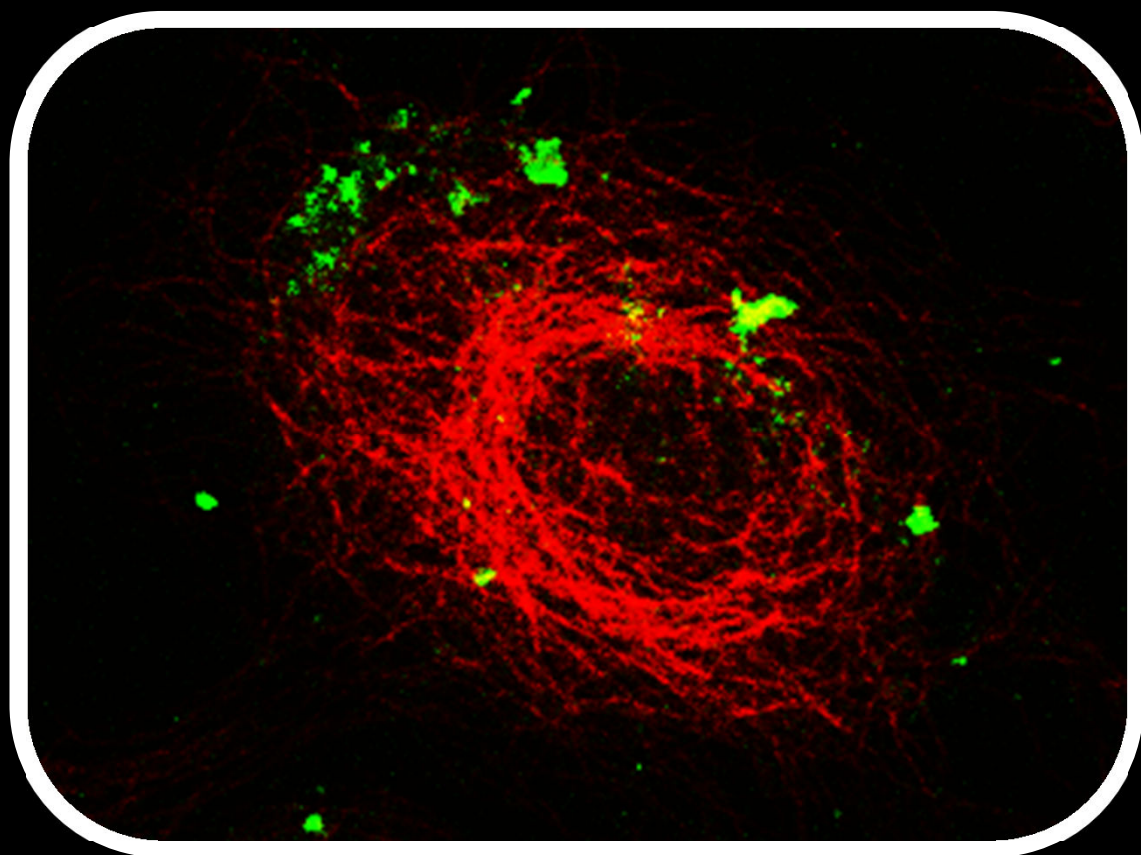# Protein glycosylation of exosomes from ovarian carcinoma cells

Structures and biological roles

Cristina Isabel Caniço Escrevente

Dissertation presented to obtain the Ph.D. degree in Biology
Instituto de Tecnologia Química e Biológica | Universidade Nova de Lisboa

Protein glycosylation of exosomes from ovarian carcinoma cells

Structures and biological roles

Cristina Isabel Caniço Escrevente

Dissertation presented to obtain the Ph.D. degree in Biology

Instituto de Tecnologia Química e Biológica | Universidade Nova de Lisboa

Oeiras, October, 2011

INSTITUTO
DE TECNOLOGIA
QUÍMICA E BIOLÓGICA
/UNL

Knowledge Creation

Supervisor: Dr. Júlia Costa

President of the Jury: Dr. Claudina Rodriguez-Pousada

Members of the Jury: Dr. Celso Albuquerque Reis and Dr. Margarida Sofia Pereira Amaral (opponents), Dr. Paula Maria Sanches Alves.

Cover: By author. Uptake of SKOV3 exosomes by SKOV3 cells. Detection of exosomes labelled with carboxyfluoresceine diacetate succinimidyl-ester (green) and alpha-tubulin (red) by confocal immunofluorescence microscopy.

Acknowledgments

This PhD Thesis would not have been possible without the support and assistance of a number of people to whom I would like to express my sincere gratitude.

First, I would like to acknowledge my supervisor Dr. Júlia Costa for giving me the opportunity to work on such an interesting project, and for providing me the scientific support that made this Thesis possible. Thank you for accepting me as a PhD student and for the encouragement and thoughtful guidance.

A warm thanks to Professor Peter Altevogt for the helpful suggestions that enriched the content of this thesis, for the guidance and support during all this years, and for welcoming me in his laboratory.

I am grateful to Dr. Paula Alves from the Animal Cell Technology Unit for providing me the opportunity to work with the flow cytometer and all the TCA team for the help.

I am thankful to Dr. Harald Conradt and Sebastian Kandzia from GlycoThera, Germany, for their contribution to my work, and particularly for the help given in the glycosylation profiling.

A special thanks to all my lab colleagues, present and former, for the friendly and supportive atmosphere that contributed to the final outcome of this Thesis. I am thankful to Ricardo, for being the "man" of the lab, for the endless patience, the critical opinions, and also for the proofreading of this Thesis. I thank Rita for being a good companionship in the last two years and Carla for the good advices. Your support and friendship was very important. I would like to thank Eda for being present since day one. Your sincere friendship, your practical demeanor, and the continuous support given throughout all these years were priceless. Catarina Gomes, I am grateful for your true friendship and all the good moments shared together. I thank Catarina Brito for the friendship, the generosity, and willingness to answer to all my doubts, not only then, when you were a member of the lab, but also now. I thank Vanessa for being present in the beginning and for teaching me so many important things about the science world, and finally, Angelina for the helpful discussions.

I would like to acknowledge all my good friends inside and outside the science world. Although many times distant in space they were always present in mind. Thank you, for being present whenever I needed. I believe that the world is big but friendships are bigger.

In portuguese.... Não podia deixar de agradecer à minha família que sempre acreditou em mim e me deu apoio. Obrigado, padrinhos, primas e primos, por existirem e estarem ao meu lado em todos momentos. Obrigado aos meus avós, Palmira e José, Emília e Joaquim, por terem feito parte da minha vida. Sei que ficariam orgulhosos de mim.

Agradeço o apoio dos meus sogros, Teresa e Abílio, e dos meus novos tios, Alice e Fernandes. Obrigado por me terem recebido de braços abertos na vossa família.

Um obrigado infinito aos meus pais por me terem deixado seguir os meus sonhos e terem acreditado que podia chegar onde cheguei. Espero não vos ter desiludido ao ter escolhido este caminho.

Tenho de agradecer ao Pedro, mais do que um companheiro, um amigo. Obrigado por teres escolhido Coimbra para estudar e, sobretudo, obrigado por teres decidido partilhar a tua vida comigo. A tua paciência ilimitada é, sem dúvida, a tua maior virtude.

Por último, dedico esta tese à minha filha Carolina, que apesar de ainda não ter completado um ano já faz parte do mundo da ciência. Durante nove meses trabalhou comigo no laboratório, e durante os seus primeiros meses partilhou a minha atenção com a escrita desta tese. Obrigado por seres uma boa menina e me teres deixado trabalhar de vez em quando. Obrigado pelos beijos molhados, sorrisos e gargalhadas nos dias mais difíceis. Obrigado, simplesmente e acima de tudo, por existires e fazeres parte da minha vida.

Summary

Exosomes are small membrane vesicles that are secreted by several cell types including tumour cells. They are formed intracellularly by an inward budding of the membrane of endosomal compartments which are converted to multivesicular bodies. Exosomes are then released into the extracellular environment after fusion of the multivesicular bodies with the plasma membrane. Upon internalization by other cells they may transfer proteins and RNA among cells. Tumour-derived exosomes can promote angiogenesis, cell proliferation, tumour cell invasion and immune evasion. These vesicles have been found in biological fluids such as malignant ascites and blood and can therefore be used not only to identify potential biomarkers of disease but also in vaccination.

Alterations in protein glycosylation are often associated with tumourigenesis; therefore glycan structures represent ideal targets for tumour specific diagnosis and new anti-tumour therapeutic strategies.

This research focused on the characterization and investigation of the biological role of protein *N*-glycosylation from ovarian tumour derived exosomes, with particular emphasis on the glycoprotein *disintegrin and metalloprotease* 10 (ADAM10).

Chapter 2 details the investigation of the role of *N*-glycosylation on ADAM10 intracellular localization, activity and sorting to exosomes. To accomplish this objective, individual ADAM10 *N*-glycosylation site mutants S269A, T280A, S441A, T553A were constructed using the QuickChange site directed mutagenesis approach. Western blot analysis of the ovarian carcinoma SKOV3 cells stably transfected with wild-type and *N*-glycosylation mutants of ADAM10 showed that all potential glycosylation sites were occupied by high-mannose and/or complex oligosaccharides. Mutant T280A was found to accumulate in the endoplasmic reticulum as

the non-processed precursor of the enzyme, whilst S441A showed increased susceptibility to proteolysis. Study of ADAM10 *in vivo* activity towards the cell adhesion molecule L1, in HEK293 cells and mouse embryonic fibroblasts derived from the ADAM10 knockout mouse revealed that the mutation of ADAM10 *N*-glycosylation sites did not completely abolish enzyme activity. Accordingly, all mutants exhibited proteolytic activity towards proTNF-alpha *in vitro*. However, a reduction in the shedding levels was found, especially for T280A. On the other hand, all ADAM10 *N*-glycosylation mutants cleaved to their mature form were efficiently sorted into exosomes. Overall, these results showed the importance of *N*-glycosylation for ADAM10 processing, protection from proteolysis, and full-enzyme activity.

Exosomes can interact and be internalized by target cells; however, the mechanisms involved in this process are still poorly understood. Chapter 3 describes that SKOV3 cells were found to internalize SKOV3 derived exosomes labelled with carboxyfluoresceine diacetate succinimidyl-ester, by immunofluorescence microscopy, via an energy-dependent process. Partial colocalization with the endosome marker EEA1 and inhibition by chlorpromazine suggested the involvement of clathrin-dependent endocytosis. On the other hand, an uptake inhibition in the presence of 5-ethyl-*N*-isopropyl amiloride, cytochalasin D and methyl-beta-cyclodextrin suggested the involvement of additional endocytic pathways. Furthermore, proteins present in exosomes and at SKOV3 cell surface were at least partially required for internalization, as shown by the decrease in the uptake levels following proteinase K treatment.

The analysis of the glycosylation profiles of SKOV3 exosomes using lectins with different specificities revealed that they were enriched in specific mannose- and sialic acid-containing glycoproteins that were not present in cellular extracts and that may constitute exosome markers. The effect of glycosylation on exosome uptake was also assessed. Sialic acid

removal led to an increase in uptake efficiency whilst cell incubation with monosaccharides D-galactose, α-L-fucose, α-D-mannose, D-*N*-acetylglucosamine and the disaccharide β-lactose reduced exosome uptake to a level comparable to that of the control D-glucose.

Chapter 4 addresses the further characterization of the *N*-glycan profile of vesicles secreted by ovarian tumour cells. A detailed structure analysis of the *N*-glycans of SKOV3 and OVM secreted vesicles, microsomal and plasma membrane fractions was performed by high performance anion exchange chromatography with pulsed amperometric detection (HPAEC-PAD) and matrix assisted laser desorption/ionization time-of-flight mass spectrometry (MALDI-TOF-MS). Glycans of the di-, tri- and tetraantennary type with proximal fucose were found in secreted vesicles of SKOV3 and OVM cells, as well as in the plasma membrane and microsomal fraction. SKOV3 cells were found to contain predominantly proximally fucosylated complex partially agalactosylated glycan structures in all fractions. Moreover, the terminal GalNAcβ4GlcNAc (LacdiNAc) motif was also found in SKOV3 secreted vesicles. OVM secreted vesicles contained predominantly complex intact glycans of the di-, tri- and tetraantennary types.

In conclusion, this research has contributed to the knowledge of protein glycosylation present in vesicles secreted by ovarian tumour cells. This information should provide the basis for further exploration of the mechanisms of protein sorting and exosome biogenesis. Moreover, the identification of specific glycoproteins and *N*-glycans in exosomes might open new perspectives in biomarker discovery and cancer vaccination.

Resumo

Exossomas são pequenas vesículas membranares secretadas por diversos tipos de células, incluindo células tumorais. Eles são formados intracelularmente, pela invaginação da membrana de compartimentos endossomais que dão origem aos corpos multivesiculares. A fusão dos corpos multivesiculares com a membrana plasmática resulta na libertação dos exossomas para o ambiente extracelular. Após internalização por outras células, os exossomas podem transferir proteínas e RNA entre células. Exossomas secretados por células tumorais podem promover a angiogénese, proliferação celular, invasão tumoral e evasão do sistema imunitário. Estas vesículas foram encontradas em fluidos biológicos, tais como, ascites e sangue, e como tal, podem ser usadas para identificar potenciais biomarcadores de doenças e também em vacinação.

Proteínas com glicosilação alterada encontram-se frequentemente associadas com o processo de tumorigénese; como tal, estruturas glicosídicas representam alvos ideais para o diagnóstico específico de tumores e para o desenvolvimento de novas estratégias terapêuticas anti-tumorais.

Esta Tese visou a caracterização e investigação do papel biológico da *N*-glicosilação em proteínas presentes em exossomas secretados por células do carcinoma do ovário, com particular ênfase na glicoproteína *desintegrina e metaloprotease* ADAM10.

O Capítulo 2 descreveu a investigação do papel da *N*-glicosilação na localização intracelular, actividade e transporte para os exossomas da proteína ADAM10. Para alcançar esse objectivo foi utilizada a metodologia de mutagénese dirigida para construir mutantes em que os locais de *N*-glicosilação foram individualmente eliminados: S269A, T280A, S441A, T553A. A análise por Western blot de células de carcinoma do ovário SKOV3, transfectadas estavelmente com o tipo selvagem ou com os

mutantes de *N*-glicosilação da ADAM10, mostrou que todos os potenciais locais de *N*-glicosilação se encontravam ocupados com oligossacáridos do tipo oligomanose ou complexo. O mutante T280A foi encontrado acumulado no reticulo endoplasmático, na forma precursora não processada da enzima, enquanto o mutante S441A mostrou um aumento na susceptibilidade à proteólise. O estudo da actividade *in vivo* da ADAM10 monitorizando a molécula de adesão celular L1 como substrato, em células HEK293 e em fibroblastos de ratinhos silenciados para a ADAM10, revelou que a mutação individual dos diferentes locais de *N*-glicosilação da ADAM10 não aboliu por completo a actividade da enzima. Da mesma forma, todos os mutantes exibiram actividade proteolítica *in vitro* usando o péptido proTNF-alpha como substrato. No entanto, foi observada uma redução nos níveis de clivagem, especialmente com o mutante T280A. Por outro lado, todos os mutantes de *N*-glicosilação da ADAM10 que foram processados para a forma matura foram eficientemente transportados para os exossomas. No global, estes resultados mostram a importância da *N*-glicosilação no processamento, protecção contra a proteólise e actividade enzimática da ADAM10.

Os exossomas podem interagir e ser internalizados por células-alvo, no entanto, os mecanismos envolvidos nesse processo ainda são pouco compreendidos. O Capítulo 3 mostrou, por microscopia de fluorescência, a internalização de exossomas de células SKOV3 marcados com succinimidil éster diacetato de carboxifluoresceína por células SKOV3, através de um mecanismo dependente de energia. A colocalização parcial com o marcador de endossomas EEA1 e a inibição com clorpromazina sugeriu o envolvimento da via de endocitose mediada por clatrina. Por outro lado, a inibição da internalização na presença de 5-etil-*N*-isopropil amiloride, citocalasina D e metil-beta-ciclodextrina sugeriu o envolvimento de outras vias endocíticas. Para além disso, foram necessárias, pelo menos parcialmente, proteínas presentes nos exossomas e na superfície

das células SKOV3 para a internalização, como mostrado pela diminuição nos níveis de internalização após tratamento com proteinase K.

A análise do perfil de glicosilação dos exossomas de células SKOV3, usando lectinas com diferentes especificidades, revelou que eles eram enriquecidos em glicoproteínas específicas com manose e ácido siálico. Essas glicoproteínas não se encontravam nos extractos celulares podendo constituir marcadores de exossomas. Adicionalmente, foi investigado o papel da glicosilação na internalização de exossomas. A remoção do ácido siálico levou a uma tendência para um aumento na eficiência da internalização, enquanto que a incubação com os monossacáridos D-galactose, α-L-fucose, α-L-manose, D-*N*-acetiglucosamina e o dissacárido β-lactose reduziu a internalização para níveis comparáveis ao do controlo com D-glucose.

O Capítulo 4 visou a caracterização pormenorizada do perfil de *N*-glicanos presentes em células do carcinoma do ovário. A análise detalhada da estrutura dos *N*-glicanos presentes nas vesículas secretadas, fracção microssomal e membrana plasmática de células SKOV3 e OVM foi efectuada por cromatografia de troca iónica de elevada "performance" com detecção amperométrica pulsada (HPAEC-PAD) e por espectometria de massa com "matrix assisted laser desorption/ionization time-of-flight" (MALDI-TOF-MS). Glicanos do tipo bi-, tri- e tetra-ramificados com fucose próxima foram encontrados nas vesículas secretadas pelas células SKOV3 e OVM, bem como na membrana plasmática e fracção microssomal. Todas as fracções das células SKOV3 apresentaram, predominantemente, estruturas glicosídicas parcialmente agalactosiladas com fucose próxima. Para além disso, o motivo terminal GalNAcβ4GlcNAc (LacdiNAc) também foi encontrado nas vesículas secretadas pelas células SKOV3. As vesículas secretadas pelas células OVM apresentaram predominantemente glicanos intactos do tipo complexo bi-, tri- e tetraramificados.

Em conclusão, este estudo contribuiu para o conhecimento da glicosilação de proteínas presentes em vesículas secretadas por células do carcinoma do ovário. Esta informação poderá fornecer uma base para a exploração futura dos mecanismos de selecção de proteínas e biogénese dos exossomas. Além disso, a identificação de glicoproteínas e *N*-glicanos específicos nos exossomas poderá abrir novas perspectivas na descoberta de biomarcadores e na vacinação contra o cancro.

Table of contents

Chapter 4 - *N*-glycosylation of secreted vesicles from ovarian tumour cells 87

xvi

Thesis Outline

Exosomes are secreted by several cell types, including ovarian tumour cells and are found in biological fluids such as blood and malignant ascites. The role of these vesicles in tumour progression has been studied but the role of protein glycosylation is not known.

The major objective of this work was to characterize and investigate the biological role of protein *N*-glycosylation from ovarian tumour derived exosomes. Furthermore, the role of *N*-linked glycans in ADAM10 localization, activity and sorting to exosomes has also been investigated.

This dissertation begins with a general introduction to ovarian cancer biology, which is followed by an overview about protein glycosylation, with focus on the *N*-glycosylation biosynthetic pathway and abnormal glycosylation properties found in cancer cells. Exosome biogenesis, composition and function are described in detail and particular relevance is given to tumour-derived exosomes as potential biomarkers and therapeutic targets. Finally, a brief characterization of the metalloprotease and disintegrin ADAM10 is given, including protein structure, activity and role in cancer.

In Chapter 2, the role of *N*-linked oligosaccharides on ADAM10 intracellular localization, activity and sorting to exosomes was investigated.

Chapter 3 describes the mechanisms involved in the uptake of labelled exosomes from SKOV3 cells by SKOV3 cells. Furthermore, the glycosylation profile of these secreted vesicles was analysed by lectin blot using different lectins.

In Chapter 4, the glycosylation of ovarian tumour secreted vesicles, microsomal and plasma membrane enriched fractions were compared by lectin blot analysis. The *N*-glycan structures from glycoproteins present in

these fractions were also analysed in detail by HPAEC-PAD and MALDI-TOF-MS.

Finally, Chapter 5 consists of a general discussion with future perspectives, and conclusions of the work presented in this Thesis.

List of Figures

List of Figures (continued)

List of Tables

Abbreviations

Abbreviation	Full form
ACN	acetonitrile
ADAM	*a disintegrin and metalloprotease*
BCA	bicinchoninic acid
BMS	Brystol meyer squibb
BSA	bovine serum albumin
CFSE	carboxyfluoresceine diacetate succinimidyl-ester
Con A	concanavalin A
dHex	deoxyhexose
DMEM	Dulbecco's modified Eagle's medium
EndoH	endoglycosidase H
EEA1	early endosome antigen 1
EIPA	5-ethyl-*N*-isopropyl amiloride
ER	endoplasmic reticulum
ERGIC	endoplasmic reticulum-Golgi intermediate compartment
ESCRT	endosomal sorting complex required for transport
Exos	exosomes
Fuc	fucose
Gal	galactose
GalNAc	*N*-acetylgalactosamine
GlcNAc	*N*- acetylglucosamine
Glc	glucose
GM130	*cis*-Golgi matrix protein of 130 kDa
HEK	human embryonic kidney
Hex	hexose
HexNAc	*N*-acetylhexosamine

Abbreviation	Full form
HPAEC-PAD	high performance anion exchange chromatography with pulsed amperometric detection
HRP	horseradish peroxidase
LacNAc	*N*-acetyllactosamine
LAMP1	lysosomal-associated membrane protein
MAL	*Maackia amurensis* lectin
MALDI-TOF-MS	matrix assisted laser desorption/ionization time-of-flight mass spectrometry
Man	mannose
MEFs	mouse embryonic fibroblasts
MVBs	multivesicular bodies
NeuAc	*N*-acetylneuraminic acid
PBS	phosphate-buffered saline
PCR	polymerase chain reaction
PNGase F	peptide-*N*-glycosidase F
PVDF	polyvinyledene difluoride
SDS-PAGE	sodium deodecyl sulphate - polyacrylamide gel electrophoresis
sLe^a	sialyl-Lewis^a
sLe^x	sialyl-Lewis^x
SNA	*Sambuccus nigra* lectin
TBS	tris-buffered saline
TFA	trifluoroacetic acid
TGN	*trans*-Golgi network
TNF-α	tumour necrosis factor α
Tris	tris(hydroxymethyl)aminomethane
WFA	*Wisteria floribunda* lectin
wt	wild-type

Amino Acid nomenclature

Abbreviations		Amino acid name
Ala	A	Alanine
Arg	R	Arginine
Asn	N	Asparagine
Asp	D	Aspartate (Aspartic Acid)
Cys	C	Cysteine
Gln	Q	Glutamine
Glu	E	Glutamate (Glutamic Acid)
Gly	G	Glycine
His	H	Histidine
Ile	I	Isoleucine
Leu	L	Leucine
Lys	K	Lysine
Met	M	Methionine
Phe	F	Phenylalanine
Pro	P	Proline
Ser	S	Serine
Thr	T	Threonine
Trp	W	Tryptophan
Try	T	Tyrosine
Val	V	Valine

Chapter 1

General introduction

1. General introduction

1.1. Ovarian cancer

Ovarian cancer is the leading cause of death from gynaecological malignancies in the Western world. The high death rate associated with this disease is mainly due to the absence of specific symptoms, rapid growth rate and to lack of an effective screening, and as a result most patients are diagnosed at an advanced stage when the disease is already disseminated throughout the abdominal cavity.

Ovarian cancers are a heterogeneous group of neoplasms and are traditionally divided into three major categories according to their presumed histogenesis: sex cord-stromal, germ cell, and epithelial tumours. Epithelial ovarian tumours, which represent 90% of malignant ovarian tumours, are further grouped into histological types: serous, mucinous, endometrioid, clear cell, transitional cell tumours, carcinosarcoma, mixed epithelial tumour, undifferentiated cancers, and others (reviewed in Scully, 1987; Kaku *et al.*, 2003).

The biological mechanisms of transformation in ovarian cancer are poorly understood. Mutations in the BRCA1 and BRCA2 tumour suppressor genes are responsible for a great number of hereditary ovarian cancers (Holschneider and Berek, 2000), however, the majority of ovarian cancers are sporadic, in which the disease arises from a multistep process requiring a large number of genetic changes involving both activation of oncogenes and loss of tumour-suppressor genes (Cvetkovic, 2003).

Ovarian cancers diagnosed while still limited to the ovaries (stage I), allow that 90% of patients can be cured with conventional surgery and

chemotherapy. Cure rates decrease substantially after tumour metastasis to the pelvic organs (stage II), the abdomen (stage III) or beyond the peritoneal cavity (stage IV) (Bast *et al.*, 2009). Early detection of ovarian cancer might significantly improve the overall survival rate. Nevertheless, given the heterogeneity of the disease, it is unlikely that any single marker will be sufficiently sensitive to provide an effective initial screen. Probably, the combination of multiple serum markers may help achieve the sensitivity and specificity required for the screening of ovarian cancer (Badgwell and Bast, 2007).

1.2. Protein glycosylation

Glycosylation is the major post-translational modification of proteins and lipids and is estimated to be present in more than half of all proteins in nature. Glycosylation of proteins can be of the *N-* or *O-*linkage type depending on glycans site of attachment. An *N-*glycan is a sugar chain covalently linked via an *N-*acetylglucosamine (GlcNAc) residue to an asparagine (Asn) residue of a polypeptide chain within the consensus peptide sequence Asn-X-Ser/Thr. *N-*glycans share a common pentasaccharide core region and can be generally divided into three main types: high mannose, complex, and hybrid. An *O-*glycan is typically linked to the polypeptide via an *N-*acetylgalactosamine (GalNac) residue to a serine (Ser) or threonine (Thr) residue and can be extended into a variety of different structural core classes (Varki *et al*., 2009).

The function of the glycans presented in glycoconjugates can be crucial for the growth, development, and survival of cells and organisms. Glycans have been shown to participate in recognition events and host-pathogen interactions such as bacterial and viral infections. They are involved in protein folding and sorting, vesicular trafficking, cell signalling,

cell adhesion and motility, organogenesis and immunological defence (reviewed in Varki, 1993; Ohtsubo and Marth, 2006). Additionally, glycosylation can affect protein plasma residence time, it provides steric protection from proteases, and it plays a role on enzyme activity, substrate targeting and specificity (reviewed in Skropeta, 2009).

1.2.1. *N*-glycosylation

The biosynthesis of *N*-linked oligosaccharides occurs in the endoplasmic reticulum (ER) and Golgi complex (Figure 1, A). During the synthesis of *N*-linked glycans a 14-saccharide "core" unit is assembled as a membrane bound dolichylpyrophosphate precursor by enzymes located on both sides of the ER membrane. The structure of this precursor is common to most eukaryotes and contains 3 glucose, 9 mannose, and 2 GlcNAc residues ($Glc_3Man_9GlcNAc_2$). The completed core oligosaccharide is transferred from the dolichylpyrophosphate carrier to the nascent polypeptide chain, and is coupled through an *N*-glycosidic bond to the side chain of an asparagine residue. The oligosaccharyltransferase responsible for this transfer is a complex enzyme with its active site in the ER lumen and that recognizes a specific conformation of the glycosylation sequon (Asn-X-Ser/Thr), where X can be any amino acid except proline. Of all sequons, it has been estimated that 90% are glycosylated (Gavel and Heijne, 1990). Before exiting the ER, a terminal glucose, and mannose residues are removed from the *N*-glycan by ER glucosidases and mannosidases. When the glycoprotein moves to the Golgi complex, the glycan chains undergo further trimming of mannoses before further extension of the glycan branches. Subsequent step-wise adding of sugars to different positions of the extending glycan is catalyzed by a number of

glycosyltransferases, each adds a particular monosaccharide through a specific glycosidic bond (Helenius and Aebi, 2001; Varki *et al*., 2009).

N-glycan structures are generally classified into three principal categories: high mannose, complex and hybrid (Figure 1, B), all of them share a common tri-mannosyl ($Man_3GlcNAc_2$) core structure. The high mannose glycans have 5 to 9 mannose ($Man_{5-9}GlcNAc_2$) sugars. Those with two GlcNAc's attached to the tri-mannosyl core are called complex type. The hybrid type are a combination of high mannose and complex glycans, and have at least three mannose sugars, but only one GlcNAc on one nonreducing mannose (Helenius and Aebi, 2001; Varki *et al*., 2009).

The removal of N-glycans from proteins, either individually or in combination has revealed their role in many cellular processes (reviewed in Skropeta, 2009) and total inhibition of N-glycosylation lead to death in early embryogenesis (Marek *et al*., 1999). Nevertheless, lysosomal targeting is probably the best characterized role of N-linked glycosylation, the binding of mannose 6-phosphate on N-linked oligosaccharides in the trans-Golgi mediate the targeting of glycoproteins to the lysosome. Attachment of N-glycans is also an essential requirement for some glycoproteins to exit the secretory pathway. The ER is known to have a primary quality control function by ensuring the fidelity and proper native conformation of proteins that cross this compartment (Helenius and Aebi, 2001).
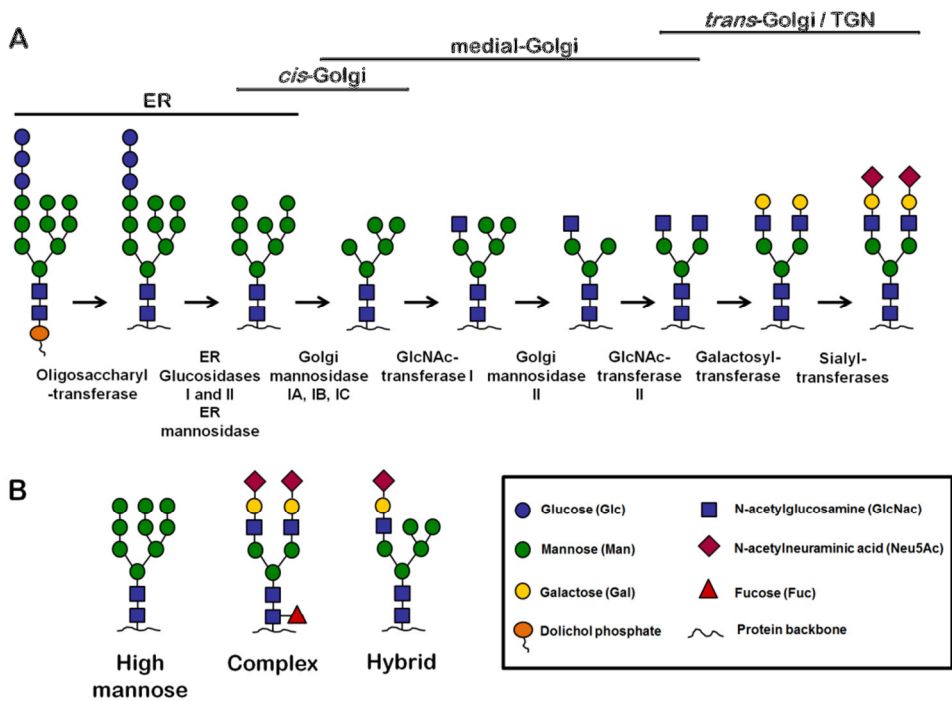
Figure 1. **_N_-glycosylation processing and representation of the different _N_-glycan types.** (A) *N*-linked oligosaccharides processing involves a series of steps that occur in different compartments of the secretory pathway. (B) Schematic representation of high mannose, complex and hybrid *N*-glycans. ER, endoplasmatic reticulum; TGN, *trans*-Golgi network. Adapted from Taylor and Drickmer, 2006; Varki *et al.*, 2009.

1.2.2. *O*-glycosylation

In *O*-linked glycosylation, monosaccharide residues are sequentially added onto the protein, in the Golgi apparatus. There is no consensus sequence and there are several possible *O*-glycosidic linkages.

The main forms of *O*-glycans on higher eukaryotic secretory proteins are mucin-type glycans and proteoglycans (Ungar, 2009). Mucin

synthesis starts with the addition of an GalNAc residue to a Ser/Thr side chain. This is followed by the formation of one of four distinct core structures by the addition of Gal and GlcNAc residues in various linkages. These core structures are the basis for the synthesis of a large variety of different glycans containing largely Gal, GlcNAc and NeuAc sugars. The hallmark of proteoglycans is the extensive modification of sugar residues with sulfate to create charged surfaces that interact with the extracellular matrix. Their glycan chains are linked to serine hydroxyls through a tetrasaccharide comprising xylose-Gal-Gal-glucuronic acid (GlcA) residues. The main proteoglycan oligosaccharides are repetitive structures formed by GlcNAc-GlcA or GlcNAc-iduronic acid dimers often containing *N*-linked (on GlcNAc only) or *O*-linked sulfate groups (Ungar, 2009).

1.2.3. Glycosylation in cancer

Glycosylation alterations are typical for all kinds of cancers, including ovarian cancer, and include increased and/or reduced expression of certain structures, the persistence of incomplete or truncated structures, the accumulation of precursors, and the appearance of novel structures. Some of these alterations affect tumour progression by increasing cells detachment from the extracellular matrix, cell motility, adhesion to activated endothelial cells or metastasis. Glycoconjugates released by tumours have been detected in the blood stream and have been used in diagnosis as cancer markers and targets for therapeutic approaches (Varki *et al*., 2009; Peracaula *et al*., 2008).

Described changes in glycosylation comprise increased β1–6GlcNAc branching of *N*-glycans; changes in the amount, linkage, and acetylation of sialic acids; reexpression of *N*-glycolylneuraminic acid; overexpression of specific carbohydrate antigens that lead to terminal

structures like sialyl-Lewis^x (sLe^x), sialyl-Lewis^a (sLe^a), or polysialic acid; expression of selectin ligands; altered expression and enhanced shedding of glycosphingolipids; increased expression of galectins and polylactosamines; altered expression of the ABH(O) blood-group-related structures; alterations in sulfation of GAGs; increased expression of hyaluronan; or loss of expression of glycophospholipid anchors. In many cases the formation of these aberrant structures depends on altered regulation of one or more key glycosyltransferases or glycosidases (Varki *et al*., 2009; Peracaula *et al*., 2008).

The most widely used tumour marker in ovarian cancer is CA125 (MUC16), a large mucin protein containing both *N*- and *O*-glycosylation. CA125 is increased in 80-90% of patients with advanced stage ovarian cancer, but it is only elevated in 50% of patients with stage I disease. Moreover, CA125 lacks specificity since it is not expressed in all forms of ovarian cancer and might be elevated in various benign conditions (Gupta and Lis, 2009; Jelovac and Armstrong, 2011). Since aberrant glycosylation also occurs in ovarian cancer, several studies have been performed to identify abnormal oligosaccharides present on the glycoproteins of ovarian cancer cell lines and human serum from ovarian cancer patients. Cell surface antigens such as Lewis^y, sLe^x, sialyl-Tn, and Tn antigens were found in primary ovarian carcinomas and their metastases (Davidson *et al*., 2000). Furthermore, mucinous tumours were found to intensively express sialyl-Tn, Lewis^a, and sLe^a, whereas serous and endometrioid tumours strongly expressed Lewis^y and H-type 2 antigen (Federici *et al*., 1999). Bisecting glycans have also been described in tissues of endometrioid ovarian cancers (Abbott *et al*., 2008).

Specific changes in the serum of ovarian cancer patients include increase of core fucosylated, agalactosylated complex type diantennary glycans originated from immunoglobulin G, along with the sLe^x determinant (Saldova *et al*., 2007). Alterations in fucosylation and branching in α1-acid

glycoprotein have also been proposed as potential biomarkers of ovarian cancer (Imre *et al.*, 2008). Furthermore, an increase in sialylation with a shift in sialic acid linkage from α2,3- to α2,6- was observed in ovarian cancer serum glycoproteins (Saldova *et al.*, 2007).

Alterations in the functions of the glycosyltransferases responsible for the formation of these antigens are also a consequence of ovarian tumour development and have been reported in several studies. These modifications include alterations in mRNA levels of α2,3- and α2,6-sialyltransferases in the tissues of serous ovarian cancer (Wang *et al.*, 2005), elevated expression of *N*-acetylglucosaminyltransferase V in mucinous ovarian carcinoma tissues (Takahashi *et al.*, 2009), elevated α6-fucosyltransferase in serous adenocarcinomas (Takahashi *et al.*, 2000), and elevated α3/4-fucosyltransferase activities in ovarian cancer (Chandrasekaran *et al.*, 1992).

Ovarian carcinoma cell lines, SKOV3, GG, OVM, and m130 were also characterized with respect to their glycosylation using anti-carbohydrate antibodies and lectins (Escrevente *et al.*, 2006). These cell lines contained variable amounts of Lewis carbohydrate motifs and glycoproteins recognized by Concanavalin A, a lectin that binds α-mannosyl containing-branched glycans predominantly of the high mannose followed by hybrid and diantennary complex structures to a lower extent, and Sambucus nigra lectin that binds structures containing terminal α2,6-linked sialic acid. In addition, structure analysis of the *N*-linked glycans from total glycoproteins derived from SKOV3 ovarian carcinoma cells confirmed the abundance of high mannose and proximally fucosylated complex partially agalactosylated glycan structures as well as the presence of the LacdiNAc motif (Machado *et al.*, 2011).

1.3. Exosomes

Exosomes are small microvesicles that are released into the extracellular environment by a variety of different cells. The release of exosomes has been described for the first time for maturing reticulocytes (Johnstone *et al*., 1987) but since then it has been observed for a multitude of other hematopoietic cells, including B cells (Raposo *et al*., 1986), dendritic cells (Théry *et al*., 1999), mast cells (Raposo *et al*., 1997), and T-cells (Blanchard *et al*., 2002). In addition, they can be released by cells with different origins such as intestinal epithelial cells (van Niel *et al*., 2001), kidney cells (Hoorn *et al*., 2005), neurons (Faure *et al*., 2006) and tumour cells (Andre *et al*., 2002). Furthermore, exosomes have been detected in various bodily fluids such as blood plasma (Caby *et al*., 2005), urine (Pisitkun *et al*., 2004), saliva (Ogawa *et al*., 2008), breast milk (Admyre *et al*., 2007), and malignant pleural effusions (Bard *et al*., 2004).

Exosomes from different origins all share certain common characteristics, including size (40-100 nm), structure (lipid-bilayer), shape (cup-shaped morphology), density in sucrose gradient (1.13-1.19 g/ml) and general protein and lipid composition (Simons and Raposo, 2009; Théry *et al*., 2009).

Exosomes can be isolated based on their size, density and/or biochemical properties. The most commonly used procedure is based on differential sedimentation and involves several centrifugations to remove dead cells, large debris and other cellular contaminants, followed by a final high-speed ultracentrifugation to pellet small vesicles. This pellet contains exosomes, which can be further purified by a sucrose density gradient (Théry *et al*, 2006) to remove contaminating vesicles of distinct sizes and densities that are also produced by healthy (Figure 2) or apoptotic/ dying cells (Théry *et al*., 2009). Other methods including membrane ultrafiltration

(Lamparski *et al*., 2002) and immunoaffinity capture (Clayton *et al*., 2001) can also be used depending on the sample source and applications intended.

1.3.1. Biogenesis and secretion

The uptake of material from the exterior of the cells occurs via endocytosis. The endocytic vesicles are then transported to early endosomes and recycled back to the plasma membrane, or delivered to late endosomes together with other proteins (Figure 2). In late endosomes, proteins are sorted into intraluminal vesicles by inward budding of the limiting membrane into the endosomal lumen, forming multivesicular endosomes, classified on the basis of their morphology as multivesicular bodies (MVBs). Consequently, proteins are incorporated into the invaginating membrane, thus maintaining the same topological orientation as the plasma membrane while cytosolic components are engulfed (Février and Raposo, 2004).

The mechanisms underlying sorting of proteins into intraluminal vesicles at the endosomal-limiting membrane are largely unknown. One mechanism described involves the recognition of ubiquitinated proteins by the Endosomal Sorting Complex Required for Transport (ESCRT). The ESCRT machinery is organized into four heteromeric protein complexes. The ESCRT-0, -I and –II complexes recognize and sequester ubiquitinated proteins in the endosomal membrane, whereas the ESCRT-III complex seems to be responsible for membrane budding (reviewed in Lakkaraju and Rodriguez-Boulan, 2008; Simons and Raposo, 2009). However, some proteins present in the exosomes are not ubiquitinated, suggesting that other mechanisms such as oligomerization or partitioning of protein into lipid raft domains may be involved (de Gassart *et al*., 2003; Lakkaraju and

Rodriguez-Boulan, 2008; Schorey and Bhatnagar, 2008). Recently, an ESCRT-independent mechanism of protein sorting into MVBs involving the sphingolipid ceramide has been described (Trajkovik *et al.*, 2008).
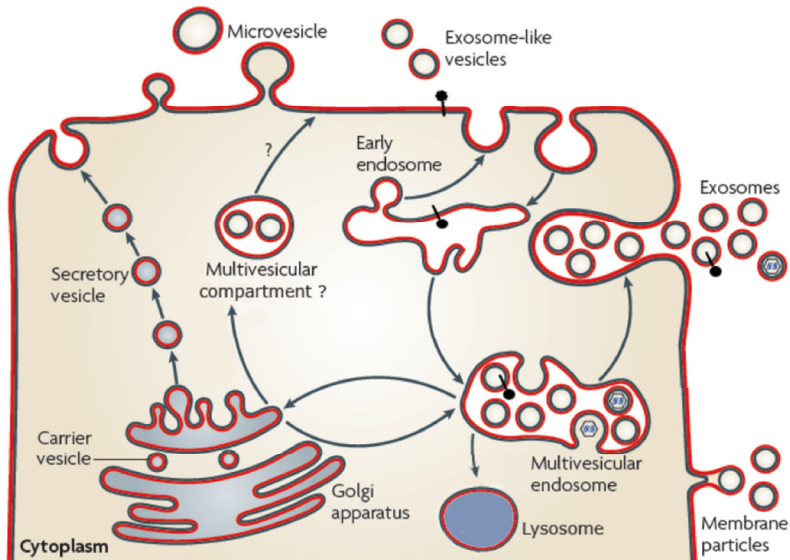
Figure 2. Exosome biogenesis and different types of membrane vesicles. Membrane proteins are internalized and delivered to early endosomes. In early endosomes, the proteins can be recycled to the plasma membrane or delivered to late endosomes. Proteins are sorted to intraluminal vesicles by budding of the endosomal limiting membrane into the endosomal lumen, forming multivesicular endosomes. Multivesicular endosomes can dock and fuse with the plasma membrane resulting in exosomes (40-100 nm) secretion. Some viruses, such as retroviruses, hijack the exosomal machinery and are secreted by the same mechanism. Microvesicles (100-1000 nm) and membrane particles (50-80 nm) can also be secreted by cells by direct budding from the plasma membrane into the extracellular space. Exosome-like vesicles (20-50 nm) are also thought to originate from internal multivesicular compartments, although the nature of these compartments is not clear. Adapted from Février and Raposo, 2004; Théry *et al.*, 2009.

In a final step, multivesicular endosomes can either fuse with lysosomes for protein degradation or with the plasma membrane, resulting in the release of exosomes (Figure 2). The mechanism that leads to exosomes secretion, though still poorly understood, appears to involve two Ras family monomeric proteins Rab27A and Rab27B (Ostrowski *et al*., 2010).

In addition to exosomes other vesicles may be secreted from mammalian cells and they have been classified based on their biogenesis and physiochemical properties, namely diameter (Figure 2) (Théry *et al*., 2009).

1.3.2. Composition

Exosomes contain a variety of molecules, including proteins, RNA and lipids reflecting the cell type from which they originate and possibly their functional role.

Although the protein content of exosomes varies depending on their source, the proteomic analysis of exosomes from a wide variety of cells and body fluids has identified several proteins that are well conserved and are commonly used as exosomal markers. Nearly all exosomes contain proteins involved in membrane transport and fusion (RabGTPases, annexins, flotillin), in MVBs biogenesis (Alix, TSG101), metabolic enzymes (peroxidases, pyruvate and lipid kinases) and cytoplasmic proteins (tubulin, actin). Moreover, exosomes are enriched with heat shock proteins (hsp70 and 90), integrins and tetraspanins (CD63, CD9, CD81) (reviewed in Simpon *et al*., 2008, Schorey and Bhatnagar, 2008; Simons and Raposo, 2009; Mathivanan and Simpson, 2010) and were shown to carry active proteases, such as ADAM10 and ADAM17 (Stoeck *et al*., 2006).

Recent studies have demonstrated that exosomes also carry and deliver mRNA and small RNAs, including microRNA (Valadi *et al*., 2007; Skog *et al*., 2008). A compendium of exosomes RNAs and proteins is available at "Exocarta" (http://exocarta.ludwig.edu.au).

Moreover, exosomes display a specific lipid composition different from the parental cells. They are particularly enriched in raft-lipids such as cholesterol, sphingolipids, ceramide and glycerophospholipids with long and saturated fatty-acyl chains (Subra *et al*., 2007; Trajkovik *et al*., 2008).

1.3.3. Function

Exosomes were originally observed as a mechanism to remove unnecessary proteins, namely the transferrin receptor during reticulocytes maturation (Johnstone *et al*., 1987). However, since then many other functions have been proposed such as intercellular communication, induction of immune responses, and transfer of infectious agents, among several others.

The ability of exosomes to interact with cells has important biological implications, such as cell-cell communication, and the delivery of proteins and genetic material conferring new functional properties to the recipient cells. Several types of interaction between exosomes and cells have already been proposed based on indirect evidence and *in vitro* studies. Exosomes can associate with the plasma membrane through ligand-receptor interactions (Théry *et al*., 2009) or lipids, such as phosphatidylserine (Keller *et al*., 2009). The process of internalization can occur through direct fusion of the exosomes with the plasma membrane, releasing the exosomal content into the cell cytoplasm. Alternatively, exosomes can enter the cells by receptor-mediated endocytosis and later fuse with the limiting membrane of the endosome releasing the exosomal

content to be recycled to the cell surface or to be degraded in the lysosome (Théry *et al*., 2009; Coccusi *et al*., 2009). Exosome uptake was shown to occur via clathrin-mediated endocytosis in dendritic cells (Morelli *et al*., 2004), as well as phagocytosis in monocytes and macrophages (Feng *et al*., 2010).

One of the most studied roles of secreted exosomes is their powerful effect on the immune system. Exosomes secreted from different sources can have both an activating or a tolerogenic or even inhibitory effect on immune cells. In general, exosomes produced by antigen-presenting cells such as dendritic cells, macrophages and B cells are immune activating. They activate directly or indirectly immune effector mechanisms such as cytotoxicity, antibody and cytokine production, and priming of T cells. On the other side, exosomes produced by epithelial cells and the great majority of tumours are immune inhibitory, playing an important role on tumour dissemination (Théry *et al*., 2009).

Exosomes can also participate in the propagation of infectious agents. Février *et al*. showed that the prion protein and the scrapie forms of the protein (PrPc and PrPsc, respectively) can be secreted in association with exosomes (Février *et al*., 2005). Moreover, a role for exosomes in the intercellular trafficking of human immunodeficiency virus (HIV-1) infectivity has also been suggested (Gould *et al*., 2003; Wiley and Gummuluru, 2006; Izquierdo-Useros *et al*., 2008).

Furthermore, exosomes have been proposed as a novel platform for ADAM-mediated cleavage. The proteolysis of cell adhesion transmembrane molecules like L1 and CD44 by ADAMs can occur in MVBs and exosomes, in addition to the plasma membrane (Stoeck *et al*., 2006; Keller *et al*., 2006).

1.3.4. Tumour cell-derived exosomes

The biological significance of exosomes secretion by tumours, and the presence of these vesicles in malignant effusions such as ascites, is not clear. Tumours reported to release exosomes include cancers of the ovary, breast, oral cavity, colorectum, brain, bladder, prostate, and melanomas (reviewed in Zhang and Grizzle, 2011).

Tumour-secreted vesicles, including exosomes, can contribute to tumour invasion and progression by transferring aggressive cancerous phenotypes (Al-Nedawi *et al*., 2008), modifying the tumour microenvironment (Castellana *et al*., 2009), conferring multi-drug resistance (Shedden *et al*., 2003; Safaei *et al*., 2005), and promoting angiogenesis, tumour growth and metastasis (reviewed in Muralidharan-Chari *et al*., 2010).

Some reports point to a role of cancer exosomes in immune activation (reviewed in Théry *et al*., 2009). Wolfers *et al*, (Wolfers *et al*., 2001) showed that tumour-derived exosomes were able to transfer antigens from tumour cells to dendritic cells and, therefore, function in antigen-cross presentation on syngeneic and allogeneic established mouse tumours. However, recent studies point to the increasing evidence that cancer exosomes might instead suppress the immune system facilitating tumour growth and invasion (reviewed in Valenti *et al*., 2007; Zhang and Grizzle, 2011). This can occur through several mechanisms such as induction of myeloid-derived suppressor cells (Iero *et al*., 2008) and inhibition of dendritic cell maturation (Yu *et al*., 2007) or T cell function (Clayton *et al*., 2007).

The role of exosomes in immune suppression and ovarian tumour progression has been investigated. Ascites-derived exosomes induced apoptosis of cells of the immune system (Peng *et al*., 2011) and resulted in

the growth of an ovarian carcinoma *in vivo*, after systemic administration (Keller *et al*., 2009). Moreover, exosomes derived from ovarian carcinoma cell lines and patient's ascites were shown to act as platforms for ectodomain shedding, being an important source of soluble adhesion molecules like L1 and CD44 that could regulate tumour cell function in an autocrine/paracrine fashion (Gutwein *et al*., 2005; Stoeck *et al*., 2006), and exhibited gelatinolytic activity, responsible for increasing tumour invasion into the stroma (Runz *et al*., 2007. Exosomes derived from human ovarian carcinoma cells have also been implicated in drug resistance, acting as a mechanism of efflux for the drug cisplatin (Safaei *et al*., 2005).

1.3.5. Exosomes in diagnosis and therapeutics

The presence of exosomes in biological fluids such as, blood plasma (Caby *et al*., 2005) and urine (Pisitkun *et al*., 2004), and the fact that they can be easily collected using non-invasive methods holds significant potential. Exosomes can be used for obtaining novel and complex sets of biomarkers for the early detection and diagnosis of diseases, for determining prognosis, and for therapeutic interventions such as the development of vaccines.

Urinary exosomes have been extensively studied having in view the discovery of potential disease biomarkers of bladder (Welton *et al*., 2010) and prostate cancer (Nilsson *et al*., 2009). Similarly, exosomes collected from blood plasma have also been investigated. MicroRNA profiling of circulating exosomes was explored as a diagnostic marker for biopsy profiling and to screen asymptomatic populations with ovarian (Taylor and Gercel-Taylor, 2008) and lung cancer (Rabinowits *et al*., 2009). Blood derived-exosomes of women with ovarian cancer contained high levels of claudin-4, a membrane protein whose expression is elevated in ovarian

cancer (Li *et al*., 2009), and exosomes derived from sera and malignant ascites showed the presence of tumour progression related proteins (L1, ADAM10, CD24, and EpCAM) (Gutwein *et al*., 2005; Runz *et al*., 2007).

Since both tumour and immune cells are able to secrete exosomes, the application of these vesicles in immunotherapy has become a promising area of research in cancer (reviewed in Tan *et al*., 2010), infectious (Beauvillain *et al*., 2009) and autoimmune diseases (Kim *et al*., 2005). The ability of exosomes released from dendritic cells, pulsed with tumour antigens to stimulate T-cells and to induce the eradication of tumours in mice (Zitvogel *et al*., 1998) has led to their use as therapeutic agents for the stimulation of anti-tumoral immune responses. Exosomes have already been used in phase I clinical trials with patients showing advanced stage melanomas (Escudier *et al*., 2005), non-small cell lung carcinomas (Morse *et al*., 2005), and colorectal cancer (Dai *et al*., 2008).

1.4. ADAM10

ADAM (*A Disintegrin And Metalloprotease*) 10 is a type I transmembrane glycoprotein that belongs to the ADAMs family and to the zinc-dependent metalloproteinases (*metzincins*) superfamily.

Mammalian ADAM10 was originally isolated from bovine brain, based on its ability to cleave myelin based protein in *in vitro* preparations (Chantry *et al*., 1989), but later work showed that it is widely expressed among different tissues and several species.

The gene locus for human ADAM10 was matched to chromosome 15 at position 15q21.3-q23 (Yamazaki *et al*., 1997) and codes for a protein with 748 amino acids that has four potential *N*-glycosylation sites, N267, N278, N439 and N551 (Figure 3).

ADAM10 is synthesized in the rough endoplasmic reticulum and is maturated in the late Golgi compartments. Subcellular localization analysis revealed that human ADAM10 is mainly located at the plasma membrane (Gutwein *et al*., 2003) but it also colocalizes with Golgi markers and it was found in secreted vesicles identified as exosomes (Lammich *et al*., 1999; Gutwein *et al*., 2003).

The major role of ADAM10 is the proteolytic cleavage of transmembrane proteins with important physiological and pathological roles. The severe phenotype of ADAM10$^{-/-}$ embryos implies that ADAM10 has a crucial role on early vertebrate embryogenesis. In fact, the knockout of ADAM10 in mice is embryonic-lethal at 9.5 days and showed evidence of pronounced defects of the developing central nervous system, somites, and cardiovascular system due to disrupted Notch signalling (Hartmann *et al*., 2002).

1.4.1. Structure

ADAM10 is characterized by a conserved domain structure common to other ADAMs consisting of an N-terminal signal sequence that directs the protein to the secretory pathway, followed by a prodomain, a metalloprotease and disintegrin domains, a cystein-rich region, a transmembrane domain, and finally an SH3-enriched cytoplasmic tail (Wolfsberg *et al*., 1995) (Figure 3).

ADAMs structural domains have been shown to play specific roles. ADAM10 prodomain keeps the metalloprotease inactive, through a "cystein switch" mechanism. The Zn^{2+} is coordinated by three histidines in the catalytic site, the free sulfhydryl group of the cystein residue provides a fourth coordination site and inhibits the entrance of the water molecule which is responsible for hydrolysis (Schlondorff and Blobel, 1999). The

catalytically active form of ADAM10 is generated by proteolytic removal of the prodomain by proprotein convertases furin and/or PC7 in the Golgi compartments (Anders *et al.*, 2001). Evidence suggests that the prodomain also plays an important role as a chaperone in the proper folding of the proenzyme in the ER, particularly the metalloprotease domain (Fahrenholz *et al.*, 2000). More recently, the isolated prodomain of ADAM10 was shown to act as a potent, selective inhibitor of the active mature form of the protein (Moss *et al.*, 2007).

The metalloprotease domain is well conserved among ADAMs and is similar in sequence to the snake venom metalloproteases. Although not all ADAMs yield metalloprotease activity, ADAM10 contains the consensus active site sequence HEXGHNLGXXHD, which binds the zinc ion in an appropriate configuration around the glutamate residue required for catalytic activity.
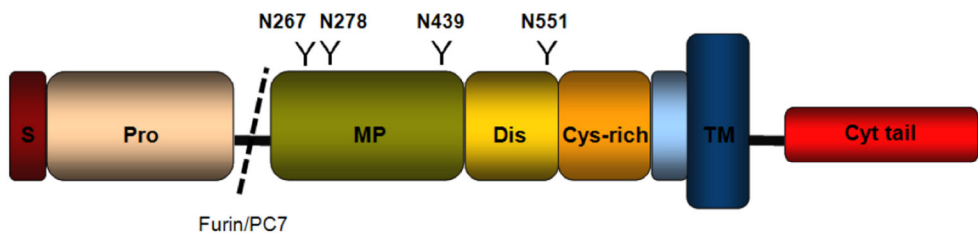
Figure 3. Domain structure of ADAM10. It consists of a signal peptide (S), a prodomain (Pro), a metalloprotease domain (MP), a disintegrin domain (Dis), a cystein-rich region (Cys-rich), a transmembrane region (TM), and a cytoplasmic tail (Cyt tail). ADAM10 has four potential *N*-glycosylation sites, three located in the metalloprotease domain, N267, N278 and N439, and one in the disintegrin domain, N551.

ADAMs disintegrin and cystein-rich domains were described as being directly involved in cell-cell adhesion processes through interactions with integrins and other receptors (White, 2003). Although no disintegrin activity has been reported for ADAM10, Janes *et al*. demonstrated that these domains are essential for ephrinA5/EphA3 substrate recognition (Janes *et al*., 2006). The formation of the ephrinA5/EphA3 complex creates a high affinity binding site for the cysteine-rich domain of ADAM10 which leads to a conformational switch that consents ADAM10 metalloprotease domain to cleave EphA5 in *trans*.

ADAMs cytoplasmic tails were proposed to be involved in the regulation of the metalloprotease activity, oligomerization, signalling and/or control of maturation and subcellular localization. ADAMs tails contain binding site motifs for SH3 domain-containing proteins and potential sites for phosphorylation. There are a number of adaptor proteins such as MAD2, Lck, Eve-1, PACSIN3 and synapse associated protein-97 with binding capacity to the cytoplasmic tail of ADAM10 (reviewed in Edwards *et al*., 2008). Moreover, a proline-rich stretch in the cytoplasmic domain of ADAM10 has been shown to be important for the correct basolateral localization of the protein in polarized epithelial cells promoting is metalloprotease activity (Wild-bode *et al*., 2006). Similarly, the binding of synapse associated protein-97 to ADAM10 cytoplasmic tail is also responsible for the correct localization of ADAM10 in synaptic membranes (Marcello *et al*., 2007).

1.4.2. Activity

The metalloprotease activity of ADAM10 is responsible for the proteolytic cleavage of several transmembrane proteins and release of their extracellular domain. This process is referred to as ectodomain shedding

and occurs both constitutively and in response to a variety of stimuli, including intracellular calcium concentration, phorbol esters and protein kinase C activation (Pandiella and Massague, 1991; Reiss and Saftig, 2009).

ADAM10 has more than 40 known protein substrates with important roles in development, cell signalling and disease pathologies, such as central nervous system disorders, inflammation and cancer (Figure 4) (Pruessmeyer and Ludwig, 2009). ADAM10 substrates include the cell adhesion molecule L1 (Mechtersheimer *et al*., 2001), pro-tumour necrosis factor α (Lunn *et al*., 1997), type IV collagen (Millichip *et al*., 1998), amyloid precursor protein (APP) (Lammich *et al*., 1999), ephrin-A2 (Hattori *et al*., 2000), epidermal growth factor receptor (EGFR) (Yan *et al*., 2002), Notch (Dallas *et al*., 1999; Hartmann *et al*., 2002), pro-heparin-binding epidermal growth factor (Lemjabbar and Basbaum, 2002), fractalkine (Hundhausen *et al*., 2003), CD44 (Nagano *et al*., 2004), N-cadherin (Reiss *et al*., 2005), betacellulin (Sanderson *et al*., 2005), and the low-affinity immunoglobulin E receptor CD23 (Weskamp *et al*., 2006), among others.

ADAM10 mediated proteolysis leads to the release of soluble factors like growth factors and chemokines, and is associated with extracellular signalling events. The released peptides can bind to their receptors and mediate signals in an autocrine or paracrine fashion. Moreover, ADAM10 mediated shedding can also play a role in intracellular signalling by regulated intramembrane proteolysis (RIP) (Brown *et al*., 2000). The ectodomain shedding of transmembrane proteins can promote further proteolysis of the remaining transmembrane fragment by the γ-secretase complex, for type I transmembrane proteins, or by the signal peptide peptidase like proteins (SPPLs), for type II transmembrane proteins, leading to the intracellular release of soluble substrate fragments, which might be translocated into the nucleus leading to the transcriptional

activation of target genes (Reiss *et al.*, 2005, Maretzki *et al.*, 2005; Martin *et al.*, 2008).

Besides signalling functions, ADAM10-mediated ectodomain shedding is also an important mechanism to regulate cell surface proteins like cell adhesion molecules and to inactivate receptors (reviewed in Reiss *et al.*, 2008). Recently, it has also been proposed that ADAM10 may function itself as a signalling protein in addition to its role as protease. ADAM10 can undergo ectodomain shedding by ADAM9 and ADAM15 followed by γ-secretase intramembrane proteolysis and translocation of ADAM10 intracellular domain into the nucleus where it is thought to be involved in gene regulation (Parkin and Harris, 2009; Tousseyn *et al.*, 2009).
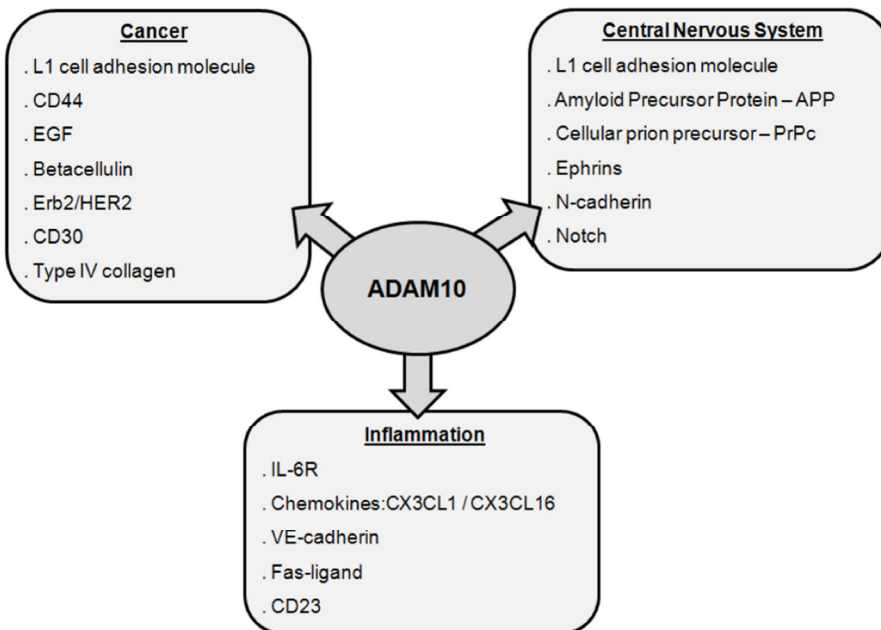
Figure 4. ADAM10 substrates. ADAM10 substrates have important functions in central nervous system, cancer and inflammation.

The factors that determine the substrate selectivity of ADAM10 are still not fully understood. Substrates have highly variable cleavage sites and there are no identified cleavage sequences. Moreover, many of ADAM10 substrates are also cleaved by other proteases, such as ADAM17 that shares high homology both in sequence and in substrate specificity with ADAM10. There is evidence that localization of both enzyme and substrate at particular subcellular microdomains is important for recognition and cleavage (Tellier *et al*., 2006). The secondary structure of the substrate justamembrane stalk is also an important factor for recognition (Seals and Courtneidge, 2003) and recent studies suggest that ADAM10 recognize preferentially cleavage sequences with large residues, primarily leucine, but also aromatic residues, while ADAM17 prefers smaller aliphatic residues (Caescu *et al*., 2009).

Regulation of ADAMs activity might occur at different levels, such as transcriptional control, alternative splicing, post-translational modifications, interaction with other proteins, cellular localization, and substrate availability (reviewed in Huovilla *et al*., 2005). Furthermore, ADAM10 activity can also be inhibited by tissue inhibitors of matrix metalloproteinases (TIMPs) 1 and 3 (Amour *et al*., 2000). More recently, synthetic inhibitors have also been developed mainly to be used as therapeutic agents to block ADAM10 activity in cancer (Moss *et al*., 2008).

1.4.3. Role in cancer

The sheddase activity of ADAM10 plays an important role in cellular signalling pathways and is critical for the survival of cancer cells. ADAM10 was found upregulated in several tumours, such as uterine, and ovarian carcinomas (Fogel *et al*., 2003), human haematological malignancies (Wu *et al*., 1997), neuroblastomas (Yavari *et al*., 1998), prostate cancer

(McCulloch *et al*., 2004), gastric carcinoma cells (Tanida *et al*., 2004), colon cancers (Gavert *et al*., 2005) and oral squamous cell carcinoma (Ko *et al*., 2005).

ADAM10 contributes to tumorigenesis and metastasis through cleavage and activation of several membrane proteins such as growth factors and cell adhesion molecules, and by regulating the adhesion and motility of cells, as a result of its role on extracellular matrix degradation (reviewed in Reiss *et al*., 2006). ADAM10-mediated L1 release was reported to enhance tumour dissemination by increasing cell migration in ovarian and uterine carcinomas (Fogel *et al*., 2003). Moreover the ectodomain shedding of cell adhesion molecules like L1 and CD44 can enable cells to escape from the surrounding tissue and mediate cell signalling that can promote cell proliferation, survival, and motility (Gutwein *et al*., 2003; Nagano *et al*., 2004).

As mentioned before, ADAM10 can also be found in secreted vesicles, identified as exosomes (Gutwein *et al*., 2003). Moreover, ADAM10 present in exosomes from ovarian carcinoma cells and ascites fluid was found to be functionally active and able to cleave both L1 and CD44 (Stoeck *et al*., 2006). These findings suggest that exosomes serve as a major platform for ectodomain shedding and as a vehicle for the export of soluble molecules that might have a role on tumour progression.

Since ectodomain shedding has been implicated as a pathological mechanism in cancer, ADAM10 inhibition has been explored as a target for cancer therapeutic drugs. Several inhibitors for ADAM10 have been described, but the lack of selectivity has contributed to adverse side effects and to the failure in clinical trials (reviewed in Reiss *et al*., 2006). Moreover, ADAM10 inhibition could have a profound negative effect in situations where ADAM10-mediated cleavage has a protective role, for example in Alzheimer's disease where ADAM10 cleavage of APP leads to a decrease in amyloide plaque formation.

1.5. Aims of this Thesis work

Exosomes are small membrane vesicles that are secreted by several cell types, including ovarian tumour cells, and have been found in biological fluids such as blood and malignant ascites. They can contribute to tumour invasion and progression by several mechanisms, and they are potential targets for the discovery of new disease biomarkers and for therapeutic interventions such as the development of vaccines.

Glycosylation is one of the most important post-translational modifications and alterations in cell surface glycosylation are often related to malignant transformation.

To date, little was known about the *N*-glycosylation profile of glycoproteins that are sorted to exosomes. The major goal of this work was to characterize and investigate the biological role of *N*-glycosylation from proteins present in exosomes of ovarian tumour cell lines. Furthermore, the glycoprotein metalloprotease ADAM10 has been studied in detail.

ADAM10 is a transmembrane protein with four potential *N*-glycosylation sites that is found in exosomes secreted from ovarian carcinoma cell lines. The first objective of this thesis work was to mutate each individual *N*-glycosylation site of ADAM10 and to understand the role played by *N*-glycosylation on ADAM10 intracellular localization, *in vivo* and *in vitro* activities. Furthermore, the presence of wild-type and mutant forms of ADAM10 in exosomes from ovarian carcinoma cells was also monitored, in order to evaluate if *N*-glycosylation site occupancy was required for ADAM10 sorting to exosomes.

The mechanisms of exosomes interaction and uptake by target cells are still poorly understood. Therefore, the second objective consisted of exploring the mechanisms of internalization of labelled exosomes by SKOV3 ovarian tumour cells. Several endocytic pathways were explored

using endocytosis inhibitors and colocalization studies by immunofluorescence microscopy. Furthermore the roles of cell surface proteins and exosomes surface proteins, as well as, oligosaccharides were investigated in the uptake. In addition, the glycosylation profile of the exosomes was analysed and compared with total cellular extracts using lectins with different specificities.

Since the exosomes had specific glycosylation patterns, as detected with lectins, the third objective consisted of the detailed structure analysis of the *N*-glycans from the secreted vesicles of SKOV3 and OVM ovarian carcinoma cell lines, as well as plasma membrane and microsomal fractions. The techniques used were HPAEC-PAD and MALDI-TOF-MS.

Chapter 2

Functional role of *N*-glycosylation from ADAM10 in processing, localization and activity of the enzyme

The majority of the work presented in this chapter has been included in the following manuscript:

Escrevente C, Morais VA, Keller S, Soares CM, Altevogt P, Costa J (2008). Functional role of *N*-glycosylation from ADAM10 in processing, localization and activity of the enzyme. *Biochim Biophys Acta*. 1780: 905-13.

2. Functional role of *N*-glycosylation from ADAM10 in processing, localization and activity of the enzyme

2.1. Summary

A disintegrin and metalloprotease 10 (ADAM10) is a type I transmembrane glycoprotein with four potential *N*-glycosylation sites (N267, N278, N439, and N551) that cleaves several plasma membrane proteins. In this work, ADAM10 was found to contain high mannose and complex glycans. Individual *N*-glycosylation site mutants S269A, T280A, S441A, T553A were constructed, and results indicated that all sites were occupied. T280A was found to accumulate in the endoplasmic reticulum as the non-processed precursor of the enzyme. Furthermore, it exhibited only residual levels of metalloprotease activity *in vivo* towards the L1 cell adhesion molecule, as well as *in vitro*, using a proTNF-alpha peptide as substrate. S441A showed increased ADAM10 susceptibility to proteolysis. Mutation of N267, N439, and N551 did not completely abolish enzyme activity, however, reduced levels were found.

ADAM10 is sorted into secretory vesicles, the exosomes. Here, a fraction of ADAM10 from exosomes was found to contain more processed *N*-linked glycans than the cellular enzyme.

In conclusion, *N*-glycosylation is crucial for ADAM10 processing and resistance to proteolysis, and results suggest that it is required for full-enzyme activity.

2.2. Introduction

ADAM (*a disintegrin and metalloprotease*) 10 is a type I transmembrane glycoprotein that belongs to the ADAMs protein family. It is characterized by a conserved domain structure, consisting of an *N*-terminal signal sequence that directs the protein to the secretory pathway followed by a prodomain, a metalloprotease, a disintegrin domain, a cystein-rich region, a transmembrane domain, and an SH3- enriched cytoplasmic tail (Wolfsberg *et al.*, 1995). In order to be catalytically active ADAM10 prodomain has to be cleaved by proprotein convertases furin and/or PC7 in the Golgi compartments (Anders *et al.*, 2001; Schlondorff and Blobel, 1999; Seals and Courtneidge, 2003).

ADAM10 metalloprotease domain is known to mediate the proteolytic cleavage of transmembrane proteins in their juxtamembrane region resulting in the release of the extracellular domain as a soluble form (shedding). ADAM10 can cleave a variety of proteins with importance in development, cell signalling and disease, such as the cell adhesion molecule L1 (Mechtersheimer *et al.*, 2001), pro-tumour necrosis factor-alpha (Lunn *et al.*, 1997), type IV collagen (Millichip *et al.*, 1998), amyloid precursor protein (Lammich *et al.*, 1999), ephrin-A2 (Hattori *et al.*, 2000), epidermal growth factor receptor (Yan *et al.*, 2002), notch (Dallas *et al.*, 1999; Hartmann *et al.*, 2002), pro-heparin-binding epidermal growth factor (Lemjabbar and Basbaum, 2002), fractalkine (Hundhausen *et al.*, 2003), CD44 (Nagano *et al.*, 2004), N-cadherin (Reiss *et al.*; 2005), betacellulin (Sanderson *et al.*, 2005), and low-affinity immunoglobulin E receptor CD23 (Weskamp *et al.*, 2006), among others. Moreover, ADAM10 is overexpressed in tumours, such as uterine and ovarian carcinomas (Fogel *et al.*, 2003), human haematological malignancies (Wu *et al.*, 1997), neuroblastomas (Yavari *et al.*, 1998), prostate cancer (McCulloch *et al.*,

2004), gastric carcinoma cells (Tanida *et al*., 2007), colon cancers (Gavert *et al*., 2005), and oral squamous cell carcinoma (Ko *et al*., 2007), suggesting a role in tumour progression and dissemination.

ADAMs disintegrin and cystein-rich domains were described as being directly involved in cell-cell adhesion processes through interactions with integrins and other receptors (White, 2003).

ADAM10 can be found in various cellular compartments. It has been shown to colocalize with Golgi markers and was found on the cell surface (Lammich *et al*., 1999; Gutwein *et al*., 2003). More recently, it was also detected in secreted vesicles identified as exosomes (Gutwein *et al*., 2003). Exosomes are small membrane vesicles (30-100 nm diameter) secreted by various cell types as a consequence of fusion of multivesicular late endosomes/lysosomes with the plasma membrane. Exosomes secretion has first been reported in a variety of cells, including cancer cells, neurons, B lymphocytes, T lymphocytes, dendritic cells, mast cells, and platelets (Caby *et al*., 2005). Exosomes secreted from tumour cells could promote cellular invasion and migration during metastasis (Stoeck *et al*., 2006).

ADAM10, like other ADAMs, is *N*-glycosylated. It has four potential *N*-glycosylation sites (N-X-S/T, X≠Pro), three located in the metalloprotease domain (N267, N278, and N439) and one in the disintegrin domain (N551). Glycosylation is one of the most important post-translational modifications in newly synthesized proteins which may influence the physicochemical and biological properties of glycoproteins. *N*-glycosylation has been related with protein folding and quality control of glycoproteins in the endoplasmic reticulum with consequences for processing and trafficking (reviewed in Helenius and Aebi, 2004; Morais *et al*., 2003), targeting in the secretory pathway, namely to the lysosome (via the mannose 6-phosphate receptor) (Hauri *et al*., 2000), dynamics of plasma membrane proteins (Cai *et al*., 2005; Brooks *et al*., 2006; Turner *et al*., 2006), cell-cell interactions, e.g.,

during metastases formation (Dube *et al*., 2005), or inflammation (Dube *et al*., 2005; Lowe *et al*., 2003), among others.

In cancer, aberrant glycosylation, particularly of cell surface glycoconjugates, is a hallmark associated with the disease (Dube *et al*., 2005). Altered glycosylation is the consequence of changes in glycosyltransferase expression and localization along the secretory pathway and also depends on the availability of sugar nucleotide donors in the Golgi lumen.

In the present work, the four potential *N*-glycosylation sites of bADAM10 were found to be occupied. By mutating each of those sites we observed that glycans from N278 were crucial for the intracellular processing of bADAM10, with the enzyme being accumulated as the precursor in the endoplasmic reticulum. Concerning N439, the *N*-glycans protected against proteolytic cleavage. *N*-glycans from each mutant were required for full *in vivo* activity. On the other hand, a fraction of human endogenous ADAM10 from exosomes was found to contain more processed *N*-linked glycans than the cellular counterpart.

2.3. Materials and methods

2.3.1. DNA constructs

The plasmid pcDNA3-ADAM10wt (Mechtersheimer *et al*., 2001) coding for wild-type bovine ADAM10 with the HA tag at the *C*-terminus was used as template for the construction of the *N*-glycosylation mutants: pbADAM10S269A, pbADAM10T280A, pbADAM10S441A, and pbADAM10T553A. Site-directed mutagenesis was done using

QuickChange cloning techniques (Stratagene, La Jolla, CA, USA), following the manufacturer's instructions. The serine or threonine from the *N*-glycosylation site (N-X-S/T) were replaced by an alanine residue following a strategy previously used (Morais *et al*., 2003; Morais *et al*., 2006).

The PCR reactions were carried out with 50-115 ng pcDNA3-ADAM10wt as template, 2.5 mM dNTPs mix, 2.5 U/µl Pfu Turbo DNA Polymerase and 10 µM of mutagenic primers. The primers used to obtain pbADAM10S269A, pbADAM10T280A, pbADAM10S441A, and pbADAM10T553A were, respectively as follows: $^{5'}$GGA ATT CGT AAC ATC GCT TTC ATG GTG AAA CGC ATA AG$^{3'}$, $^{5'}$GC ATA AGA ATC AAC ACA GCT GCT GAT GAG AAG G$^{3'}$, $^{5'}$GT AGT ATT AGA AAT ATA GCT CAA GTT CTT GAG AAG AAG$^{3'}$, $^{5'}$GAT CCT AAA CCG AAC TTC GCA GAC TGT AAT AGA CAT ACG$^{3'}$. Standard molecular biology techniques were used for PCR product restriction and analysis. Mutations of the bADAM10 *N*-glycosylation sites were confirmed by automatic DNA sequencing analysis.

2.3.2. Cell culture and protein expression

Human ovarian cancer SKOV3 cells, human embryonic kidney HEK293 cells and mouse embryonic fibroblasts (MEFs) were grown at 37 °C, 5% CO_2 in Dulbecco's Modified Eagle Medium (DMEM) (Sigma) supplemented with 10% fetal calf serum (Gibco), 1% penicillin/streptomycin solution (Gibco).

SKOV3 and HEK293 were transfected with each of the plasmids indicated in 2.3.1 or pcDNA3-L1 by the calcium phosphate technique using 5 µg of plasmid DNA and selection of stably-transfected cells was performed using 2 and 1 mg/ml geneticin sulphate G-418 (Gibco), respectively. For transient expression, HEK293 cells and MEFs were

transfected with 2 or 2.5 µg of plasmid DNA, respectively, using Lipofectamine 2000 (Invitrogen), following manufacturer's instructions.

2.3.3. Isolation of membrane vesicles

Confluent SKOV3 cells were cultivated for 24 h in serum-free medium. When indicated, cells were incubated with 10 µM TAPI-0 (Calbiochem) for 16 h. Supernatant was collected and centrifuged, at 4 °C, for 10 min, at 500 × g followed by 20 min at 10,000 × g to remove dead cells and cell debris, respectively. Membrane vesicles were collected by centrifugation at 100,000 × g, for 2 h, at 4 °C.

For sucrose-density fractionation, membrane vesicles resuspended in 0.25 M sucrose were loaded on the top of a step gradient comprising different sucrose concentrations: 2, 1.3, 1.16, 0.8, 0.5, and 0.25 M as previously described (Stoeck *et al*., 2006). The gradients were centrifuged at 100,000 × g for 2.5 h. Twelve 1 ml fractions were collected from the top of the gradient and precipitated with chloroform/methanol (1:4, v/v).

Samples were solubilized in sample buffer with or without β-mercaptoethanol for SDS-PAGE and Western blot analysis.

2.3.4. *In vivo* cleavage assay

HEK293 cells were stably-transfected with pcDNA3-L1 (HEK-L1), and the selected stable cell lines were then transiently-transfected with pcDNA3-ADAM10wt or one of the *N*-glycosylation mutants. MEFs were transiently-double transfected with pcDNA3-L1 and pcDNA3.1-LacZ, pcDNA3-ADAM10wt, or one of the *N*-glycosylation mutants. Forty-eight hours after transfection, supernatant corresponding to a 24 h-production in

serum-depleted medium, was centrifuged at 500 x *g*, 10 min and 10.000 x *g*, 20 min. When indicated, MEFs were incubated with the ADAM17 inhibitor Bristol Meyer Squib (BMS) (kindly provided by Dr. J. Arribas) for 24 h in serum-depleted medium. Cell supernatant was analysed by Western blot.

2.3.5. SDS-PAGE and Western blot analysis

Total protein lysates were obtained by solubilization of centrifuged cells in RIPA buffer (50 mM Tris-HCl pH 7.5, 150 mM NaCl, 0.1% SDS, 1% sodium deoxycholate, 1% Triton X-100, 1:50 complete protease inhibitors cocktail (Roche), for 10 min. Protein was precipitated with ethanol and solubilized in reducing SDS-PAGE sample buffer. Endogenous hADAM10 analysis was performed in non-reducing SDS-PAGE. For SDS-PAGE 7.5% acrylamide gels or pre-casted 4-12% acrylamide Bis-Tris gels (Invitrogen) were used. Western blot was performed using the following primary antibodies: rabbit anti-ADAM10 antibody AB387 (1:1000) raised against amino acids 732-748 of ADAM10 of human origin produced and purified by Davids Biotechnologies, mouse anti-ADAM10 monoclonal antibody MAB1427 (1:1000) (R&D), mouse anti-HA tag 6E2 monoclonal antibody (1:1000) (Cell Signalling), mouse anti-L1 11A (1:3), mouse antihuman CD9 (1:5000), mouse anti-annexin I monoclonal antibody (1:5000) (BD Biosciences), and mouse anti-ubiquitin P4D1 monoclonal antibody (1:1000) (Santa Cruz Biotechnology). Secondary antibodies were sheep anti-mouse IgG coupled to HRP (1:4000) or donkey anti-rabbit IgG coupled to HRP (Amersham) (1:3000). Antibody detection was accomplished with ECL Plus Western Blotting Detection Reagent (GE Healthcare).

2.3.6. Protein deglycosylation

For glycosidase hydrolysis cell lysates (approximately 1×10^6 cells) were incubated with endoglycosidase H (Endo H) (New England Biolabs) and peptide: *N*-glycosidase F (PNGase F) (New England Biolabs or Roche), according to supplier's protocol. Briefly, cell lysates were denatured in glycoprotein denaturing buffer (0.5% SDS with or without 1% β-mercaptoethanol) at 100 °C for 10 min, and incubated with deglycosylation enzyme (PNGase F or Endo H) in the corresponding buffer. Hydrolysis was carried out at 37 °C for 3 h or overnight. The samples were further analyzed by SDS-PAGE and Western blot.

2.3.7. Immunoprecipitation

Exosomes were lysed with BOG buffer (20 mM Tris-HCl pH 8.0, 50 mM β-octylglucopyranoside (BOG), 1 mM phenylmethylsulphonylfluoride (PMSF), 10 mM sodium fluoride, 10 mM sodium orthovanadate, 1:50 complete protease inhibitors cocktail (Roche) for 30 min at 4 °C with occasional vortexing.

Pre-cleared lysates were incubated for 1 h at 4 °C with a rabbit anti-HA.11 polyclonal antibody (Covance) previously coupled to protein A/G Plus agarose beads (Santa Cruz Biotechnologies). Immunoprecipitated proteins were washed three times with BOG buffer and were eluted at 100 °C for 5 min with sample buffer. Samples were analysed by SDS-PAGE and Western blot.

2.3.8. Confocal immunofluorescence microscopy

Cells were grown on glass coverslips until they reached 80% confluence, they were washed with PBS containing 0.5 mM MgCl$_2$, fixed with 4% paraformaldehyde and permeabilized with methanol/acetone (1:1) solution for 10 min at -20 °C. Blocking was done with 1% BSA in PBS for 1 h and primary and secondary antibodies were incubated at room temperature for 2 and 1 h, respectively. Antibody solutions were prepared in blocking solution and washes were performed with PBS. Coverslips were mounted in Airvol and examined on a Leica Confocal (SP2+AOBS) microscope. Primary antibodies were: rabbit anti-HA.11 (1:1000) (Covance), goat IgG anti-calnexin C-20 (1:500) (Santa Cruz), mouse IgG anti-ERGIC53 (1:1000) (Alexis Biochemicals), mouse IgG anti-GM130 (1:200) (BD Biosciences), mouse IgG anti-EEA1 (1:100) (BD Biosciences), and mouse IgG anti-LAMP1 H4A3 (1:100) (BD Biosciences).

Secondary antibodies were: donkey anti-rabbit IgG AlexaFluor 594 (1:500), donkey anti-goat IgG AlexaFluor 488 (1:500), and donkey anti-mouse IgG AlexaFluor 488 (1:500) (Molecular Probes).

For each picture, laser intensities and amplifier gains were adjusted in order to avoid pixel saturation. Each fluorophore used was excited independently and sequential detection was performed. Each picture consisted of a *z*-series of 20 images of 1024-1024 pixel resolution with a pinhole of 1.0 airy unit. Colocalization analysis was performed using the open source Image J version 1.37 (http://rsb.info.nih.gov/ij/).

2.3.9. Peptide cleavage assay

ADAM10-HA immunoprecipitates in 90 µl were incubated with 10 µl (final concentration 50 mM) fluorescent quenching peptide Abz-Leu-Ala-Gln-Ala-Val-Arg-Ser-Ser-Ser-Arg-Dap(dnp)-NH2 (Peptide International, Louisville, Kentucky, USA). Cleavage was followed in a fluorescent plate reader (Fluoroskan Ascent FL Thermo-Electron Corporation) using filters for excitation at 320 nm and emission at 405 nm.

2.3.10. ADAM10 structure

Comparative modelling methods (Sali *et al*., 1993) were used to derive the structure of the metalloprotease domain of bovine ADAM10 on basis of the same domain from human ADAM17, the closest homologue with three-dimensional structure determined (Maskos *et al*., 1998) (PDB code 1BKC). These two domains have 39% identity, which should be enough for deriving a model for ADAM10 with reasonable quality (Sanchez *et al*., 1997).

The program MODELLER (Sali *et al*., 1993) version 7.7 was used in the comparative modelling procedures. Resulting structures were analysed with PROCHECK (Laskowski *et al*., 1993). A large number of models were calculated, and the one having the lowest value of the objective function was selected. Problems on the alignment were corrected and new models were calculated in an iterative manner. A Ramachandran plot analysis of the final model showed it to have 87.0% residues in most favored regions, 12.5% in additional allowed regions and 0.5% (1 residue) in disallowed regions. This residue is Cys 344, which is involved in a disulphide bridge with Cys 451, and corresponds to a cystein residue in the ADAM17

template (Cys 365) that is also located in a disallowed zone of the Ramachandran plot.

2.4. Results

2.4.1. The *N*-glycosylation sites of hADAM10 are occupied

ADAM10 contains four potential *N*-glycosylation sites in the mature form of the protein (Figure 5). Three of these sites are located in the metalloprotease domain: N267, N278 and N439 and one in the disintegrin domain: N551. Endogenous human ADAM10 from SKOV3 ovarian carcinoma cells appeared as a major band with an apparent molecular mass of approximately 68 kDa (Figure 6, A). By enzymatic digestion with Endo H, that removes *N*-linked glycans of the high mannose and hybrid type, we observed that the hADAM10 mature form underwent a downward shift of approximately 5 kDa. On the other hand, hydrolysis with PNGase F, that removes both high mannose, hybrid, and complex type *N*-linked glycans, reduced the molecular mass by 9 kDa to the expected value for the hADAM10 core protein without the prodomain and with no post-translational modifications (59 kDa) (Figure 6, A). These results indicated that ADAM10 contained high mannose as well as complex *N*-glycans.
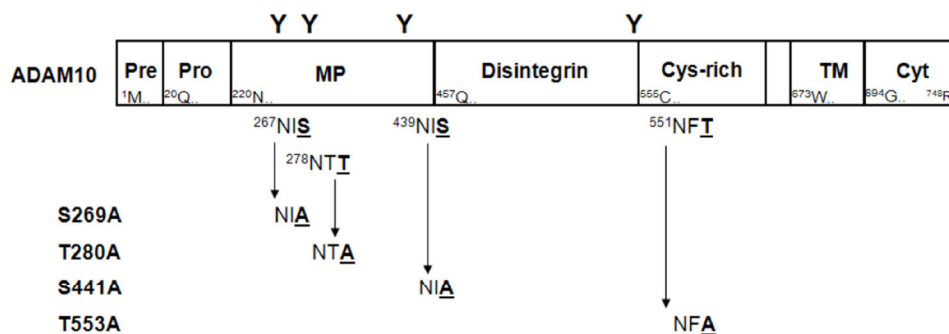
Figure 5. Schematic representation of ADAM10 and *N*-glycosylation mutants.
Signal peptide-Pre; prodomain-Pro; metalloprotease domain-MP; disintegrin domain-Disintegrin; cystein-rich region-Cys-rich; transmembrane region-TM and cytoplasmic tail-Cyt. The four potential *N*-glycosylation sites (Y) are located in the MP (N267, N278, and N439), and in the disintegrin domain (N551). ADAM10 *N*-glycosylation mutants were created by mutating the Ser or Thr residues from the *N*-glycosylation sites (N-X-S/T) to Ala residues.

To investigate the functional role played by the *N*-linked glycans, each potential *N*-glycosylation site was mutated. We used HA-tagged bovine ADAM10, which shares high homology with human ADAM10 protein sequence (97%), since several attempts to mutate the *N*-glycosylation sites of hADAM10 were not successful. Serine or threonine residues of each bADAM10 *N*-glycosylation site (N-X-T/S) were replaced by alanine, creating four bADAM10 *N*-glycosylation mutants: S269A, T280A, S441A, and T553A (Figure 5).

SKOV3 ovarian cancer cells were stably-transfected with the pcDNA3 vector coding for bADAM10wt or S269A, T280A, S441A, and T553A mutants. Stable cell lines were established and recombinant protein expression was analysed by SDS-PAGE and Western blot, using a mouse anti-HA tag antibody (Figure 6, B). All mutants were detected at lower molecular masses than the wild-type form, which indicated that all *N*-glycosylation sites were occupied. Most striking was the observation that

mutant T280A accumulated as the precursor format approximately 100 kDa, the mature form being detected at very low levels, which indicated that *N*-linked glycans from N278 were required for bADAM10 processing. Mutant S441A underwent proteolysis with an abundant cleavage product at 52 kDa. Therefore, the *N*-linked glycans from N439 protected bADAM10 from proteolysis. The highest shift was observed for T553A, which suggested that this site contained complex glycans, whereas the others contained high mannose glycans.

To investigate the type of glycans present in each *N*-glycosylation site, Endo H and PNGase F digestion of bADAM10wt and mutants was performed (Figure 6, C). Forms containing only high mannose glycans exhibited similar shifts in SDS-PAGE after deglycosylation with each of the enzymes, whereas forms containing high mannose and complex glycans exhibited higher shifts after PNGase F than after Endo H deglycosylation. In view of this, it was concluded that the mature form of bADAM10wt contained high mannose and complex glycans similarly to endogenous hADAM10. The precursor form of bADAM10wt contained high mannose and complex glycans, which indicated that it was transported beyond the ER to the Golgi, where it is known to be processed. On the other hand, precursor T280A contained only high mannose glycans suggesting that it probably accumulated in the ER. Mature S441A and T553A only contained high mannose *N*-glycans, which suggested that either N439 or N551 could contain complex *N*-glycans.
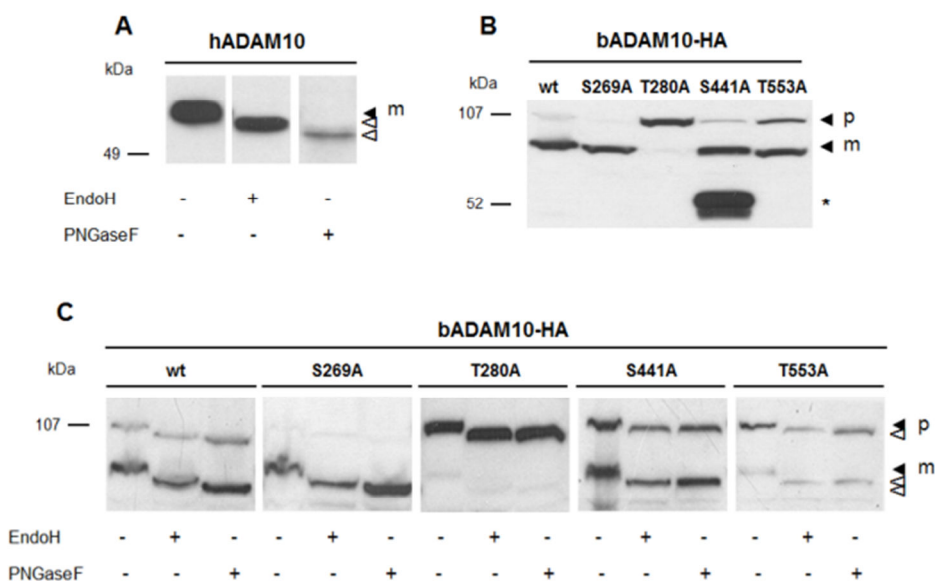
Figure 6. Western blot analysis of ADAM10 and *N*-glycosylation mutants from SKOV3 cells. (A) Deglycosylation of endogenous hADAM10 (1×10^6 cells/lane) with Endo H and PNGase F. Analysis was performed under non-reducing conditions using a mouse anti-ADAM10 antibody MAB1427. (B) Analysis of cells stably transfected with either bADAM10wt or *N*-glycosylation mutants under reducing conditions using a mouse anti-HA tag antibody. (C) Deglycosylation of bADAM10wt and bADAM10 *N*-glycosylation mutants with Endo H and PNGase F. Precursor (p) or mature (m) ADAM10 are indicated with closed arrowheads. Corresponding deglycosylated bands are shown with open arrowheads and the asterisk indicates bADAM10 cleavage product.

2.4.2. Intracellular localization of bADAM10 *N*-glycosylation mutants

In agreement with previous reports (Dallas *et al*., 1999; Reiss *et al*., 2005), the analysis of the localization of endogenous hADAM10 by confocal microscopy of SKOV3 ovarian carcinoma cells showed predominant localization of the protein at the perinuclear region and at the cell surface

where it appeared as punctuated dots evenly distributed at the plasma membrane (results not shown).

Since it has been reported that removal of *N*-glycosylation sites from proteins can affect protein transport and intracellular localization (Martina *et al*., 1998), bADAM10wt and mutants were colocalized with markers of the secretory pathway using confocal immunofluorescence microscopy. The markers used were: endoplasmic reticulum (ER) - calnexin, ER - Golgi intermediate compartment (ERGIC) - ERGIC53, Golgi - GM130, early endosomal antigen-1 - EEA1, and late endosome/lysosome-associated membrane protein 1 - LAMP1 (Figure 7).

Bovine ADAM10wt colocalized with the EEA1 marker (Figure 7, D), which indicated that it was present in the endosomes. Low levels of protein were also found to colocalize with calnexin (Figure 7, A), and to a lower extent with GM130 (Figure 7, C) and ERGIC53 (Figure 7, B), probably corresponding to protein in traffick through the ER, Golgi and ERGIC. No colocalization with LAMP1 was observed (Figure 7, E). All mutants, with the exception of T280A, showed a similar staining profile (results not shown). T280A mutant showed higher colocalization with calnexin (Figure 7, F). These results showed that this mutant was retained in the ER and agreed with T280A precursor accumulation and its sensitivity to both Endo H and PNGase F.

Moreover, membrane protein biotinylation confirmed that most mature hADAM10 and bADAM10wt mature forms were localized at the plasma membrane. All *N*-glycosylation mutants showed comparable expression levels, at the cell surface, compared with bADAM10wt, with the exception of T280A that was almost undetectable (results not shown).
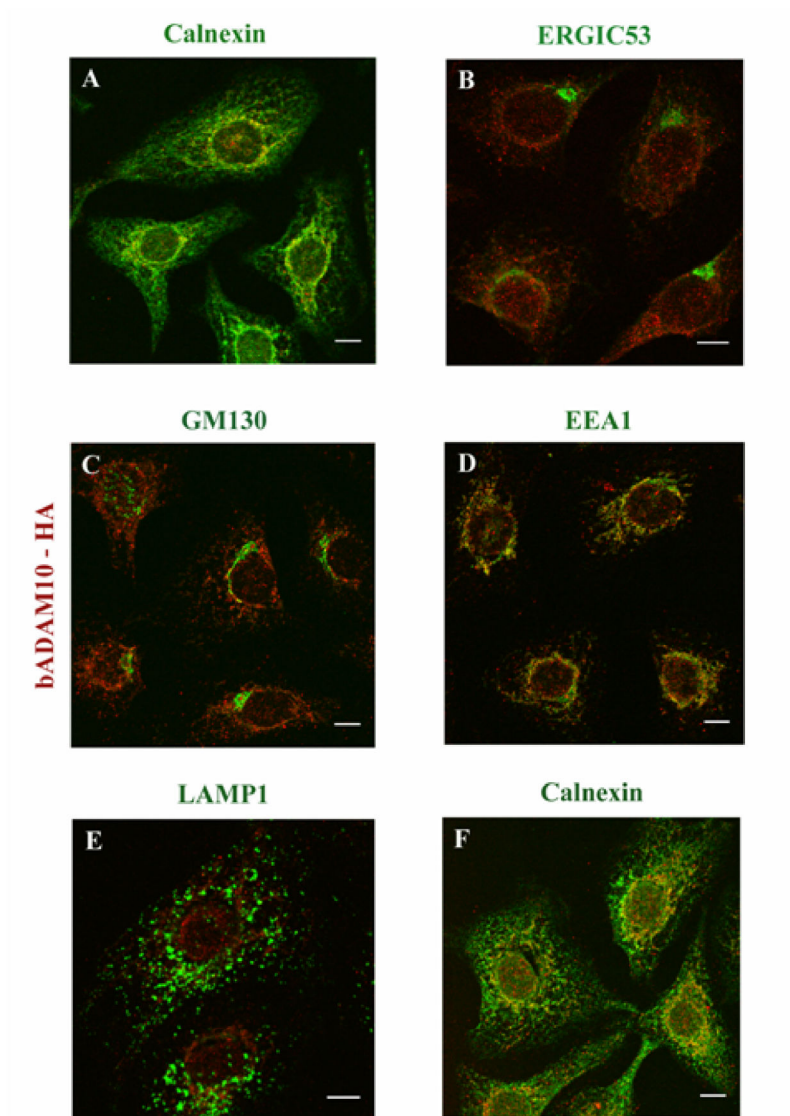
Figure 7. Colocalization of bADAM10wt and T280A mutant, with markers of the secretory pathway by confocal immunofluorescence microscopy. SKOV3 cells stably-transfected with bADAM10wt (red) were fixed in 1:1 methanol/acetone and double labelled with rabbit anti-HA tag antibody and one of the following markers (green): (A) goat anti-calnexin; (B) mouse anti-ERGIC53; (C) mouse anti-GM130; (D) mouse anti-EEA1 or (E) mouse anti-LAMP1. (F) T280A mutant (red) was double labelled with rabbit anti-HA tag antibody and goat anti-calnexin (green). Secondary antibodies were donkey anti-rabbit IgG AlexaFluor 594, donkey anti-mouse IgG AlexaFluor 488 and donkey anti-goat IgG AlexaFluor 488. Scale bars, 10 μm.

2.4.3. *In vivo* and *in vitro* activity of bADAM10wt and *N*-glycosylation mutants

The shedding activity of bADAM10wt and glycosylation mutants towards the L1 cell adhesion molecule was investigated. L1 is a 220 kDa type I membrane glycoprotein of the immunoglobulin family that is overexpressed in many human tumour cell lines, such as neuroblastomas, melanomas (Fogel *et al*., 2003), colon (Gavert *et al*., 2005), and ovarian carcinomas (Fogel *et al*., 2003), as well as in neural, hematopoietic, and certain epithelial cells. L1 cleavage by ADAM10 occurs in intracellular compartments, predominantly at the plasma membrane, and exosomes, and results in two distinct fragments: a fragment of approximately 32 kDa that remains attached to the cell membrane and a soluble fragment of approximately 200 kDa that is released and can be detected in the supernatant.

HEK293 cells were selected for this study since they show low expression levels of endogenous hADAM10 and L1, and almost no L1 shedding (Figure 8, Ctr). Therefore, HEK293 cells were stably transfected with pcDNA3-L1 (HEK-L1), and the selected stable cell lines were then transiently transfected with bADAM10wt and glycosylation mutants. Forty eight hours after transfection, L1 from the cell supernatants corresponding to a 24 h-production in serum depleted medium, was analyzed by Western blot and a representative blot is shown (Figure 8, upper panel). As controls L1 and bADAM10 from the corresponding cell extracts were also analyzed by Western blot. Mature full-length L1 probably at the plasma membrane was detected (Figure 8, middle panel). Bovine ADAM10wt and mutants were detected as mature form and precursor (Figure 8, lower panel). Mutant T280A exhibited very low levels of mature form.

Transient overexpression of bADAM10wt in cells stably-overexpressing L1 led to the detection of a higher level of shed L1 to the supernatant (Figure 8). Mutation of N278 caused a decrease in the amount of shed L1 to almost undetectable levels. Transfection with the other mutants did not completely abolish the production of soluble L1, however, the levels appeared to decrease.
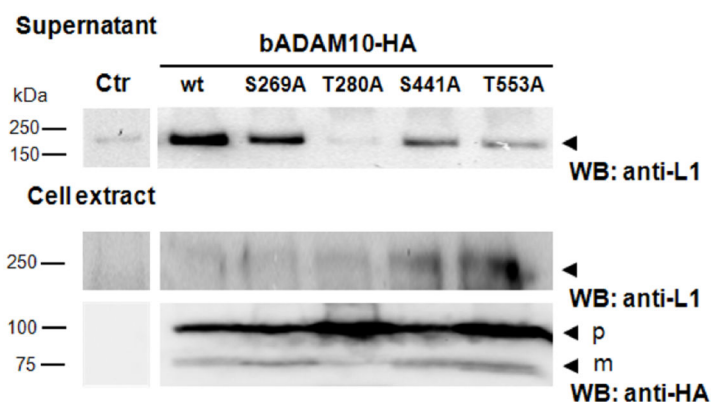
Figure 8. L1 cleavage by bADAM10wt and *N*-glycosylation mutants in HEK293 cells. HEK293-L1 cells were co-transfected with bADAM10wt or each of the *N*-glycosylation mutants. Cell supernatants were analyzed by Western blot using a mouse anti-L1 11A antibody to detect cleaved L1. Results shown are from a representative blot from two independent experiments done in duplicate. Controls for corresponding full-length L1 and bADAM10 are shown in middle and lower panels, respectively.

The effect of ADAM10 *N*-glycosylation mutations in L1 protein cleavage, *in vivo*, was also investigated in primary mouse embryonic fibroblasts knockout for ADAM10 (ADAM10$^{-/-}$ MEFs) (Hartmann *et al*., 2002). These cells are Simian virus large T antigen (SV-T)-immortalized and derive from ADAM10-deficient mice. As a positive control we used ADAM10$^{+/+}$ MEFs that express endogenous ADAM10 (Figure 9, A).

MEFs were transiently-double transfected with pcDNA3-L1 and the empty vector pcNA3.1-LacZ, bADAM10wt, or one of the *N*-glycosylation mutants. Forty-eight hours after transfection, the supernatant corresponding to a 24 h-production in serum-depleted medium, was collected and analysed by Western blot (Figure 9, B). As controls L1 and bADAM10 from the corresponding cell extracts were also analyzed by Western blot (Figure 9, B).

Figure 9. L1 cleavage in ADAM10$^{-/-}$ MEFs transiently overexpressing pcDNA3-L1 and pcDNA3.1-LacZ, bADAM10wt or each of the *N*-glycosylation mutants. (A) Analysis of endogenous mADAM10 protein in ADAM10$^{-/-}$ and ADAM10$^{+/+}$ MEFs using the polyclonal antibody rabbit anti mouse ADAM10 AB387. (B) L1 cleavage in MEFs in the absence or presence of 5 µM of the ADAM17 inhibitor, BMS. MEFs supernatants were analyzed by Western blot using a mouse anti-L1 11A antibody to detect cleaved L1. Controls for corresponding full-length L1 and bADAM10 are shown in middle and lower panels, respectively.

Although, L1 cleavage levels in ADAM10$^{-/-}$ MEFs were lower than in ADAM10$^{+/+}$ MEFs, the production of soluble L1 was not completely abolished (Figure 9, B). It has been described that in wt MEFs two ADAM protein family members can cleave L1: while ADAM10 cleaves L1 constitutively, ADAM17 needs to be induced by phorbol-12-myristate-13-acetate (PMA) or methyl-β-cyclodextrin (MCD) (Maretzy *et al*., 2005). Nevertheless, it is possible that in absence of ADAM10, ADAM17 can compensate and contribute to the constitutive L1 cleavage.

Since there was still cleavage of L1 in ADAM10$^{-/-}$ MEFs, that could possibly be attributed to ADAM17 (Gutwein *et al*., 2005; Maretzky *et al*., 2005), L1 cleavage assay was done in the presence of 5 μM ADAM17 inhibitor - BMS. After incubation with BMS a decrease in L1 cleavage levels was observed both for ADAM10$^{-/-}$ and ADAM10$^{+/+}$ MEFS. In addition, in agreement with the results obtained above using HEK293 cells (Figure 8), mutation of N278 caused a decrease in the amount of shed L1 (Figure 9, B).

Since the *in vivo* activity is influenced by the catalytic activity of ADAM10 as well as its intracellular localization, we determined the proteolytic activity using a cell-free assay for mutants T280A and S269A that had the highest and the lowest alterations of *in vivo* activity, respectively. HEK293 cells were transiently doubly-transfected with bADAM10wt or with S269A and T280A mutants solubilized in lysis buffer and subjected to immunoprecipitation with anti-HA antibody to isolate the proteins. After washing, the precipitated proteins were incubated with the fluorescent quenching peptide Abz-Leu-Ala-Gln-Ala-Val-Arg-Ser-Ser-Ser-Arg-Dap(dnp)-NH2 containing the ADAM cleavage site of TNF-alpha.

Bovine ADAM10wt and glycosylation mutant forms were efficiently purified from cell lysates of HEK293 cells and were able to cleave the TNF-alpha peptide in a time dependent fashion. A reduced cleavage of the peptide to approximately 60% of the value obtained for bADAM10wt was

found for S269A (Figure 10). On the other hand, a reduction to 28% was observed for the T280A mutant, which could be due to an inactivating effect or to the lower level of mature form. Due to double transient transfection, high levels of precursor were detected, which most likely did not contribute to cleavage since to this date no proteolytic activity has been described for the precursor form, and only minor amounts of mature ADAM10 were detected. Similar results were obtained when the proteins were expressed in SKOV3 cells (data not shown). In transient transfections ADAM17 also accumulates as the pro-form in the early secretory pathway, while little or no processed form can be detected (reviewed in Arribas *et al*, 2005). These results corroborated the findings of the *in vivo* L1 cleavage assay.

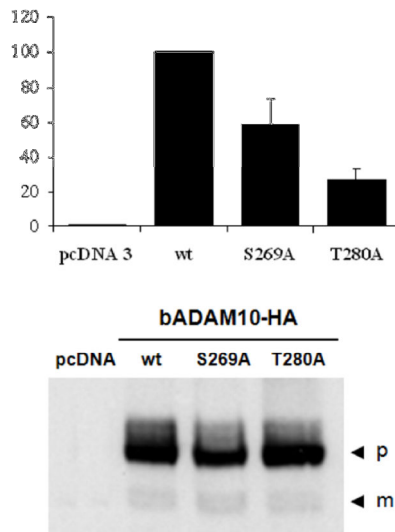**Figure 10. Measurement of the proteolytic activity of bADAM10wt and S269A, T280A *N*-glycosylation mutants using a fluorescent TNF-alpha peptide cleavage assay.** The analysis was carried out in triplicate. Data are represented as mean values ± SD. Transfection efficiency was monitored by Western blot using a mouse anti-HA tag antibody (lower panel). Precursor (p) or mature (m) bADAM10 are indicated with closed arrowheads.

2.4.4. Characterization of ADAM10 from exosomes

ADAM10 has been found in exosomes, where it promotes the shedding of several substrates, such as L1 and CD44 (Gutwein *et al*., 2003; Stoeck *et al*., 2006). To investigate if glycosylation would play a role in glycoprotein sorting to exosomes, endogenous hADAM10 from cell extracts and exosomes was analysed by SDS-PAGE and Western blot, and further digested with Endo H and PNGase F (Figure 11 A, B).

Exosomes were collected in the pellet after ultracentrifugation of cleared supernatants from SKOV3 cells followed by sucrose-density fractionation as previously described (Stoeck *et al*., 2006). Since hADAM10 was only detected in fractions that are positive for the exosomal marker CD9 (Figure 11, A), the remaining studies were performed using exosomes obtained after ultracentrifugation without further fractionation.

Endogenous human ADAM10 from the exosomes appeared as a double band, the lighter one co-migrating with that from the cell extract (see Figure 11, A). The heavier band was resistant to digestion with Endo H but sensitive to PNGase F whereas the lighter band was sensitive to both Endo H and PNGase F (Figure 11, B). The products of digestion with PNGase F also resulted in a double band. These results suggested that the heavier band contained complex glycans, whereas the lighter band contained both high mannose and complex glycans similarly to hADAM10 from the cell extract. The presence of two bands after PNGase F digestion indicated an additional post-translational modification for the heavier band or proteolytic degradation.

On the other hand, a proteolytic product of hADAM10 was detected in exosomes but not in the cellular extract. Further experiments showed that such proteolysis was catalyzed by a metalloprotease since it was prevented when the cells were incubated with TAPI-0, a metalloprotease inhibitor (Mohler *et al*., 1994) (Figure 11, C, upper panel). As control for the

presence of exosomes the same blot was probed with anti-annexin I, an exosomal marker (Figure 11, C, lower panel).
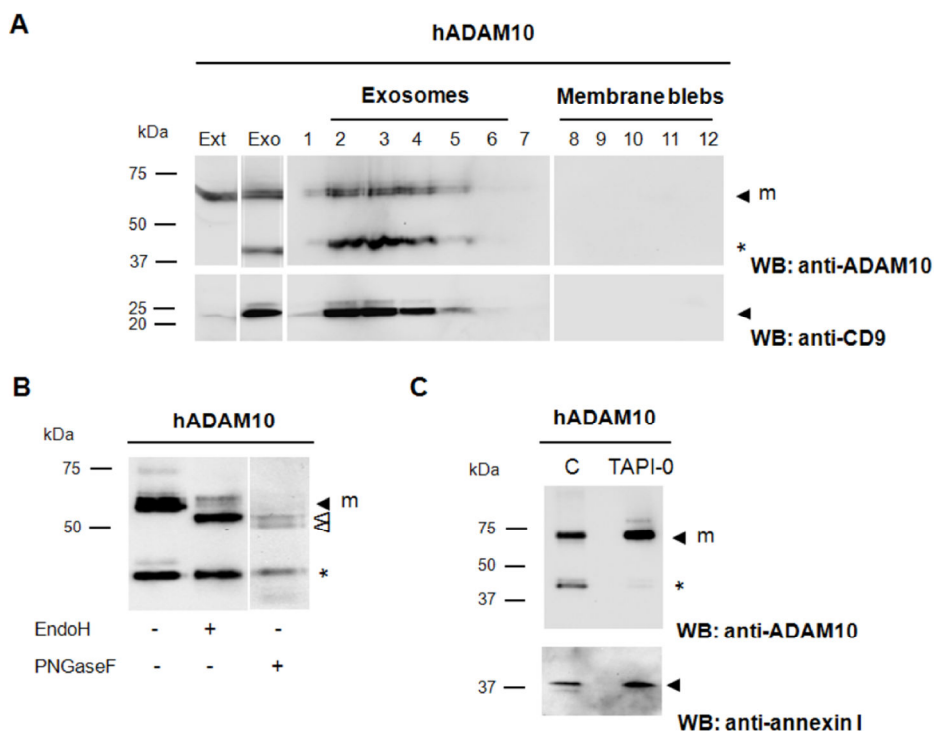

Figure 11. Western blot analysis of endogenous hADAM10 from SKOV3 cell extracts and exosomes. (A) Total protein from cell extracts (Ext; $1x10^6$ cells/lane), exosomes (Exo; $1.5x10^7$ cells), and exosomes fractionated by centrifugation in sucrose gradient, were analysed under non-reducing conditions using the mouse anti-ADAM10 antibody MAB1427. Exosomal marker CD9 was detected as a control using a different concentration gel. (B) Deglycosylation of hADAM10, from exosomes obtained after ultracentrifugation, with Endo H and PNGase F. (C) Exosomes were incubated for 16 h with the metalloprotease inhibitor TAPI-0. Annexin I, an exosomal marker was detected as an input control. Precursor (p) or mature (m) ADAM10 are indicated with closed arrowheads. Corresponding deglycosylated bands are shown with open arrowheads and asterisk indicates ADAM10 cleavage product.

For comparison, recombinant bADAM10wt and mutants overexpressed in SKOV3 cells were analysed (Figure 12, A). Precursor T280A was not found in the exosomes, which is in agreement with the previous results indicating that it is retained in the ER. Mature forms of bADAM10wt, S269A, S441A, and T553A were found in the exosomes, however, they were not detected as a double band, contrary to endogenous hADAM10, probably due to the low levels of bADAM10 expression. In addition, they all migrated at a slightly higher molecular mass than their cellular counterparts. The increased mass estimation could be due to post-translational modifications, such as *N*-glycosylation or ubiquitination. Immunoprecipitation of bADAM10wt followed by Western blot analysis using an anti-ubiquitin antibody allowed the identification of three bands (Figure 12, B). The heavier band co-migrated with the mature form of bADAM10wt, therefore suggesting that it was ubiquitinated. The other two bands possibly corresponded to other ubiquitinated proteins that may interact with bADAM10wt. As controls total cellular and exosomal proteins were also analysed (Figure 12, B). Exosomal proteins were heavily ubiquitinated in comparison with cellular proteins. High proteolytic activity from the exosomes hindered PNGase F digestion analysis.

Proteolytic cleavage also occurred for exosomal bADAM10wt and mutants similarly to endogenous hADAM10. This cleavage was particularly evident for mutant S441A. These results further support the importance of the *N*-linked glycans from N439 to protect the protein against proteolysis. Deglycosylation of exosomal bADAM10 remained inconclusive due to high level of protein degradation.

Detection of CD9, an exosomal marker, revealed no differences in the amount of secreted vesicles produced in all the four *N*-glycosylation mutants when compared with the bADAM10wt (results not shown).
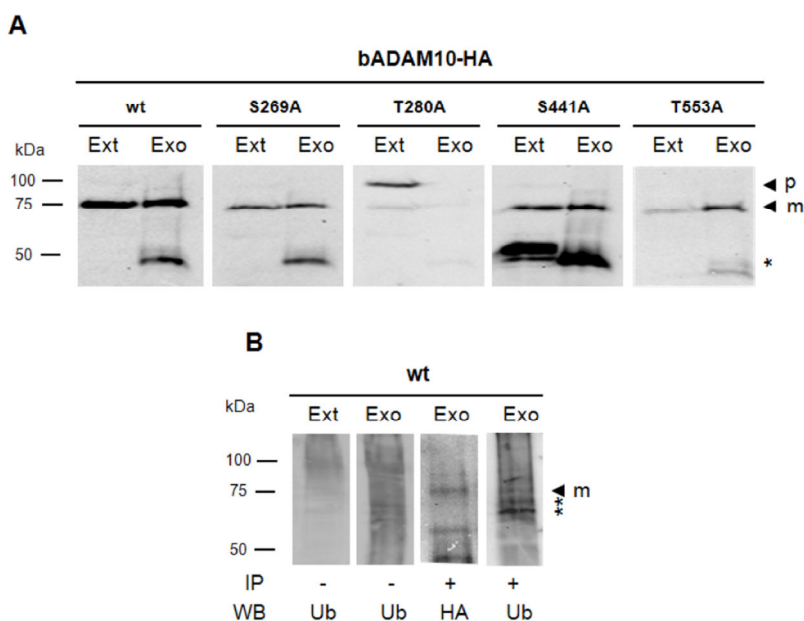
Figure 12. Western blot analysis of bADAM10wt and *N*-glycosylation mutants from stably transfected SKOV3 cells. (A) Total protein from cell extracts (Ext; 1×10^6 cells/lane) and exosomes (Exo; 1.5×10^7 cells) were analysed using a mouse anti-HA tag antibody. Precursor (p) or mature (m) bADAM10 are indicated with closed arrowheads and asterisk indicates bADAM10 cleavage product. (B) Protein ubiquitination of cell extract (100 µg total protein), corresponding exosomes (70 µg total protein) and immunoprecipitated exosomal bADAM10wt. Analysis was performed using mouse anti-Ubiquitin P4D1 (Ub) and mouse anti-HA tag antibodies (HA). Mature (m) bADAM10 is indicated with closed arrowhead and asterisk indicates ubiquitinated proteins that interact with bADAM10.

2.4.5. Modelling of the 3D structure of bADAM10 metalloprotease domain

A model of bADAM10 metalloprotease domain based on its homology with ADAM17 (39% identity) was constructed to investigate the structural basis for the decreased *in vitro* activity of S269A, the absence of T280A processing and the susceptibility of S441A to proteolytic

degradation, as well as significantly decreased *in vivo* activities of T280A and S441A (Figure 13). Both N267 and N278 glycosylation sites are located in exposed zones before and after beta-strands, respectively, in loop regions as expected. The N267 residue has one glycosylation counterpart in ADAM17 (N264) in a spatially related region (not sequence related). The N278 has no counterpart on ADAM17. Surprisingly, the N439 glycosylation site is located inside an alpha-helix. In a related spatial zone in ADAM17, there is potential glycosylation site N452, which is, however, located at the beginning of the helix and not inside it as in the case of ADAM10.
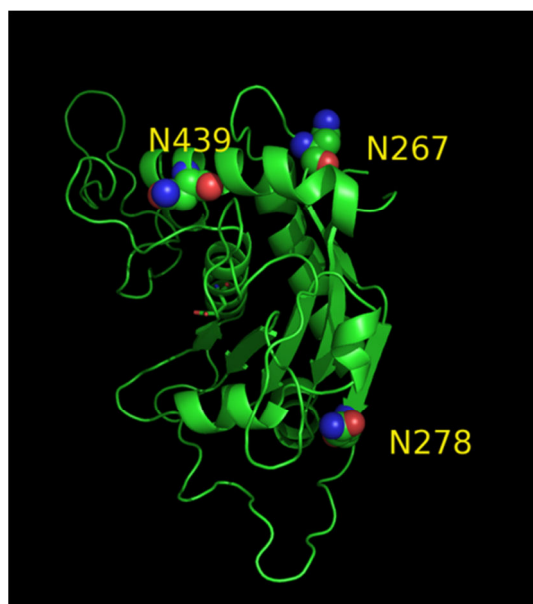

Figure 13. Representation of the three-dimensional model for bADAM10 metalloprotease domain, rendered using cartoons. The potential *N*-glycosylation residues are highlighted using CPK models and labelled. Figure produced using PyMol (DeLano, Palo Alto, 2002).

2.5. Discussion

Glycosylation is an important post-translational modification that plays an important role in a number of physiological and biochemical properties of a glycoprotein including stability, folding, intracellular trafficking, or activity (Helenius *et al*., 2003). However, *N*-linked glycosylation does not occur at every potential site and the role played by glycosylation in different proteins is highly variable and depends on the individual protein.

ADAM10 is a glycoprotein with four potential *N*-glycosylation sites: N267, N278, N439, and N551 but the functional role of ADAM10 *N*-glycosylation is unknown. To investigate if *N*-glycosylation has any role on ADAM10 processing, stability, activity, and intracellular localization, the four potential sites were mutated and characterized individually.

Our results showed that all four bADAM10 *N*-glycosylation sites were occupied with high mannose or complex glycans. Moreover, the mutation of a single *N*-glycosylation consensus sequence at N278 profoundly affected the efficient processing and trafficking of bADAM10. It is well known that the interaction of glycoproteins with the lectin chaperones from the ER, calnexin or calreticulin, is required for their correct folding, reviewed in (Helenius *et al*., 2003; Morais *et al*., 2003). The time that a certain glycoprotein remains in the calnexin/calreticulin folding cycle in the ER depends on the protein, and it can vary from minutes to hours. If glycoproteins fail to attain the correct fold, they can either be accumulated in the ER as aggregates, be translocated to the cytosolic face of the ER and be degraded by the proteasome, or they can be transported to the Golgi apparatus and divert to the lysosome where they are degraded (Helenius *et al*., 2003;Trombeta *et al*., 2003). Our results suggest that the *N*-linked glycans from N278 are important for the folding of the protein

probably mediating the interaction with calnexin. In the absence of this folding step ADAM10 would fail to attain its final conformation and would be retained in the ER. As a consequence the protein would remain as an inactive precursor protein not only because of impaired folding but also because further proteolytic processing to the mature form, which takes place in the Golgi, would not occur due to compartmentalization constraints. In agreement, T280A mutant showed reduced levels of activity both *in vivo* and *in vitro*. Since only the ADAM10 mature form is active (Schlondorff and Blobel, 1999; Seals and Courtneidge, 2003) the residual activity observed for this mutant is the result of the small amount of detected mature form. The 3D-model of ADAM10 metalloprotease domain, built using comparative modelling techniques based on the 3D structure of ADAM17, showed that the N278 site is located in an exposed zone and, therefore, has a good possibility of being occupied, which agrees with the experimental results. In addition, results obtained by other authors supported that ADAM10 N278 site is occupied in human platelets (Lewandrowski *et al*., 2006). Therefore, the *N*-linked glycans probably mediate interaction with calnexin.

Mutation of the N439 glycosylation site resulted in increased susceptibility of bADAM10 to proteases. The 3D model of ADAM10 showed that N439 was found in an alpha-helix, which is a rare event but has a probability of occurring of 10.5% (Petrescu *et al*., 2004) that is a non-negligible value. Therefore, mutation of this site probably induced a conformation alteration that exposed a particular region susceptible to protease degradation. Furthermore, since N439, as well as N267, are not located near the active site of ADAM10 from the 3D model, it is probable that mutating them did not have a direct effect on substrate binding, and therefore would not abolish enzyme activity, but could cause alterations in protein conformation, explaining the decreased activities. Changes in conformation caused by mutation of glycosylation sites with consequences

for activity have been described for other proteins, for example, the Kv3.1 voltage-gated K+ channel (Brooks *et al*., 2006) or the GABA-transporter 1 (Cai *et al*., 2005).

N551 is located at the end of the disintegrin domain, juxtaposed to the Cys-rich domain. These domains have been described as mediators of protein-protein interactions and regulators of ADAM protease specificity (White, 2003). Furthermore, Janes *et al*. showed that the cystein-rich domain is the major responsible for substrate recognition and binding of the EphA3/ephrin complex (Janes *et al*., 2005). Even if the analysis of the crystallographic structure of the bADAM10 disintegrin and cystein-rich domains (PDB: 2ao7) showed that N551 is located away from the identified substrate recognition site, it is possible that mutating this site caused conformational changes of these domains leading to decreased substrate recognition specificities. This could explain the decreased *in vivo* activity of T553A.

Signals responsible for the sorting of proteins into vesicles to be released as exosomes, within MVBs are still being elucidated. Mono-ubiquitination of plasma membrane proteins acts as a signal for endocytosis and targeting to the endosomes. Furthermore, the sequestration of transmembrane proteins in exosomes could require (mono)-ubiquitination and the ESCRT-I, -II and -III protein complexes (reviewed in Keller *et al*., 2006; van Niel *et al*., 2006). Accordingly, in the present work, a comparatively higher amount of ubiquitinated proteins was found in the exosomes, and in particular, recombinant exosomal bADAM10 appeared to be ubiquitinated. Concerning endogenous exosomal hADAM10, a fraction of the protein was detected at a higher molecular mass, which could be explained by ubiquitination or another post-translational modification. In addition, this fraction exclusively presented complex *N*-glycans differently from total cellular hADAM10, which contained a mixture of complex and high mannose oligosaccharides.

Several possibilities can be admitted to explain this finding: i) more complex type glycoforms of hADAM10 are preferentially enriched during sorting and trafficking from the plasma membrane to the MVBs; ii) preferential enrichment of complex type glycoforms occurs during glycoprotein sorting into the exosomes; iii) increased proteolysis of less processed glycoforms occurs in the exosomes, thus revealing more processed glycoforms. Further experiments are required to clarify this matter, however, the low amounts of protein makes it a difficult task.

An ADAM10 cleavage product was specifically found in exosomes and it was identified as being the result of metalloprotease cleavage. It is possible that the ADAM10 and the unidentified metalloprotease are specifically sorted into the exosomes and only get in contact there.

In conclusion, the work described here provides evidence for the functional role of *N*-glycans from each of the *N*-glycosylation sites from ADAM10. They are required for the processing and activation of the enzyme, to protect the protein from proteolytic degradation, and, finally, they are required for full-enzyme activity.

2.6. Acknowledgements

CE had a Ph.D. fellowship from Fundação para a Ciência e a Tecnologia, Portugal.

Chapter 3

Interaction and uptake of exosomes by ovarian carcinoma cells

Work presented in this chapter corresponds to the following manuscript:

Escrevente C, Keller S, Altevogt P, Costa J (2011). Interaction and uptake of exosomes by ovarian carcinoma cells. *BMC Cancer*. 11:108.

3. Interaction and uptake of exosomes by ovarian carcinoma cells

3.1. Summary

Exosomes consist of membrane vesicles that are secreted by several cell types, including tumours and have been found in biological fluids. Exosomes interact with other cells and may serve as vehicles for the transfer of protein and RNA among cells.

SKOV3 exosomes were labelled with carboxyfluoresceine diacetate succinimidyl-ester and collected by ultracentrifugation. Uptake of these vesicles, under different conditions, by the same cells from where they originated was monitored by immunofluorescence microscopy and flow cytometry analysis. Lectin analysis was performed to investigate the glycosylation properties of proteins from exosomes and cellular extracts.

In this work, the ovarian carcinoma SKOV3 cell line has been shown to internalize exosomes from the same cells via several endocytic pathways that were strongly inhibited at 4 ºC, indicating their energy dependence. Partial colocalization with the endosome marker EEA1 and inhibition by chlorpromazine suggested the involvement of clathrin-dependent endocytosis. Furthermore, uptake inhibition in the presence of 5-ethyl-*N*-isopropyl amiloride, cytochalasin D and methyl-beta-cyclodextrin suggested the involvement of additional endocytic pathways. The uptake required proteins from the exosomes and from the cells since it was inhibited after proteinase K treatments. The exosomes were found to be enriched in specific mannose- and sialic acid-containing glycoproteins. Sialic acid removal caused a small but non-significant increase in uptake.

Furthermore, the monosaccharides D-galactose, α-L-fucose, α-D-mannose, D-*N*-acetylglucosamine and the disaccharide β-lactose reduced exosomes uptake to a comparable extent as the control D-glucose.

In conclusion, exosomes are internalized by ovarian tumour cells via various endocytic pathways and proteins from exosomes and cells are required for uptake. On the other hand, exosomes are enriched in specific glycoproteins that may constitute exosome markers. This work contributes to the knowledge about the properties and dynamics of exosomes in cancer.

3.2. Introduction

Exosomes are small membrane vesicles between 40-100 nm in diameter that are secreted by various cell types, including tumour cells, neurons, B- and T-lymphocytes, intestinal epithelial cells (Denzer *et al*., 2000; Keller *et al*., 2006; Simpson *et al*., 2009), and in physiological fluids (Simpson *et al*., 2009; van Niel *et al*., 2006).

Exosome biogenesis involves the inward budding of endosomes into MVBs to form intraluminal vesicles that are then released to the extracellular space. During this process transmembrane proteins are incorporated into the invaginating membrane maintaining the same topological orientation as the plasma membrane, while cytosolic components are engulfed.

The molecular basis of protein sorting during exosome formation appears to involve an ubiquitin-dependent mechanism and the endosomal sorting complexes required for transport - ESCRT (Katzmman *et al*., 2001; Lakkaraju and Rodriguez-Boulan, 2008). However, some proteins present in the exosomes are not ubiquitinated, suggesting that other mechanisms such as oligomerization or partitioning of protein into lipid raft domains may be involved (Lakkaraju and Rodriguez-Boulan, 2008; de Gassart *et al*., 2003; Schorey and Bhatnagar, 2008; Trajkovic *et al*., 2008).

Exosomes are released by MVBs fusion with the plasma membrane and the mechanism appears to involve Rab27A and Rab27B (Ostrowski *et al*., 2010). Recent studies have suggested their participation in different physiological and/or pathological processes such as tumour progression, stimulation of the immune system, coagulation and inflammation, and intercellular transfer of infectious agents, such as proteins and RNA (van Niel *et al*., 2006; Lakkaraju and Rodriguez-Boulan, 2008; Schorey and Bhatnagar, 2008).

Many of the functions described for exosomes depend on their ability to specifically interact with a target cell and several types of interaction have already been proposed based on indirect evidence and *in vitro* studies. Exosomes can associate with the plasma membrane through ligand-receptor interactions (Théry *et al*., 2009) or lipids, such as phosphatidylserine (Keller *et al*., 2009). The process of internalization can occur through direct fusion of the exosomes with the plasma membrane, leading to the release of the exosomal content into the cell cytoplasm. Alternatively, exosomes can enter the cells by receptor-mediated endocytosis and later fuse with the limiting membrane of the endosome releasing the exosomal content to be recycled to the cell surface or to be degraded in the lysosome (Théry *et al*., 2009; Cocucci *et al*., 2009). Exosome uptake was shown to occur via clathrin-mediated endocytosis in dendritic cells (Morelli *et al*., 2004), as well as phagocytosis in monocytes and macrophages (Feng *et al*., 2010).

Exosomes have a unique protein and lipid composition that varies depending on the cells from which they originate. Nevertheless, as a consequence of their endosomal origin nearly all exosomes contain proteins involved in membrane transport and fusion (RabGTPases, annexins, flotilin), in MVBs biogenesis (TSG101, Alix), heat shock proteins (Hsc70, Hsc90), integrins, and tetraspanins (CD9, CD63, CD81, CD82) (Simons and Raposo, 2009; Stoorvogel *et al*., 2002). In addition, they are enriched in raft-lipids such as cholesterol, sphingolipids, and ceramide. In exosomes, an enrichment of certain glycosylated motifs has also been observed (Krishnamoorthy *et al*., 2009).

Glycosylation is a post-translational modification that plays an important role in several properties of proteins including stability, folding, intracellular trafficking, and recognition. Lectins and their interactions with carbohydrates have been found to play a role in exosome uptake by dendritic cells (Hao *et al*., 2007) and macrophages (Barres *et al*., 2010).

In the present work, the SKOV3 ovarian carcinoma cell line has been shown to internalize exosomes derived from the same cells via various endocytic pathways. Proteins from exosomes and from cells were required for the uptake. On the other hand, exosomes were highly enriched in specific glycosylated sialic acid- and mannose-containing glycoproteins, and sialic acid removal caused a small though non-significant increase in uptake.

3.3. Materials and methods

3.3.1. Cell culture

Human ovarian cancer SKOV3, embryonic kidney HEK293, and neuroglioma H4 cell lines were grown in DMEM (Sigma) at 37 °C, 5% CO_2 supplemented with 10% fetal calf serum (Gibco), 1% penicillin/streptomycin solution (Gibco).

3.3.2. Isolation of secreted membrane vesicles

Confluent SKOV3, HEK293 and H4 cells were cultivated for 24 h in serum-free medium. The supernatant was collected and centrifuged, at 500, 10,000 and 100,000 x *g* 10, 20 and 120 min, respectively, at 4 °C. The pellet of the last centrifugation consisted of secreted membrane vesicles. Sucrose-density fractionation was performed as described previously (Stoeck *et al*., 2006).

3.3.3. Glycoprotein detection using lectins and immunoblot

Cellular extracts were obtained by solubilization of centrifuged cells in Triton X-100 buffer (50 mM Tris-HCl pH 7.5, 5 mM EDTA, 1% Triton X-100, 0.02% complete protease inhibitors cocktail (Roche)), for 30 min. Total protein concentration was determined by the bicinchoninic acid (BCA) method.

Glycoproteins from total cellular extracts and secreted membrane vesicles were stained after transfer to polyvinylidene difluoride (PVDF) membrane with lectins. Concanavalin A (Con A) (Sigma), biotinylated *Sambucus nigra* (SNA) and *Maackia amurensis* lectin (MAL) (Galab Technologies) were used. Glycoproteins were fixed on the PVDF membrane with 25% (v/v) 2-propanol and 10% (v/v) acetic acid for 5 min. The membranes were blocked for 1 h with TBS, 0.1% Tween-20 (TTBS) for Con A or with TTBS containing 2% BSA for SNA and MAL. For Con A detection the membrane was incubated overnight with 25 µg/ml Con A in TTBS containing 1 mM $CaCl_2$ and 1 mM $MgCl_2$ (TTBSS) followed by 1 h incubation with 0.5 µg/ml horseradish peroxidase type I (Sigma) in TTBSS. For SNA and MAL detection, membranes were incubated overnight in TTBS with 0.5 or 5 µg/ml SNA or MAL lectin, respectively. Membranes were further incubated for 1 h with 0.02 µg/ml streptavidin-peroxidase (Sigma). Detection was performed with the Immobilon Western chemiluminescent HRP substrate (Millipore).

Immunoblot was performed as previously described (Chapter 2). The following antibodies were used: mouse anti-CD9 (1:5000) and mouse anti-L1 (L1 11A) (1:3).

3.3.4. Glycosidase treatment

Hydrolysis of α2,3- and α2,6-linked NeuAc from total protein cellular extracts and exosomes was carried out overnight at 37 ºC by the addition of 15 mU neuraminidase from *Vibrio cholerae* or from *Arthrobacter urefaciens* (Roche) in 50 mM sodium acetate pH 5.5 containing 4 mM CaCl$_2$, and 50 mM sodium acetate pH 5.0, respectively. For specific hydrolysis of α2,3-linked NeuAc, 9 U neuraminidase from *Streptococcus pneumonia* (Prozyme, Glyko) in 50 mM sodium phosphate pH 6.0 were used, for 1 h at 37 ºC.

3.3.5. Uptake of SKOV3 exosomes by SKOV3 cells

SKOV3 exosomes were labelled with carboxyfluoresceine diacetate succinimidyl-ester (CFSE) (Invitrogen) as previously described (Keller *et al.*, 2009). Briefly, exosomes (20 μg) collected after a 100,000 x *g* ultracentrifugation were incubated with 7.5 μM CFSE for 30 min at 37 ºC in a final volume of 200 μl PBS containing 0.5% BSA. Labelled exosomes (Exos-CFSE) were 65-fold diluted with DMEM supplemented with 10% vesicles-free fetal calf serum and pelleted by ultracentrifugation for 16 h at 10,0000 x *g*, 12 ºC. Exos-CFSE were resuspended in DMEM and incubated with SKOV3 cells at 37 or 4 ºC

When indicated Exos-CFSE or cells were treated for 30 min with 100 μg/ml proteinase K, or for 2 h with 15 mU neuraminidase from *V. cholerae* or from *A. urefaciens*, before uptake. SKOV3 cells were also incubated, 30 min prior to and during uptake, with the inhibitors 10 μg/ml chlorpromazine, 5 μg/ml cytochalasin D, 50 μM 5-ethyl-*N*-isopropyl amiloride (EIPA) or 2% methyl-beta-cyclodextrin, or with 150 mM of the

monosaccharides D-glucose, D-galactose, α-L-fucose, α-D-mannose, D-*N*-acetylglucosamine, and the disaccharide β-lactose (Sigma).

Uptake assays were always performed in the presence of the compounds and analyzed after 2 or 4 h by immunofluorescence microscopy or flow cytometry.

3.3.6. Immunofluorescence microscopy

Immunofluorescence microscopy was done as previously described (Chapter 2). Primary antibodies were: mouse IgG anti-alpha-tubulin DM1A (1:2000) (Sigma), mouse IgG anti-EEA1 (1:100) (BD Biosciences), mouse IgG anti-LAMP1 H4A3 (1:100) (BD Biosciences) and mouse IgG anti-caveolin-1 (1:50) (Santa Cruz). Secondary antibody was donkey anti-mouse IgG AlexaFluor 594 (1:500) (Molecular Probes). Images were acquired on a Leica DMRB microscope using a DFC340FX camera coupled to the microscope, and Leica application suite V3.3.0 software. For colocalization, images were acquired on a confocal SP5 microscope. Each picture was acquired with laser intensities and amplifier gains adjusted to avoid pixel saturation. Each fluorophore used was excited independently and sequential detection was performed. Each picture consisted of a z-series of 20 images of 1024-1024 pixel resolution with a pinhole of 1.0 airy unit. Colocalization analysis was performed using the open source Image J version 1.38 (http://rsb.info.nih.gov/ij/).

3.3.7. Flow cytometry

SKOV3 cells incubated with Exos-CFSE for 4 h at 37 or 4 ºC were washed with PBS, detached using trypsin and resuspended in PBS with 2%

fetal calf serum (Gibco). Flow cytometry analysis was performed on a Cyflow ML cytometer (Partec) using Flowmax software 2.56 (Partec). Gate was set on living cells based on forward/side scatter properties and a minimum of 103 events within the gated live population were collected per sample. Exos-CFSE uptake by SKOV3 cells was measured by the shift in peak fluorescence intensity of CFSE, calculated by the geometric mean of the population. SKOV3 cells with no Exos-CFSE uptake (unlabelled) were used as controls for cell autofluorescence. Results were expressed as means ± S.D. and comparison between two means was performed by Student t-test. A p value lower than 0.05 was considered significant.

3.4. Results

3.4.1. Uptake of SKOV3 exosomes by SKOV3 cells

Since it has been shown that SKOV3 exosomes can be internalized by NK cells (Keller *et al*., 2009) here we have investigated if they are internalized by the cell line from where they originated. With that purpose exosomes produced in the absence of fetal bovine serum and collected at 100,000 x *g* were labelled with CFSE (Exos-CFSE) and incubated with SKOV3 cells. CFSE is a membrane permeable non-fluorescent compound that becomes fluorescent after cleavage of its acetate groups by intracellular esterases (Parish *et al*., 1999). A punctuated green fluorescent pattern corresponding to Exos-CFSE interaction/internalization was observed after 30 min and it increased up to 4 h of incubation (Figure 14, A). To obtain a higher sensitivity exosomes were also biotinylated and detected with streptavidin Alexa-488, and the interaction was observed

already 0.5 min after incubation (data not shown). Colocalization studies by immunofluorescence confocal microscopy of Exos-CFSE and alpha-tubulin, a microtubule marker, showed that Exos-CFSE were localized in the same z-stacks as microtubules, thus, confirming their internalization (Figure 14, B). Supporting this conclusion was the observation that the exosomes were not removed by acid wash of cells pre-exposed to Exos-CFSE (data not shown).
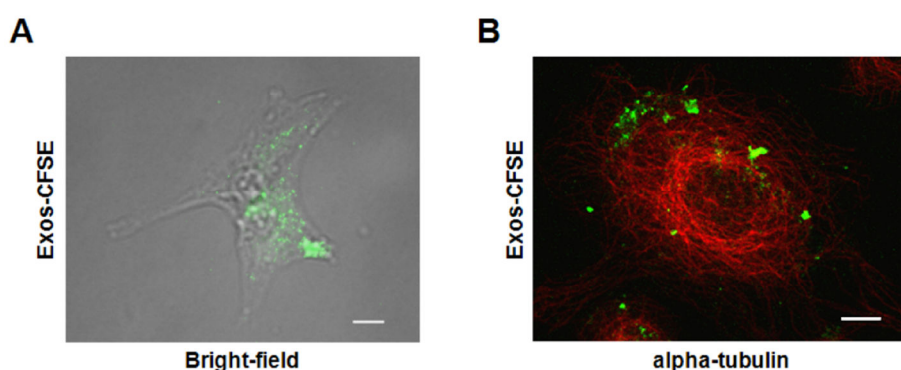

Figure 14. Uptake of SKOV3 exosomes by SKOV3 cells. (A) SKOV3 cells were incubated with Exos-CFSE (20 µg protein; green) for 4 h and were visualized in bright-field merged with fluorescence microscopy. Scale bar = 20 µm. (B) Detection of Exos-CFSE (green) and alpha-tubulin (red) by confocal immunofluorescence microscopy. Scale bar = 10 µm.

Several endocytic mechanisms have been described to mediate the entry of material into the cells (Doherty *et al*., 2009). Here, we observed that a decrease in temperature from 37 to 4 °C caused a reduction of 80 ± 8% (n=6) in the number of labelled cells as well as a decrease of 77 ± 9% (n=6) in the uptake for the positively labelled cells, based on the shift in fluorescence intensity corresponding to the geometric mean of the population peaks (Figure 15, A). These results indicated that exosomes uptake was mediated by endocytosis in an energy-dependent process.

Exos-CFSE were also found to partially colocalize with the endosomal marker EEA1 (Figure 15, B), thus showing the participation of clathrin-mediated endocytosis in exosome uptake. This conclusion was further supported by uptake inhibition (19 ± 18%, n=4) (Figure 15, C) with 10 µg/ml chlorpromazine, which blocks clathrin-mediated endocytosis (Wang *et al*., 1993). Colocalization with the lysosomal marker LAMP1 (Figure 15, B) indicated that at least a part of the exosomes were targeted to the lysosome.

In addition, other inhibitors have been tested. First, cells incubated with 5 µg/ml cytochalasin D, which is known to inhibit actin polymerization and consequently inhibit phagocytosis (deFife *et al*., 1999) as well as other endocytic pathways (Tian *et al*., 2010) showed an uptake reduction of 32 ± 7% (n=4) (Figure 15, C). EIPA at 50 µM, which is known to block macropinocytosis (West *et al*., 1989), caused an uptake reduction of 36 ± 13% (n=5) (Figure 15, C), thus suggesting that exosomes were internalized via macropinocytosis. Methyl-beta-cyclodextrin, that is used to deplete cholesterol from cellular membranes (Rodal *et al*., 1999), decreased Exos-CFSE uptake (44 ± 8%, n=5) (Figure 15, C). However, there was no colocalization with caveolin-1 (Figure 15, B), which is a marker of caveolae that are enriched in cholesterol rich domains. These results indicated that exosome uptake could occur via a cholesterol associated pathway independent of caveolae or that methyl-beta-cyclodextrin affected exosomes membrane integrity, thus decreasing uptake efficiency.

Exos-CFSE did not colocalize with the Golgi marker GM130, the *trans*-Golgi network marker TGN46 or the endoplasmic reticulum marker calnexin (data not shown).
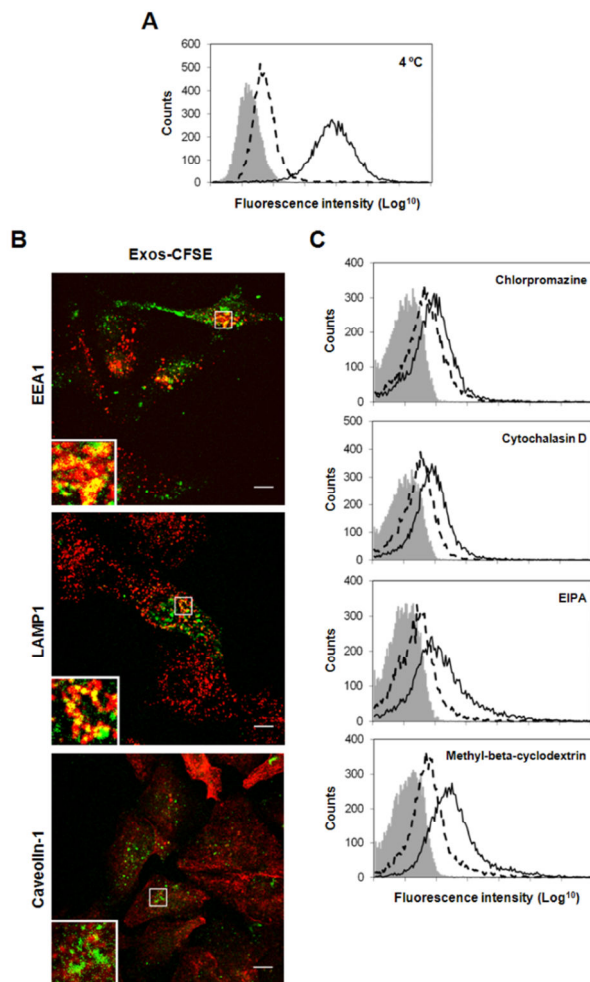
Figure 15. Path of internalization of exosomes in SKOV3 cells. (A) Exos-CFSE (20 µg protein; green) were incubated with SKOV3 cells at 37 or 4 °C and uptake was monitored by flow cytometry analysis of cell fluorescence intensity. Solid and dashed lines represent Exos-CFSE uptake at 37 and 4 °C, respectively. (B) Colocalization of Exos-CFSE (20 µg protein; green) with EEA1 (red), LAMP1 (red), and caveolin-1 (red). Secondary antibody was donkey anti-mouse IgG AlexaFluor 594. Colocalization is indicated in yellow. Images in the left bottom represent 4x magnifications of selected areas. Scale bars = 10 µm. (C) Effect of chlorpromazine, cytochalasin D, EIPA, and methyl-beta-cyclodextrin (30 min pre-incubation) on Exos-CFSE uptake (4, 4, 4 and 2 h, respectively) monitored by flow cytometry analysis (dashed lines). Controls consist of SKOV3 cells with no treatment for chlorpromazine and methyl-beta-cyclodextrin, or treated with DMSO for cytochalasin D and EIPA (solid lines). Unlabelled SKOV3 cells (grey) were used as control for cell autofluorescence. The results shown are representative of three independent experiments.

3.4.2. Proteins are required for exosomes uptake

The recognition between exosomes and the target cell has been reported to involve proteins present at the cell surface of both exosomes and target cells (Théry *et al.*, 2009; Morelli *et al.*, 2004). Here, Exos-CFSE or SKOV3 cells were digested with proteinase K, a broad specificity protease, and uptake efficiency was analyzed by flow cytometry analysis. Uptake levels of digested Exos-CFSE were found to be lower (45 ± 12%, n= 6) than Exos-CFSE without treatment (Figure 16, A). As control, fluorescence of Exos-CFSE was not affected by proteinase K treatment (data not shown). Furthermore, a decrease of 32 ± 8% (n= 6) in uptake was observed in SKOV3 cells treated with proteinase K (Figure 16, B). Therefore, proteins present in exosomes and also in SKOV3 cells are required, at least in part, for internalization by target cells.
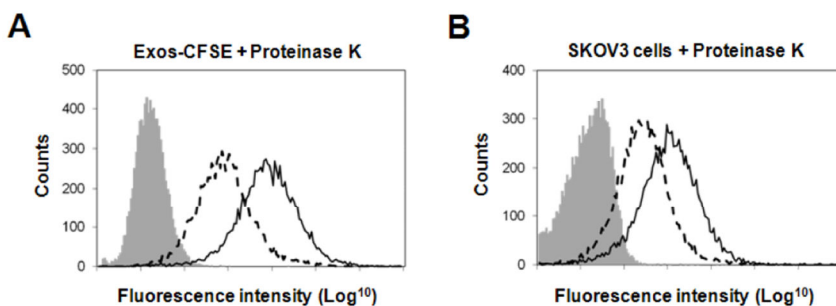

Figure 16. Effect of proteinase K treatment in SKOV3 exosomes uptake. (A) Exos-CFSE (20 µg protein; green) or (B) SKOV3 cells were treated with 100 µg/ml proteinase K for 30 min. Uptake was determined after 4 h of incubation by flow cytometry analysis and compared with uptake of Exos-CFSE with no treatment (solid lines). Unlabelled SKOV3 cells (grey) were used as control for cell autofluorescence. Dashed lines represent Exos-CFSE uptake after proteinase K digestion. The results shown are representative of three independent experiments performed in duplicate.

3.4.3. Enrichment of specific glycoproteins in exosomes and relevance in uptake

Glycan-lectin interactions have been suggested to play a role in the uptake of exosomes by target cells (Hao *et al*., 2007; Barres *et al*., 2010), therefore, we have investigated if glycans would play a role in exosome uptake by SKOV3 cells.

First, glycoproteins of cellular extracts and secreted vesicles from SKOV3 cells were detected with the lectins Con A (binds α-mannosyl containing branched glycans predominantly of the high-mannose followed by hybrid- and diantennary complex type structures to a lower extent) (Bhattacharyya *et al*., 1989), SNA (recognizes NeuAcα2,6Gal/GalNAc) and MAL (binds NeuAcα2,3Galβ1,4GlcNAc/Glc) (Knibbs *et al*., 1991).

The profile from secreted vesicles was distinct from that of cellular extracts with the three lectins (Figure 17, A). Detection with SNA and MAL was almost totally abolished after digestion with *V. Cholerae* and *A. urefaciens* neuraminidases (cleave terminal α2,3- and α2,6-linked NeuAc), whereas only MAL binding was abolished after *S. pneumoniae* (cleaves only α2,3-linked NeuAc) digestion (Figure 17, B), thus confirming that SNA and MAL binding to secreted vesicles glycoproteins was specific. The sialic acid was not present in sialylated Lewis epitopes, since there was no detection with anti-sialyl-Lewis[a] or anti-sialyl-Lewis[x] antibodies (data not shown).

SKOV3 secreted vesicles are constituted by exosomes and apoptotic vesicles, which can be fractionated by using a sucrose gradient, as previously described (Stoeck *et al*., 2006; Escrevente *et al*., 2008). CD9 is a tetraspanin protein that has been used as exosome marker (Février and Raposo, 2004; Lamparski *et al*., 2002). After sucrose gradient separation of the secreted vesicles all the SNA and MAL binding was found

in the exosome-containing fractions (fractions 2-5) and not in the apoptotic blebs (fractions 8-11) (Figure 8, C).
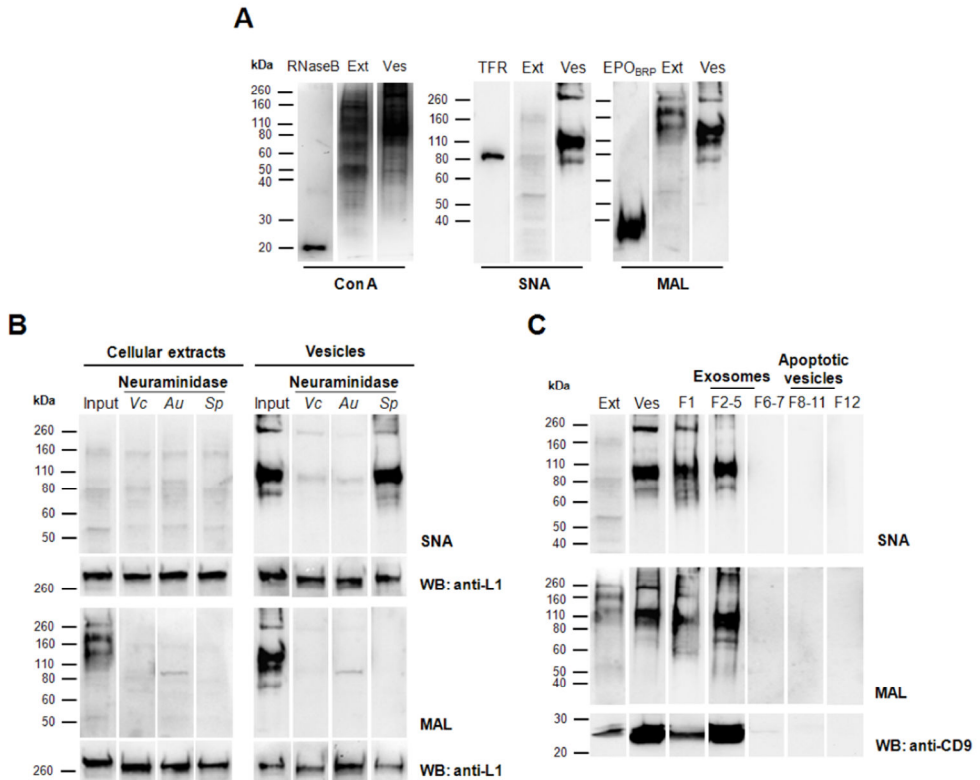

Figure 17. Western blot and lectin detection of glycoproteins from SKOV3 cellular extracts (Ext) and secreted vesicles (Ves). (A) Con A, SNA, and MAL lectin detection in SKOV3 cellular extract and vesicles. Three µg total protein were applied per lane. As positive controls, 200 ng ribonuclease B (RNase B) (Fu *et al.*, 1994), human plasma transferrin (TFR) (Spik *et al.*, 1975) and erythropoietin (EPO[BRP]) (Sasaki *et al.*, 1988) were used. (B) SNA and MAL lectin analysis of desialylated SKOV3 cellular extracts and vesicles. Total proteins (3 µg) were digested with neuraminidases from *V. cholerae* (Vb), *A. urefaciens* (Au) and *S. pneumonia* (Sp). Input consisted of cellular extracts and exosomes without treatment. As loading control L1 was detected. (C) Vesicles from 1.5×10^7 SKOV3 cells were fractionated in a sucrose gradient. Cellular extracts (Ext), secreted vesicles from 100,000 x *g* pellet (Ves), pooled fractions 2-5 (F2-5) (3 µg total protein), 20% of F1, F6-7, F8-11 and F12 were analysed. As positive control for exosomes, CD9 was detected. Detection was performed using the chemiluminescent method.

Specific patterns of protein glycosylation were also found for exosomes from two other human cell lines, embryonic kidney HEK293 and neuroglioma H4 cells (Figure 18).

To investigate a possible role for glycosylation in exosome uptake Exos-CFSE were desialylated with *V. cholerae* and *A. urefaciaens* sialidases and exosomes uptake was monitored by immunofluorescence microscopy and flow cytometry analysis of cell fluorescence intensity. Uptake efficiency of exosomes after neuraminidase treatment was slightly increased (16 ± 14%, n= 6) when compared with exosomes incubated with neuraminidase buffer (Figure 19, A), however, the observed increase was not statistically significant using the Student *t*-test (p=0.0764). In addition, increases in the uptake of exosomes incubated with neuraminidase (38 ± 13%, n=6) or neuraminidase buffer (23 ± 14%, n=6) were detected when compared with Exos-CFSE without treatment (Figure 19, A).
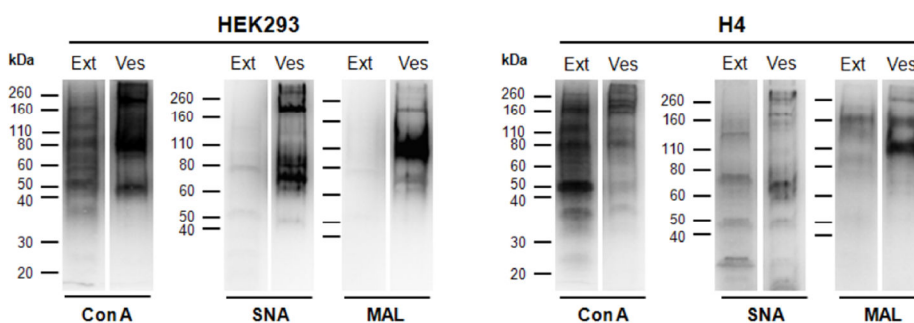

Figure 18. Con A, SNA, and MAL lectin detection of glycoproteins from HEK293 and H4 cellular extract (Ext) and secreted vesicles (Ves). For the analysis, 3 µg of total protein were applied per lane. Detection was performed using the chemiluminescent method.

The uptake assay was also performed in the presence of 150 mM of the monosaccharides D-glucose (control), D-galactose, α-L-fucose, α-D-mannose and D-*N*-acetylglucosamine, and the disaccharide β-lactose. Decreases of 23 ± 7%, 24 ± 14%, 25 ± 16%, 27 ± 8%, 19 ± 15%, and 20 ± 8% (n=6), respectively, in the uptake of Exos-CFSE in comparison with control without sugar were observed. The incubation with α-D-mannose led to a higher decrease in uptake relatively to the control sugar D-glucose, however the difference was not statistically significant (Figure 19, B).
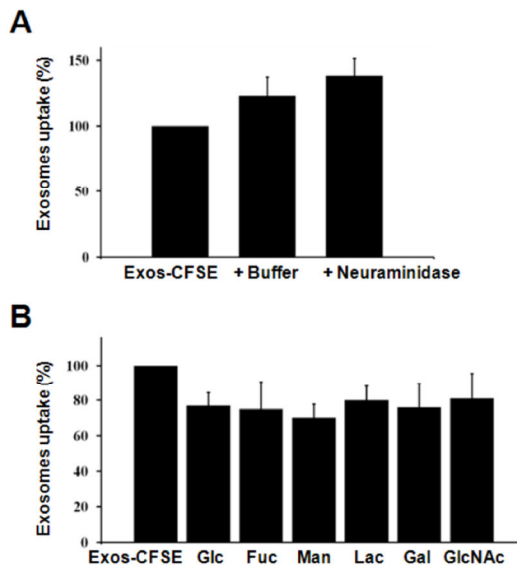

Figure 19. Effects of neuraminidase and sugars on SKOV3 exosomes uptake. (A) Exos-CFSE (20 µg protein) were incubated with 15 mU *V. cholera* neuraminidase or corresponding buffer for 2 h before Exos-CFSE uptake. (B) Effect of 150 mM D-glucose (Glc), α-L-fucose (Fuc), α-D-mannose (Man), β-lactose (Lac), D-galactose (Gal) and D-*N*-acetylglucosamine (GlcNAc) (30 min pre incubation) on Exos-CFSE uptake (4 h) monitored by flow cytometry analysis. Uptake efficiency was calculated relatively to the uptake without treatment, considered as 100%. Results are displayed in relative percentages ± S.D. The results shown are representative of three independent experiments performed in duplicate.

3.5. Discussion

Exosomes are small membrane vesicles that are secreted by several cell types, including tumours and they have been found in biological fluids. They contain several membrane and cytoplasmic proteins and, in cancer, they play a role in cell migration and metastases. They may also transfer proteins associated with deregulated signaling pathways in cancer (Al-Nedawi *et al*., 2008; Iero *et al*., 2007), therefore, contributing to the propagation of transformed phenotype. Furthermore, the exosomes may transfer mRNA and miRNA (Skog *et al*., 2008).

In the present work, we have found that the SKOV3 ovarian carcinoma cell line internalizes exosomes derived from the same cells in an energy-dependent process, via various endocytic pathways: colocalization studies with organelle markers and incubation with inhibitors have shown that the endocytosis pathway dependent on clathrin, macropinocytosis, and a cholesterol associated pathway independent of caveolae were associated with the uptake. Evidence from the literature showed that in dendritic cells exosome uptake was also inhibited at 4 °C and with cytochalasin D, and was further trafficked to the late endosomes/lysosomes (Morelli *et al*., 2004). In phagocytic cells, more specifically macrophages, internalization was also dependent on the actin cytoskeleton but not on pathways involving caveolae, macropinocytosis or clathrin coated vesicles (Feng *et al*., 2010). In the PC12 cell line exosomes uptake was also found to occur via the endocytic pathway (Tian *et al*., 2010). After internalization, exosomes could fuse with the endosomal membrane and deliver their content to the cytoplasm of the target cell. For SKOV3 cells such process could take place over a long period of time since internalized exosomes were detected in the cells for at least 20 h (data not shown).

The initial recognition events that precede uptake may involve several molecules, proteins (Simons and Raposo, 2009), and lipids (Keller *et al.*, 2009) have already been indicated as involved in this process. In this work, the impairment observed for vesicles or cells treated with proteinase K indicated that proteins from the extracellular surface from both target cells and exosomes are required for internalization. Further studies to identify which proteins play an important role in the recognition are required.

Here we also found that exosomes from SKOV3 cells are particularly enriched in specific glycoproteins with high mannose or NeuAcα2,3/6-containing structures. In this context, other authors, using lectin arrays, have also observed the enrichment in T-cells secreted microvesicles of high-mannose and sialic acid-containing structures in comparison with cell membranes (Krishnamoorthy *et al.*, 2009). Furthermore, an enrichment of more extensively glycosylated forms of PrPc has been found in the exosomes in comparison with cell lysates (Vella *et al.*, 2007).

Removal of NeuAc from the exosomes with neuraminidase led to an increase in the uptake, but non-significant. The removal of NeuAc decreased the negative charge at the exosome surface exposing galactose or *N*-acetylgalactosamine residues. This could lead to physico-chemical alterations of the membrane or create new ligands for carbohydrate binding proteins at the surface of the cells that would mediate the binding.

The monosaccharides D-galactose, α-L-fucose, α-D-mannose, D-*N*-acetylglucosamine, and the disaccharide β-lactose reduced exosomes uptake to a comparable extent as the control D-glucose probably due to increased osmotic pressure that is known to reduce endocytosis (Oka *et al.*1989). Therefore, these sugars do not play a major role in exosome interaction and uptake in SKOV3 cells. This result is different from that found in dendritic cells where exosome uptake was specifically inhibited by

mannose and *N*-acetylglucosamine, the interaction being at least in part mediated by a C-type lectin (Hao *et al*., 2007), or in macrophages where lactose diminished exosome uptake probably through its action on galectin-5 that mediated the process (Barres *et al*., 2010).

Here, certain glycoproteins were specifically detected in exosomes and may constitute markers. It will be interesting to investigate if those glycoproteins are selectively sorted to the exosomes or if only certain glycoforms from the same protein are sorted into the exosomes. It can be admitted that glycans by themselves may be important for glycoprotein sorting into exosomes. Since protein oligomerization is known to promote sorting into exosomes independently of the ESCRT machinery and ubiquitination (Simons and Raposo, 2009), the glycans could mediate oligomerization via interaction with lectins as previously described for the transferrin receptor in reticulocytes (Vidal *et al*., 1997). Moreover, glycans may interact with galectins at the cell surface, which may lead to their enrichment in membrane lipid domains as previously described (Garner and Baum, 2008). Considering that lipid microdomains play a role on exosomes biogenesis (Simons and Raposo, 2009), glycans could in that case also have a role on sorting to exosomes. Further studies are required to clarify this matter.

Exosomes contain cell surface cancer antigens, which confers them the potential for therapeutic approaches in cancer vaccination. Our observation that they are particularly enriched in glycan epitopes urges the need to further characterize the corresponding structures since one of the major changes that occur in cancer is in cell surface glycosylation, which has been largely used as biomarker. The knowledge of exosomes glycosylation with the possibility for its modulation will open new perspectives in cancer vaccination.

3.6. Acknowledgements

Chapter 4

N-glycosylation of secreted vesicles from ovarian tumour cells

4. *N*-glycosylation of secreted vesicles from ovarian tumour cells

4.1. Summary

Vesicles secreted from cells, including exosomes, are released by several cell types, including ovarian tumour cells, and are found in biological fluids such as malignant ascites and blood. They contain several membrane and cytoplasmic proteins and they play a role in cancer progression.

Aberrant glycosylation is an important aspect in malignant transformation and consequently in ovarian cancer. Exosomes from ovarian tumour cell lines have been shown to be enriched in specific glycoproteins in comparison with cellular extracts. Nevertheless, detailed knowledge about these glycan structures is not known at present.

In the present work, vesicles secreted from SKOV3 cells were compared with plasma membrane and microsomal enriched fractions and were found to contain specific glycoproteins that were distinctly recognized by the lectins Con A, SNA, MAL and *Wisteria floribunda* (WFA).

Detailed structure analysis of the *N*-glycans from SKOV3 and OVM secreted vesicles, microsomal, and plasma membrane fractions was performed by HPAEC-PAD and MALDI-TOF-MS. Complex glycans of di-, tri- and tetraantennary type with proximal fucose (Fuc) were found in all fractions of both cell lines. High mannose structures were enriched in the microsomal fraction of the two cell lines. Agalactosylated truncated structures were found predominantly in SKOV3 cells, while the terminal LacdiNAc motif was abundant in SKOV3-secreted vesicles.

The results obtained contributed to the knowledge of the glycosylation of vesicles secreted from ovarian tumour cells comparatively to other cellular membrane enriched fractions. This might open new perspective for the use of secreted vesicles as potential sources of tumour markers.

4.2. Introduction

Many cell types, including tumour cells, secrete exosomes into the extracellular space. These vesicles can also be found in the body fluids, such as blood, urine, saliva, and malignant effusions (reviewed in van Niel *et al.*, 2006), and can contribute to tumour invasion and progression by transferring genetic information that confers aggressive phenotypes (Al-Nedawi *et al.*, 2008), modifying the tumour microenvironment (Castellana *et al.*, 2009), conferring multi-drug resistance (Shedden *et al.*, 2003; Safaei *et al.*, 2005), and promoting angiogenesis, tumour growth and metastasis (reviewed in Muralidharan-Chari *et al.*, 2010). Moreover, exosomes contain proteins related with tumour progression (Gutwein *et al.*, 2005; Runz *et al.*, 2007) that might be used as tumour markers and also constitute potential targets for therapeutic approaches.

Ovarian tumour cells were found to release large amounts of vesicles and the rate of their release has been shown to correlate with tumour invasiveness (Ginestra *et al.*, 1999). Moreover exosomes were also found in blood (Taylor and Gercel-Taylor, 2008; Li *et al.*, 2009) and malignant ascites (Gutwein *et al.*, 2005; Runz *et al.*, 2007) of patients with ovarian carcinoma.

Glycosylation alterations are typical for all kinds of cancers, including ovarian carcinoma, and include several changes related to terminal carbohydrate structures, such as incomplete synthesis and modification of normally existing carbohydrates, and changes in the carbohydrate core structures (Dabelsteen, 1996). Several studies have already described specific glycosylation changes in the serum of ovarian cancer patients. They include increased core fucosylated, agalactosylated complex-type diantennary glycans originated from immunoglobulin G, along with the sLe^x determinant (Saldova *et al.*, 2007), increased sialylation with a

shift in sialic acid linkage from α2,3- to α2,6- in ovarian cancer serum glycoproteins (Saldova *et al.*, 2007), and alterations in fucosylation and branching in α1-acid glycoprotein (Imre *et al.*, 2008).

Ovarian carcinoma cell lines, SKOV3, GG, OVM, and m130 were already characterized with respect to their glycosylation using anti-carbohydrate antibodies and lectins (Escrevente *et al.*, 2006). The cells contained variable amounts of Lewis carbohydrate motifs and all contained glycoproteins recognized by Con A, a lectin that binds α-mannosyl containing-branched glycans predominantly of the high mannose followed by hybrid and diantennary complex structures to a lower extent (Bhattacharyya *et al.*, 1989), and SNA that binds structures containing terminal α2,6-linked sialic acid (Knibbs *et al.*, 1991). In addition, structure analysis of the *N*-linked glycans from total glycoproteins derived from SKOV3 ovarian carcinoma cells confirmed the abundance of high mannose and proximally-fucosylated, complex type partially agalactosylated glycan structures, as well as the presence of the LacdiNAc motif (Machado *et al.*, 2011).

SKOV3 cells exosomes have been shown to contain higher levels of certain glycosylated sialic acid- and mannose-containing glycoproteins when compared with total cellular extracts (Chapter 3). Nevertheless, detailed knowledge about the *N*-glycan structures and their role is not elucidated at present.

Lectin binding assays using Con A, SNA, MAL and WFA revealed that secreted vesicles have a unique glycosylation profile when compared with plasma membrane, and microsomal enriched fractions. The *N*-glycan analysis from SKOV3 and OVM secreted vesicles, plasma membrane and microsomal fractions by HPAEC-PAD and MALDI-TOF-MS showed that all fractions of both cell lines contained complex glycans of di-, tri- and tetraantennary type with proximal Fuc. Furthermore, high mannose type structures were found to be enriched in the microsomal fraction of the two

cell lines. Agalactosylated truncated structures were found predominantly in SKOV3 cells. Finally, the terminal LacdiNAc motif was abundant in secreted vesicles of SKOV3 cells.

4.3. Materials and methods

4.3.1. Cell culture

Human ovarian cancer SKOV3, OVM, m130, and GG cell lines were grown in DMEM (Sigma) at 37 °C, 5% CO_2, supplemented with 10% fetal calf serum (Gibco), and 1% penicillin/streptomycin solution (Gibco).

4.3.2. Isolation of cell-secreted vesicles

Cell-secreted vesicles were isolated as previously described (Chapter 3). Briefly, confluent SKOV3, OVM, m130 and GG cells were cultivated for 48 h in serum-free medium. The supernatant was collected and centrifuged at 500, 10,000 and 100,000 x *g*, 10, 20 and 120 min, respectively, at 4 °C. The pellet of the last centrifugation, consisting of secreted membrane vesicles, was resuspended in PBS.

4.3.3. Isolation of microsomal and plasma membrane enriched fractions

The isolation of the microsomal membrane fraction from SKOV3 and OVM cells was accomplished by differential centrifugation. Cells were pelleted by centrifugation, washed once with PBS, and resuspended in homogenization buffer (1 mM $NaHCO_3$, 0.2 mM $CaCl_2$, 0.2 mM $MgCl_2$, 1mM spermidine, pH 8). Cells were disrupted with a pellet pestle (Sigma) and centrifuged at 600 x g, 10 min, 4 °C. Supernatant was collected and further centrifuged at 15,000 x g and 100,000 x g, for 10 and 120 min, respectively, at 4 °C. The pellet, consisting of the microsomal membrane fraction was homogenised in PBS with a 25 gauge needle until complete resuspension. The supernatant containing the cytosolic fraction was also collected for further analysis.

The isolation of plasma membrane proteins from SKOV3 and OVM cells was performed by cell surface biotinylation. SKOV3 cells were washed with PBSCM (1 mM $CaCl_2$, 1 mM $MgCl_2$ in PBS) and biotinylated with 0.5 mg/ml sulfo-NHS-SS-biotin (Pierce) in PBSCM for 40 min at 4 °C with agitation (Sousa *et al*., 2003). After a two fold wash with PBSCM containing 50mM NH_4Cl followed by DMEM with 10% FCS and 1% P/S, cells were incubated with lysis buffer (1% Triton-X, 0.5% DOC, 0.1% SDS, 5 mM EDTA, 0.02% complete protease inhibitors cocktail (Roche)) for 30 min at 4 °C with agitation. After centrifugation the supernatants were incubated with streptavidin-agarose beads (Sigma) for 2 h, at 4 °C to pellet biotinylated proteins. The agarose beads were pelleted and washed four times with washing buffer (10 mM Tris-HCl buffer pH 8.0, 0.5 M NaCl, 1 mM EDTA and 1% NP-40). Biotinylated proteins were eluted by incubation in 0.08% Tris-HCl pH 6.8, 2% SDS, 10% glycerol, 5 min at 100 °C. Non-biotinylated proteins were also collected from the supernatant for further analysis.

4.3.4. Glycoprotein detection using lectins and immunoblot

Cellular extracts were obtained by solubilization of centrifuged cells in Triton X-100 buffer (50 mM Tris-HCl pH 7.5, 5 mM EDTA, 1% Triton X-100, 0.02% complete protease inhibitors cocktail (Roche)) for 30 min. Secreted vesicles, plasma membrane, and microsomal fractions were obtained as described above.

Total protein concentration was determined by the BCA method. Glycoproteins were stained after transfer to PVDF membrane with lectins. Con A (Sigma), biotinylated SNA, MAL (Galab Technologies), and WFA (Vector Labs) were used. Glycoproteins were fixed on the PVDF membrane with 25% (v/v) 2-propanol and 10% (v/v) acetic acid for 5 min. The membranes were blocked for 1 h with TBS, 0.1% Tween 20 (TTBS) for Con A, with TTBS containing 2% BSA for SNA, and MAL and with TBS, 0.15% Tween 20, 2% BSA for WFA. For Con A detection the membrane was incubated overnight with 25 µg/ml Con A in TTBS containing 1 mM CaCl$_2$ and 1 mM MgCl$_2$ (TTBSS) followed by 1 h incubation with 0.5 µg/ml horseradish peroxidase type I (Sigma) in TTBSS. For SNA, MAL and WFA detection, membranes were incubated overnight in TTBS with 0.5 µg/ml SNA or 5 µg/ml MAL and WFA lectin. Membranes were further incubated for 1 h with 0.02 µg/ml streptavidin-peroxidase (Sigma).

When indicated, membranes were incubated simultaneously with the lectin and the corresponding competitive sugar, 0.2 M methyl-α-D-mannopyranoside for Con A and 0.2 M *N*-acetyl-D-galactosamine for WFA. Detection was performed with the Immobilon Western chemiluminescent HRP substrate (Millipore).

4.3.5. Total *N*-glycans isolation

Total *N*-glycans isolation from SKOV3 and OVM cell-secreted vesicles, microsomal, and plasma membrane fractions were performed as previously described (Machado *et al.*, 2011). A total of 3.5 and 3 mg of total proteins corresponding to secreted vesicles and microsomal fraction, respectively, were solubilized for 30 min in PBS containing 2% (v/v) Nonidet P-40 and 0.1% benzonase (Sigma), pH 7.2. For the isolation of *N*-glycan from the plasma membrane, a solution containing 350 µg of biotinylated proteins were used. Proteins were precipitated with 4 volumes of ice-cold 100% ethanol for 2 h at −20 °C and dried in a Speed Vac concentrator (Savant Instruments Inc.). The resulting pellet was incubated for 90 min in 0.3 M Tris–HCl pH 8.3, 6 M urea, 1 mM dithioerythritol, diluted in water and incubated overnight with 70 µg of trypsin (Merk) and 0.02% sodium azide.

Trypsin inactivation was accomplished by 10 min incubation at 90 °C, followed by the addition of 0.02% complete protease inhibitor cocktail during 1 h. Next, the sample solution was subjected to buffer exchange using a 5 kDa Vivaspin concentrator (Sartorius) to PNGase F buffer (10 mM NaH_2PO_4, 5 mM ethylenediaminetetraacetic acid, pH 7.5). All incubations were performed at room temperature unless otherwise noted.

The *N*-glycan release from total glycopeptides of secreted vesicles, microsomal, and membrane fractions from SKOV3 cells were performed by overnight incubation with 50 U PNGase F (Roche) at 37 °C. The released *N*-glycans were separated from the glycoproteins by precipitation with 2.4 volumes of ice-cold 100% ethanol for 2 h at −20 °C. After centrifugation at 10,000 × *g*, for 10 min at 4 °C, the *N*-glycans in suspension were removed, and two additional washes of the glycoprotein pellet were made with ice-

cold 50% ethanol. The supernatants containing *N*-glycans were pooled and dried in a Speed Vac concentrator.

4.3.6. Analysis of desialylated *N*-glycans by HPAEC-PAD

The *N*-glycan samples were desalted using 100 mg Hypercarb cartridges (Thermo) previously washed with 80% (v/v) acetonitrile (ACN) with 0.1% trifluoroacetic acid (TFA), and six times with water. The *N*-glycans solubilized in water were then loaded onto the column, washed two times with water, and finally eluted with 40% ACN with 0.1% TFA. The eluted glycans were neutralized with 2.5% (v/v) NH_4OH and dried in a Speed Vac concentrator. The desialylated *N*-glycans were prepared by incubation with 5 mM H_2SO_4 for 90 min at 80 °C. Hydrolyzed *N*-glycans were neutralized with 50 mM NaOH and dried in a Speed Vac concentrator.

The analysis of *N*-glycan structures by HPAEC-PAD was performed using an ICS-3000 ion chromatography system (Dionex Corporation), consisting of an AS autosampler, a DC detector/chromatography module, and a DP dual pump. Samples of 20 μL were injected into an equilibrated CarboPac PA200 column equipped with a guard column (3 × 50 mm, Dionex). Released desialylated *N*-glycans were eluted by using a concentration gradient of 0.15 M sodium hydroxide (solvent A) and 0.15 M sodium hydroxide/0.6 M sodium acetate (solvent B), at a flow rate of 0.4 mL/ min. The gradient consisted of a 30 min isocratic run at 100% solvent A, followed by increasing solvent B concentration (10 min to 15%, 2 min to 30%, 3 min to 100%). The column temperature was constant at 30 °C. The electrochemical detection of the oligosaccharides was performed by application of the detection potentials and durations as recommended by the manufacturer.

For subsequent MALDI-TOF-MS analysis pools or individual fractions from the HPAEC-PAD analysis were collected after online desalting using a carbohydrate membrane desalter device (CMD-I, Dionex). Glycan fractions were dried in a Speed Vac concentrator for further analysis.

4.3.7. Analysis of *N*-glycans by MALDI-TOF-MS

Glycans were analyzed with a Bruker ULTRAFLEX time-of-flight (TOF/TOF) instrument in the linear positive ion mode. Native desialylated oligosaccharides were analyzed using a matrix of 2,5-dihydroxybenzoic acid as a UV-absorbing material. Samples of 1 µL at an approximate concentration of 1–10 pmol/µL were mixed with equal amounts of the respective matrix and sodium salt. This mixture was spotted onto a stainless steel target and dried at room temperature before analysis. Structures were tentatively assigned to various *N*-glycans based on their observed masses compared with the calculated masses of known *N*-glycans.

Mass spectrum data were analyzed with the Bruker DataAnalysis version 4 (Bruker Daltonics). Further annotation of *N*-glycans and database searches were performed using the GlycoWorkbench software (Ceroni *et al.*, 2008).

4.4. Results

4.4.1. Enrichment of specific glycoproteins in ovarian carcinoma secreted vesicles

SKOV3-secreted vesicles and exosomes were found to be highly enriched in certain glycosylated sialic acid- and mannose-containing glycoproteins when compared with total cellular extracts (Chapter 3). To investigate if secreted vesicles had a characteristic glycosylation profile that was distinct from plasma membrane and microsomal fractions, the different fractions were detected with lectins after Western blotting.

In this study, secreted vesicles isolated by ultracentrifugation of cell supernatants at 100,000 x *g* were used for analysis since this fraction has been shown to be enriched in exosomes (Théry *et al*., 2006). Previous results from our laboratory have shown that MAL- and SNA-binding glycoproteins were only detected in exosome-containing fractions after sucrose density purification (Chapter 3).

The microsomal fraction was obtained by differential centrifugation and it consisted of the 100,000 x *g* pellet after clarification of the cell extract at 15,000 x *g*, while a plasma membrane enriched fraction was obtained by cell surface protein biotinylation and separation with streptavidin-agarose. As controls, a cytoplasmic fraction consisting of post-100,000 x *g* supernatant, and an intracellular fraction containing proteins that were not biotinylated were also analysed.

Glycoproteins of SKOV3 cellular extracts (Ext), secreted vesicles (Ves), and all the other enriched fractions were detected with the lectins Con A, SNA, MAL and WFA (recognizes the LacdiNAc motif, GalNAcβ4GlcNAc). The glycosylation profile of SKOV3-secreted vesicles

was distinct from all other fractions with all the lectins tested (Figure 20). Con A was shown to strongly bind glycoproteins of SKOV3-secreted vesicles when compared with other fractions, using the same amount of total protein. The binding specificity was confirmed using 0.2 M of the competitive sugar methyl-α-D-mannopyranoside.

In SKOV3 cell secreted vesicles three glycoproteins with sizes of approximately 260 kDa and one with about 110 kDa were recognized by WFA (indicated with asterisks in Figure 20). In the plasma membrane enriched fraction only one specific glycoprotein at approximately 160 kDa was recognized. The detection was specific since it was abolished in the presence of 0.2 M of competitive sugar N-acetyl-galactosamine. The signal detected in cellular extracts, microsomal, intracellular, and cytoplasmic fractions with WFA was probably not specific since it was not inhibited after incubation with the competitive sugar (Figure 20).

Previous results have shown that specific bands from SKOV3 exosomes were strongly recognized by SNA and MAL contrary to cellular extracts (Chapter 3). In the present study, SKOV3-secreted vesicles contained two major bands identified by SNA, one with an apparent molecular mass of 260 kDa and the second between 80 and 110 kDa (indicated with asterisks in Figure 20). MAL detected two bands with high intensity in SKOV3-secreted vesicles, one band around 260 kDa and a second band between 110 and 160 kDa (indicated with asterisks in Figure 20). These specific glycoproteins were not found in microsomal or plasma membrane enriched fractions (Figure 20). Therefore, sialylated glycoproteins identified were specific to secreted vesicles, and were not found in other membrane fractions.
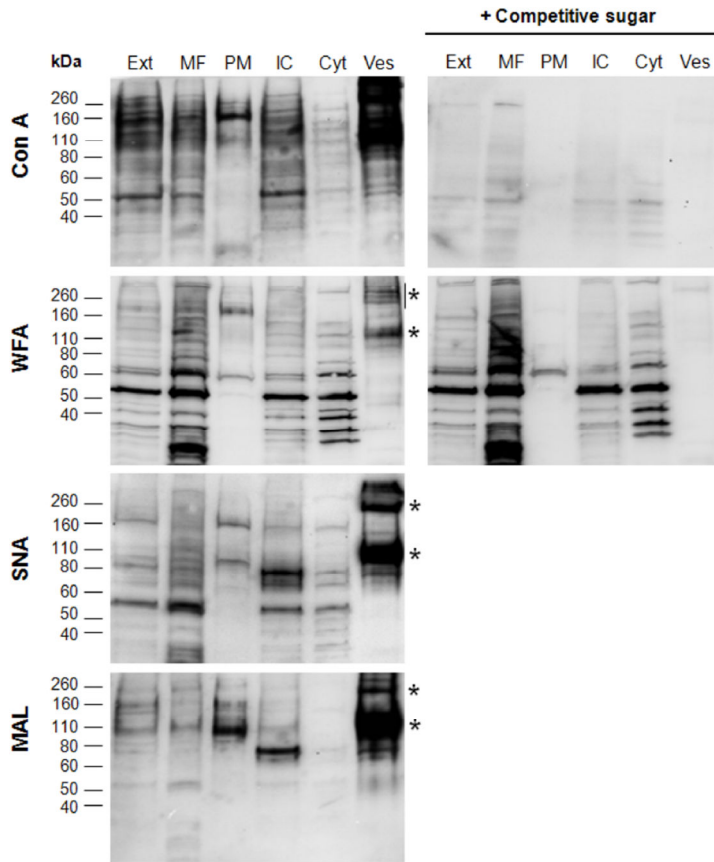
Figure 20. Western blot and lectin detection of glycoproteins from SKOV3 cellular extracts (Ext), microsomal fraction (MF), plasma membrane fraction (PM), intracellular fraction (IC), cytoplasmic fraction (Cyt) and secreted vesicles (Ves). Detection of glycoproteins with Con A, WFA, SNA and MAL. Competitive sugars used were 0.2 M methyl-α-D-mannopyranoside for Con A and 0.2 M *N*-acetyl-galactosamine for WFA. Total proteins (3 µg) were applied per lane. Detection was performed using the chemiluminescent method. Asterisks correspond to most abundant glycoproteins enriched in the secreted vesicles.

To determine if there was also an enrichment of specific sialic acid-containing glycoproteins in other ovarian carcinoma cell lines, secreted vesicles from OVM, m130, and GG cells were analysed by Western blot with SNA and MAL (Figure 21). SNA was found to bind specific glycoproteins in m130 secreted vesicles, including one protein above 260 kDa, one with approximately 160 kDa and three proteins with apparent molecular masses around 80 kDa (indicated with asterisks in Figure 21). MAL detected one major glycoprotein in m130 and OVM secreted vesicles with about 110 kDa (indicated with asterisks in Figure 21). No specific enrichment was observed for GG cells with these lectins.
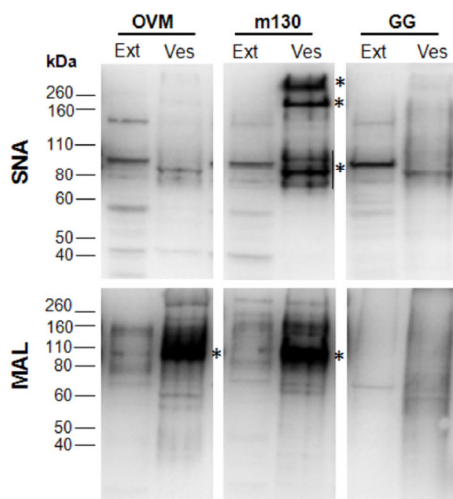

Figure 21. Western blot and SNA and MAL lectin detection of glycoproteins from OVM, m130 and GG ovarian carcinoma cell lines. For the analysis, three µg of total proteins from cellular extracts (Ext) and secreted vesicles (Ves) were applied per lane. Detection was performed using the chemiluminescent method. Asterisks correspond to most abundant glycoproteins enriched in the secreted vesicles.

4.4.2. Structural analysis of desialylated *N*-glycans from ovarian tumour secreted vesicles, plasma membrane and microsomal fractions

To further elucidate the glycan structures of secreted vesicles comparatively to cellular membranes, the *N*-linked oligosaccharides of SKOV3 and OVM cell-secreted vesicles, plasma membrane, and microsomal enriched fractions were released with PNGase F, desialylated by mild acid hydrolysis and were analyzed by HPAEC-PAD (Figure 22, C, D, and E)

The majority of the peaks eluted in the region of the chromatogram corresponding to high mannose: $Man_5GlcNAc_2$, $Man_6GlcNAc_2$, $Man_7GlcNAc_2$, $Man_8GlcNAc_2$ and $Man_9GlcNAc_2$ (9-18 min) (Figure 22, A and Figure 23, A) and complex *N*-glycans di-, tri-, and tetraantennary with and without LacNAc repeats and proximal Fuc (12-21 min) (Figure 22, B and Figure 23, B).

The HPAEC-PAD profile of secreted vesicles from SKOV3 and OVM cells was distinct from those of plasma membrane and microsomal fractions. For example, the microsomal fraction showed peaks with retention times identical to those of high mannose glycans contrary to other fractions (indicated with asterisks in Figure 22 and Figure 23).

Differences between the *N*-glycans profile of SKOV3 and OVM vesicles were also detected. For example, OVM vesicles showed a relatively larger peak co-eluting with tetraantennary glycans with proximal Fuc (Standard D, Figure 22 and Figure 23).

SKOV3 and OVM plasma membrane and microsomal fractions shared some similarities in their *N*-glycans profile, namely, a high intensity peak with a retention time of approximately 21 min that was almost undetected in the secreted vesicles (Figure 22 and Figure 23).
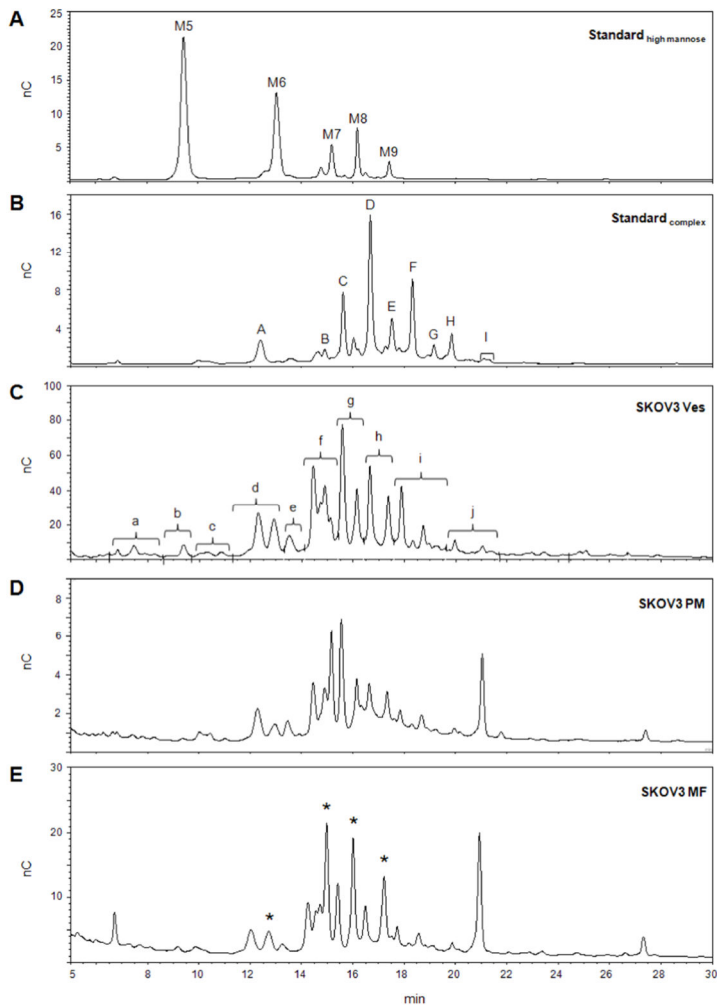
Figure 22. HPAEC-PAD analysis of the desialylated *N*-glycans released from SKOV3-secreted vesicles, plasma membrane and microsomal fractions. (A) High mannose glycan standards from RNase B, structures are: M5, $Man_5GlcNAc_2$; M6, $Man_6GlcNAc_2$; M7, $Man_7GlcNAc_2$; M8, $Man_8GlcNAc_2$; M9, $Man_9GlcNAc_2$. (B) Complex reference glycan standards from erythropoietin from chinese hamster ovary cells, structures (all proximally α6-fucosylated) are: A, diantennary; B, 2,4-triantennary; C, 2,6-triantennary; D, tetraantennary; E, triantennary + one LacNAc repeat; F, tetraantennary + one LacNAc repeat; G, triantennary + two LacNAc repeats; H, tetraantennary + two LacNAc repeats; I, triantennary + three LacNAc repeats and tetraantennary + three LacNAc repeats. (C) Total *N*-glycans of SKOV3-secreted vesicles (Ves). Fractions a–j were subjected to MALDI-TOF-MS analysis (D) Total *N*-glycans of SKOV3 plasma membrane (PM) enriched fraction. (E) Total *N*-glycans of SKOV3 microsomal fraction (MF). Peaks indicated with an asterisk correspond to high mannose glycans.
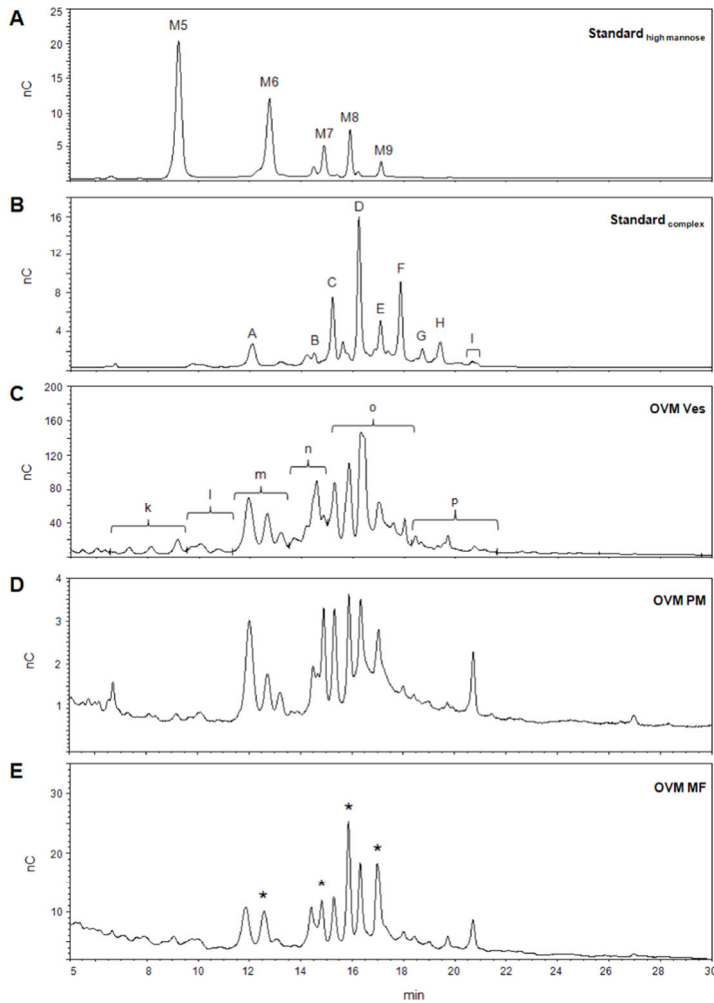
Figure 23. HPAEC-PAD analysis of the desialylated *N*-glycans released from OVM secreted vesicles, plasma membrane and microsomal fractions. (A) High mannose glycan standards from RNase B, structures are: M5, $Man_5GlcNAc_2$; M6, $Man_6GlcNAc_2$; M7, $Man_7GlcNAc_2$; M8, $Man_8GlcNAc_2$; M9, $Man_9GlcNAc_2$. (B) Complex reference glycan standards from erythropoietin from Chinese hamster ovary cells, structures (all proximally α6-fucosylated) are: A, diantennary; B, 2,4-triantennary; C, 2,6-triantennary; D, tetraantennary; E, triantennary + one LacNAc repeat; F, tetraantennary + one LacNAc repeat; G, triantennary + two LacNAc repeats; H, tetraantennary + two LacNAc repeats; I, triantennary + three LacNAc repeats and tetraantennary + three LacNAc repeats. (C) Total *N*-glycans of OVM-secreted vesicles (Ves). Fractions k-p were subjected to MALDI-TOF-MS analysis (D) Total *N*-glycans of OVM plasma membrane (PM) enriched fraction. (E) Total *N*-glycans of OVM microsomal fraction (MF). Peaks indicated with an asterisk correspond to high mannose glycans.

Due to the high complexity of the samples and to obtain more structural information, the total desialylated *N*-glycan pool released from SKOV3 and OVM cell-secreted vesicles, plasma membrane, and microsomal enriched fractions were analysed by MALDI-TOF-MS (Figure 24 and Figure 25). Furthermore, individual fractions of SKOV3 (a-j) (Figure 22, C) and OVM (k-p) (Figure 23, C) vesicles from the HPAEC-PAD profiles were also collected after on-line desalting and were analysed by MALDI-TOF-MS (Supplementary Figure 1 and Supplementary Figure 2). The results of the observed *m/z* and possible glycan structures, compatible with the proposed compositions and considering the *N*-glycosylation biosynthetic pathway of mammalian cells, are indicated in Table I and Table II for SKOV3 and OVM cells, respectively.

The major findings were as follows. Signals at *m/z* 1809.7, 2174.8 and 2539.9 were compatible with complex glycans of the di-, tri- and tetraantennary type with proximal Fuc and they were detected for the secreted vesicles as well as in the plasma membrane and microsomal fractions. The results were found in the two cell lines (Figure 24 and Figure 25).

Signals at *m/z* 1419.5, 1581.6, 1743.6 and 1905.6, compatible with high mannose structures ($Man_6GlcNAc_2$; $Man_7GlcNAc_2$; $Man_8GlcNAc_2$ and $Man_9GlcNAc_2$, respectively) were predominantly found in the microsomal fraction of the two cell lines (Figure 24, C and Figure 25, C).

Peaks at *m/z* 2012.5 and 1850.5 were compatible with agalactosylated truncated structures (triantennary minus one Gal and two Gal, respectively). Peaks at *m/z* 2377.6 and 2215.6 were compatible with tetraantennary glycans less one Gal and two Gal, respectively. These peaks were predominantly found in SKOV3 cells, in all fractions (Figure 24, A-C and Table I). For OVM cells they were found in minor amounts and only in the vesicles fraction (Figure 25, A-C and Table II).

Peaks at *m/z* 1850.5, 2215.6 and 2580.7 in SKOV3-secreted vesicles could also correspond to complex glycans of the di-, tri- and tetraantennary type bearing the LacdiNAc motif (Figure 24, A). This hypothesis agrees with the detection of SKOV3-secreted vesicles with the lectin WFA (Figure 20). These peaks were absent from OVM plasma membrane and microsomal fractions and had a low intensity (1850.5, 2215.6) or were absent (2580.7) from OVM-secreted vesicles (Figure 25, A).

The profiles for secreted vesicles were shown to be more heterogeneous than in the other fractions for the two cell lines. For OVM cells a comparatively higher amount of higher antennarity, tri- and tetraantennary glycans, relatively to diantennary glycans was detected in secreted vesicles versus plasma membrane or microsomal fractions (Figure 23 and Figure 25).
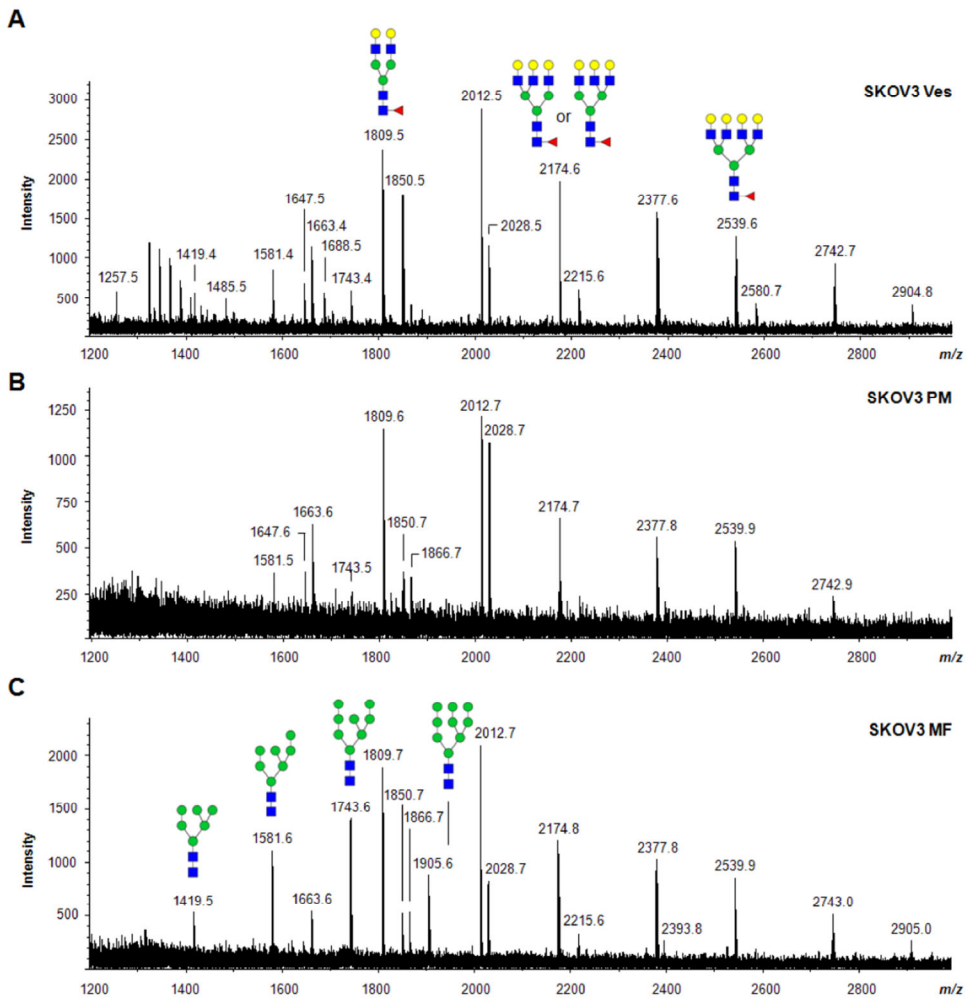
Figure 24. MALDI-TOF-MS analysis of the total desialylated *N*-glycans from SKOV3 cells. (A) secreted vesicles (Ves), (B) plasma membrane fraction (PM), (C) microsomal fraction (MF). Only one or two possible isomeric structures of selected peaks are presented. Graphical representations of glycans are consistent with the nomenclature of the Consortium for Functional Glycomics.
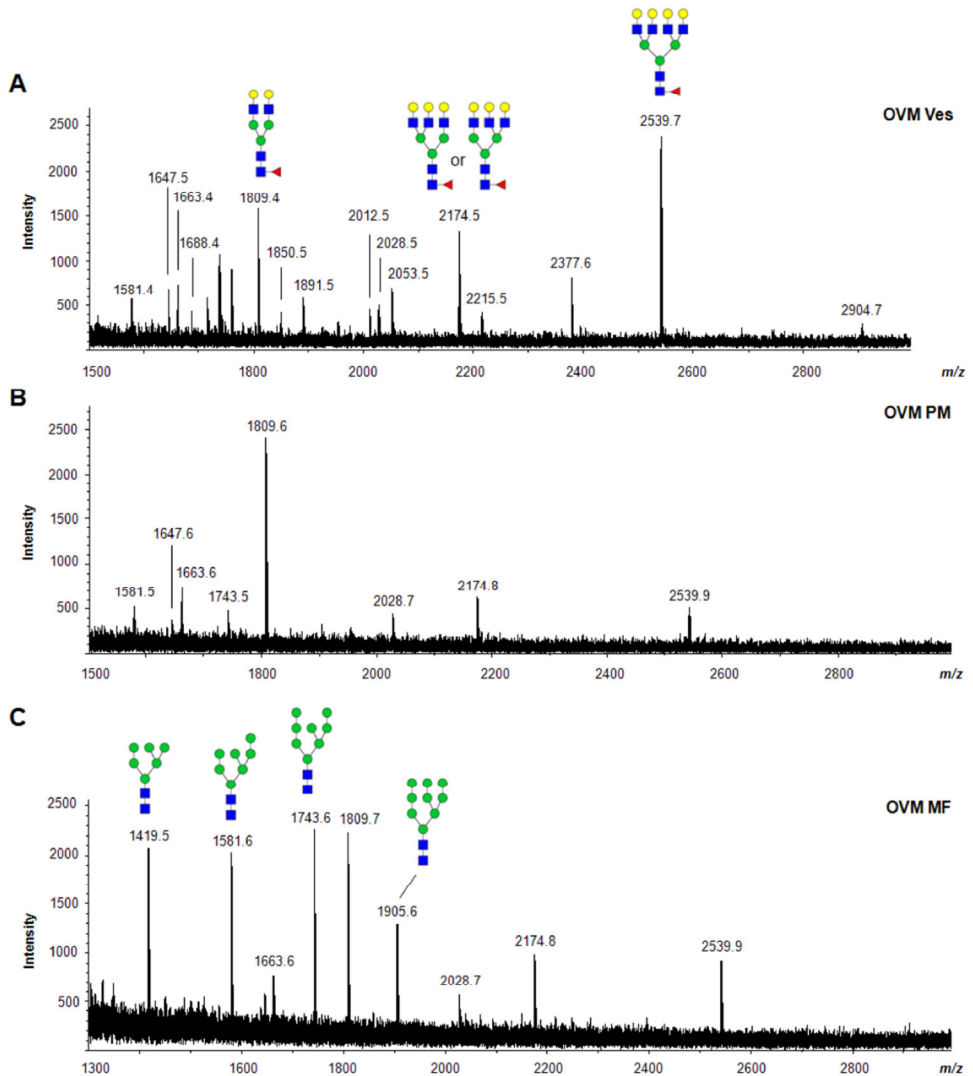
Figure 25. MALDI-TOF-MS analysis of the total desialylated *N*-glycans from OVM cells. (A) secreted vesicles (Ves), (B) plasma membrane fraction (PM), (C) microsomal fraction (MF). Only one or two possible isomeric structures of selected peaks are presented. Graphical representations of glycans are consistent with the nomenclature of the Consortium for Functional Glycomics.

Table I. Observed mass signals (*m/z*) by MALDI-TOF-MS analysis. Proposed composition and compatible structure of the major desialylated *N*-glycans from SKOV3 cells.

Calculated [M+Na]$^+$	Vesicles		Plasma membrane	Microsomal fraction	Proposed composition	Compatible structure
	m/z	HPAEC-PAD fraction	*m/z*	*m/z*		
1257.4	1257.5	b, c	-	-	HexNAc$_2$Hex$_5$	
1298.5	1298.4*	a	-	-	HexNAc$_3$Hex$_4$	
1419.5	1419.4	d, e	-	1419.5	HexNAc$_2$Hex$_6$	
1444.5	1444.5*	a	-	-	HexNAc$_3$Hex$_4$dHex	
1485.5	1485.4	a	-	-	HexNAc$_4$Hex$_3$dHex	
1581.5	1581.4	f, h	1581.6	1581.6	HexNAc$_2$Hex$_7$	
1606.6	1606.5*	c	-	-	HexNAc$_3$Hex$_5$dHex	
1647.6	1647.5	c, a, b, h	1647.6	-	HexNAc$_4$Hex$_4$dHex	
1663.6	1663.4	e	1663.6	1663.6	HexNAc$_4$Hex$_5$	
1688.6	1688.5	c	-	-	HexNAc$_5$Hex$_3$dHex	
1704.6	1704.5*	e	-	-	HexNAc$_5$Hex$_4$	
1743.6	1743.4	g, h	1743.5	1743.6	HexNAc$_2$Hex$_8$	
1809.7	1809.5	d, c, e, f, h	1809.6	1809.7	HexNAc$_4$Hex$_5$dHex	
1850.7	1850.5	a, d, c, e	1850.6	1850.7	HexNAc$_5$Hex$_4$dHex	
1866.6	1866.6*	f	1866.7	1866.7	HexNAc$_5$Hex$_5$	

Table I. Observed mass signals (*m/z*) by MALDI-TOF-MS analysis. Proposed composition and compatible structure of the major desialylated *N*-glycans from SKOV3 cells (continued).
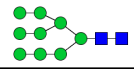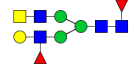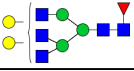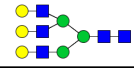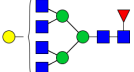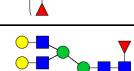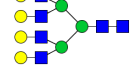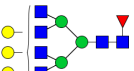
Calculated [M+Na]⁺	Vesicles		Plasma membrane	Microsomal fraction	Proposed composition	Compatible structure
	m/z	HPAEC-PAD fraction	*m/z*	*m/z*		
1905.6	1905.6*	h, i	-	1905.6	HexNAc₂Hex₉	
1996.7	1996.7*	a	-	-	HexNAc₅Hex₄dHex₂	
2012.7	2012.5	f, e, g, h	2012.7	2012.7	HexNAc₅Hex₅dHex	
2028.7	2028.5	i, j, g, h	2028.7	2028.7	HexNAc₅Hex₆	
2053.8	2053.6*	b	-	-	HexNAc₆Hex₄dHex	
2158.8	2158.7*	a	-	-	HexNAc₅Hex₅dHex₂	
2174.8	2174.6	f, g, h, i	2174.7	2174.8	HexNAc₅Hex₆dHex	
2215.8	2215.6	c, f, h	-	2215.8	HexNAc₆Hex₅dHex	
2377.9	2377.6	g, h, i, j	2377.8	2377.8	HexNAc₆Hex₆dHex	
2393.8	-	-	-	2393.8	HexNAc₆Hex₇	
2523.9	2523.8*	b	-	-	HexNAc₆Hex₆dHex₂	
2539.9	2539.6	h, i, j	2539.8	2539.9	HexNAc₆Hex₇dHex	
2580.9	2580.7	h, i	-	-	HexNAc₇Hex₆dHex	

Table I. Observed mass signals (*m/z*) by MALDI-TOF-MS analysis. Proposed composition and compatible structure of the major desialylated *N*-glycans from SKOV3 cells (continued).
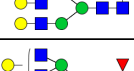
Calculated [M+Na]+	Vesicles		Plasma membrane	Microsomal fraction	Proposed composition	Compatible structure
	m/z	HPAEC-PAD fraction	*m/z*	*m/z*		
2743.0	2742.7	i, j	2742.9	2743	HexNAc$_7$Hex$_7$dHex	
2905.0	2904.8	j, i	-	2905	HexNAc$_7$Hex$_8$dHex	
3108.1	3108.1*	j	-	-	HexNAc$_8$Hex$_8$dHex	
3270.0	3270.1*	j	-	-	HexNAc$_8$Hex$_9$dHex	
3473.2	3473.2*	j	-	-	HexNAc$_9$Hex$_9$dHex	

HexNAc, N-acetylhexosamine (GlcNAc/GalNAc); dHex, deoxyhexose (Fuc); Hex, hexose (Man or Gal). Asterisk denotes compound only detected in the MALDI-TOF-MS analysis of the separated fractions from the HPAEC-PAD analysis (Figure 22, C). Letters underlined represent the HPAEC-PAD fractions where *m/z* signal was predominantly observed. Only one or two possible glycan structures, compatible with the proposed compositions, are shown. Graphical representations of glycans are consistent with the nomenclature of the Consortium for Functional Glycomics.

Table II. Observed mass signals (*m/z*) by MALDI-TOF-MS analysis. Proposed composition and compatible structure of the major desialylated *N*-glycans from OVM cells.

Calculated [M+Na]$^+$	Vesicles		Plasma membrane	Microsomal fraction	Proposed composition	Compatible structure
	m/z	HPAEC-PAD fraction	*m/z*	*m/z*		
1257.4	1257.4*	k, l	-	-	HexNAc$_2$Hex$_5$	
1339.5	1339.5*	k	-	-	HexNAc$_4$Hex$_3$	
1419.5	1419.5*	m	-	1419.5	HexNAc$_2$Hex$_6$	
1444.5	1444.5*	k	-	-	HexNAc$_3$Hex$_4$dHex	
1485.5	1485.6*	k, l	-	-	HexNAc$_4$Hex$_3$dHex	
1501.5	1501.6*	l	-	-	HexNAc$_4$Hex$_4$	
1581.5	1581.4	n, o	1581.5	1581.6	HexNAc$_2$Hex$_7$	
1606.6	1606.6*	l	-	-	HexNAc$_3$Hex$_5$dHex	
1647.6	1647.4	l, k	1647.6	-	HexNAc$_4$Hex$_4$dHex	
1663.6	1663.4	m, n, p	1663.6	1663.6	HexNAc$_4$Hex$_5$	
1688.6	1688.4	l	-	-	HexNAc$_5$Hex$_3$dHex	
1743.6	1743.6*	o	1743.5	1743.6	HexNAc$_2$Hex$_8$	
1768.6	1768.4*	n	-	-	HexNAc$_3$Hex$_6$dHex	
1809.7	1809.4	m, l, n	1809.6	1809.7	HexNAc$_4$Hex$_5$dHex	
1850.7	1850.5	k, m	-	-	HexNAc$_5$Hex$_4$dHex	

113

Table II. Observed mass signals (*m/z*) by MALDI-TOF-MS analysis. Proposed composition and compatible structure of the major desialylated *N*-glycans from OVM cells (continued).
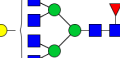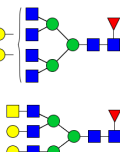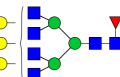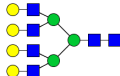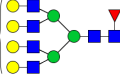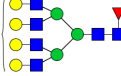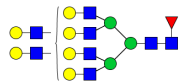
Calculated [M+Na]$^+$	Vesicles		Plasma membrane	Microsomal fraction	Proposed composition	Compatible structure
	m/z	HPAEC-PAD fraction	*m/z*	*m/z*		
1891.7	1891.5	m, n	-	-	HexNAc$_6$Hex$_3$dHex	
1905.6	1905.6*	p, o	-	1905.6	HexNAc$_2$Hex$_9$	
1955.7	1955.7*	k, m	-	-	HexNAc$_4$Hex$_5$dHex$_2$	
2012.7	2012.5	n	-	-	HexNAc$_5$Hex$_6$dHex	
2028.7	2028.5	p, o	2028.7	2028.7	HexNAc$_5$Hex$_6$	
2053.8	2053.5	n	-	-	HexNAc$_6$Hex$_4$dHex	
2174.8	2174.5	n, o, p	2174.7	2174.8	HexNAc$_5$Hex$_6$dHex	
2215.8	2215.5	o, l	-	-	HexNAc$_6$Hex$_6$dHex	
2377.9	2377.8	o	-	-	HexNAc$_6$Hex$_6$dHex	
2393.8	2393.8*	p	-	-	HexNAc$_6$Hex$_7$	
2539.9	2539.5	o, p	2539.9	2539.9	HexNAc$_6$Hex$_7$dHex	
2743.0	2742.9*	p	-	-	HexNAc$_7$Hex$_7$dHex	
2905.0	2904.7	p	-	-	HexNAc$_7$Hex$_8$dHex	

Table II. Observed mass signals (*m/z*) by MALDI-TOF-MS analysis. Proposed composition and compatible structure of the major desialylated *N*-glycans from OVM cells (continued).
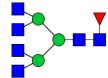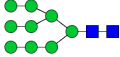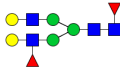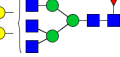
Calculated [M+Na]$^+$	Vesicles		Plasma membrane	Microsomal fraction	Proposed composition	Compatible structure
	m/z	HPAEC-PAD fraction	*m/z*	*m/z*		
3270.2	3270.1*	p	-	-	HexNAc$_8$Hex$_6$dHex	

HexNAc, N-acetylhexosamine (GlcNAc/GalNAc); dHex, deoxyhexose (Fuc); Hex, hexose (Man or Gal). Asterisk denotes compound only detected in the MALDI-TOF-MS analysis of the separated fractions from the HPAEC-PAD analysis (Figure 23, C). Letters underlined represent the HPAEC-PAD fractions where *m/z* signal was predominantly observed. Only one or two possible glycan structures, compatible with the proposed compositions, are shown. Graphical representations of glycans are consistent with the nomenclature of the Consortium for Functional Glycomics.

4.5. Discussion

Vesicles secreted by cells, including exosomes, are released by ovarian tumour cells (Gutwein *et al*., 2005) and are found in the blood and malignant ascites of the patients (Li *et al*., 2009; Runz *et al*., 2007). Furthermore, they are potential targets for the discovery of new disease biomarkers.
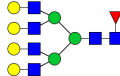
Alterations in glycosylation constitutes a common trait in many types of cancer, and antibodies against glycan epitopes at the cell surface have been used as diagnostic for several carcinomas (Peracaula *et al*., 2008). Lectin profiling studies previously performed in our group showed that exosomes secreted from ovarian tumour SKOV3 cells were enriched in specific mannose and sialic acid-containing glycoproteins (Chapter 3). In the present study we have shown by lectin blot that the glycosylation profile

of SKOV3-secreted vesicles was also different from other membrane enriched fractions, namely plasma membrane and microsomal enriched fractions. Our observations are in agreement with the results obtained using lectin microarrays in T-cells microvesicles that showed enrichment in high mannose and sialic acid-containing structures, as well as complex *N*-glycans, and fucosylated structures in comparison with cell membranes micellae (Krishnamoorthy *et al*., 2009). Furthermore, the results allowed the identification of glycoproteins that are specific for secreted vesicles and possibly constitute exosomes markers. Further studies are required to purify and characterize those proteins by lectin affinity chromatography, followed by peptide mass fingerprinting. Antibodies raised against the polypeptide part will allow clarifying if specific proteins or protein glycoform are enriched in exosomes.

In addition, lectin detection revealed that SKOV3- and OVM-secreted vesicles had specific α2,3- and/or α2,6-linked NeuAc-containing glycoproteins that were not detected in other fractions. Since altered expression of certain sialic acid types or their linkages can have prognostic significance in several human cancers (reviewed in Li *et al*., 2010) it will be interesting to analyse the profile of native oligosaccharides from secreted vesicles and from the other membrane enriched fractions.

In order to further elucidate the *N*-glycan structures in the secreted vesicles from ovarian tumour cells, relatively to plasma membrane and microsomal fractions, SKOV3 and OVM cells were analysed by HPAEC-PAD followed by MALDI-TOF-MS. As a common feature the results indicated the presence of glycans of the di-, tri- and tetraantennary type with proximal Fuc in secreted vesicles of SKOV3 and OVM cells, as well as in plasma membrane and microsomal fractions. The abundance of proximally fucosylated complex partially agalactosylated glycan structures in all fractions of SKOV3 cells was also detected.

A higher amount of high mannose structures was found in microsomal fractions of both SKOV3 and OVM cell lines. Since the endoplasmic reticulum is a major component of the microsomal fraction (Michelsen and Hagen, 2009) these high mannose glycans probably correspond to unprocessed structures characteristic of glycoproteins in transit or resident in the endoplasmic reticulum.

Moreover, the results suggested the presence of the LacdiNAc motif in SKOV3-secreted vesicles, which was in agreement with the WFA detection of specific bands in secreted vesicles. Partially agalactosylated glycans and the LacdiNAc motif have already been described in endogenous cellular and supernatant glycoproteins from SKOV3 cells (Machado *et al*., 2011). The LacdiNAc motif is associated with glycoproteins secreted by tumour cells such as ribonuclease I found in pancreatic tumour cells (Peracaula *et al*., 2003), plasminogen activator from Bowes melanoma cells (Chan *et al*., 1991), and glycodelin-A that is increased in many gynecological tumours (Horowitz *et al*., 2001).

Glycan profiles of secreted vesicles from the two cell lines studied were more heterogeneous than the plasma membrane or the microsomal fraction. The results also suggested a comparatively higher amount of more processed glycans of the tri- and tetraantennary types in secreted vesicles in comparison with plasma membrane and microsomal fractions for the OVM cells. This effect could be due to more processed glycoforms of a certain glycoprotein being enriched in exosomes, as suggested for ADAM10 (Chapter 2). Alternatively, the enrichment of specific glycoproteins with more processed glycans in exosomes would be plausible. To explore these hypothesis further work is required in characterizing purer exosome fractions, in exploring additional cell lines, and in improving glycan separation, possibly after labelling, for quantitation.

From our knowledge this is the first study endeavouring the detailed structural analysis of the *N*-glycans present in glycoproteins from ovarian

tumour-secreted vesicles. In this work, secreted vesicles were isolated by ultracentrifugation at 100,000 x g since this fraction has been shown to be enriched in exosomes (Théry *et al*., 2006). Preliminary results using Nanoparticle Tracking Analysis (Nanosight) revealed that the majority of the isolated SKOV3- and OVM-secreted vesicles had average sizes of 134 and 113 nm, respectively. Nonetheless, vesicles with smaller and larger dimensions were also detected (data not shown). Secreted vesicles can be further purified using a sucrose gradient. Purified exosomes have a density of 1.13-1.19 g/ml and have a size between 40-100 nm (Simons and Raposo, 2009). Therefore, it would be interesting to analyse the *N*-glycans from purified exosomes not only to confirm if *N*-glycan structures enriched in the secreted vesicles are found in exosomes but also to investigate if additional specific structures are found.

The knowledge of *N*-glycan structures present in purified exosomes could provide the basis for further studies on the mechanisms involved in exosomes biogenesis. In a more applied perspective, the identification of specific *N*-glycans might give new insights for biomarkers discovery and cancer vaccination.

4.6. Acknowledgements

Chapter 5

General discussion and conclusions

5. General discussion and conclusions

5.1. General discussion and perspectives

Ovarian cancer has the highest mortality rate among the gynecological malignancies in the Western world. Long-term survival has not changed significantly in the last two decades, largely due to inadequate diagnostic approaches and the lack of efficient treatments.

Aberrant protein glycosylation is an early event of oncogenic transformation; therefore, glycan structures represent ideal targets for tumour specific diagnosis and new anti-tumour therapeutic strategies. In ovarian cancer a number of proteins were found to be aberrantly glycosylated, including CA125 (Jankovic and Milutinovic, 2008), alpha-1-proteinase inhibitor, haptoglobin (Turner *et al*., 1995), immunoglobulin G, and other acute phase proteins (Saldova *et al*., 2007). Moreover, an increased sialylation of proteins and deregulated sialylation pathways were also observed (Aranganathan *et al*., 2005).

Exosomes are small membrane vesicles that are secreted by several cell types, including ovarian tumour cells (Gutwein *et al*., 2005), and have been found *in vivo* in several biological fluids, such as blood and malignant ascites of ovarian cancer patients (Caby *et al*., 2005; Runz *et al*., 2007). Exosomes have the ability to interact with other cells and were shown to contribute to tumour progression by promoting immune escape mechanisms, facilitating extracellular matrix degradation and transferring proteins and genetic material among cells (reviewed in Muralidharan-Chari *et al*., 2010).

Although many studies have been carried out to identify the protein, lipid and RNA composition of exosomes, little is known about the glycosylation profile of these secreted vesicles and the potential role of *N*-glycans in protein sorting to exosomes or in recognition and uptake of exosomes by target cells.

In this context, the intent of this Thesis was to investigate the protein glycosylation profile of vesicles secreted from ovarian tumour cells. In addition, the biological role of *N*-glycans in ADAM10 protein sorting to exosomes and in the internalization of SKOV3 exosomes by SKOV3 cells was explored.

5.1.1. Exosome specific glycoproteins/glycoforms

Proteomic studies have shown that glycoproteins, similarly to other proteins, are found in exosomes (Simpson *et al*., 2008). In addition, some reports have described the presence of heavily glycosylated forms of some proteins, such as FAS-L (Abrahams *et al*., 2003) and the prion precursor protein (Vella *et al*., 2007), in secreted vesicles that are not detected in cellular extracts. In this context, here the use of lectins with different carbohydrate specificities revealed that vesicles secreted from SKOV3 and OVM cells contained specific glycoproteins, in particular proteins containing α2,3-linked sialic acid, that were not detected in cellular extracts, plasma membrane or microsomal enriched fractions (Chapter 4). Vesicles secreted from SKOV3 cells were also found to strongly bind Con A, which recognizes predominantly high mannose glycans, compared with other fractions (Chapter 3 and Chapter 4). Furthermore, secreted vesicles from the two cell lines were found to contain a higher amount of *N*-glycans than plasma membrane or microsomal fractions, as shown by the peak intensities in the HPAEC-PAD profiles (Chapter 4). These results together

showed that specific glycoproteins and/or glycoforms were enriched in ovarian tumour secreted vesicles. The molecular mechanisms underlying this enrichment are still not known.

To date, several mechanisms of protein sorting to exosomes have been proposed. The most studied involves the recognition of ubiquitinated proteins by the ESCRT machinery (reviewed in Lakkaraju and Rodriguez-Boulan, 2008; Simons and Raposo, 2009). In SKOV3 cells, this pathway might account for the recruitment of some proteins to exosomes since exosomal proteins were found to be heavily ubiquitinated in comparison with cellular proteins (Chapter 2) and SKOV3 exosomes contained TSG101, a protein that is involved in the ESCRT sorting machinery (unpublished data). Overexpressed ADAM10-HA was also found to be ubiquitinated in exosomes, however due to the low protein expression it was not possible to determine if endogenous ADAM10 was also ubiquitinated in exosomes (Chapter 2). To substantiate the possibility of glycoproteins being sorted to exosomes via ESCRT, RNA interference targeting different mRNAs coding for proteins involved in the ESCRT machinery could be used and the presence of different glycoproteins monitored in exosomes.

Nevertheless, not all proteins found in exosomes are ubiquitinated and other sorting mechanisms might coexist in the same cells, depending on the cargo protein or even for the same protein. Mechanisms involving partitioning into cholesterol and sphingolipid-rich lipid microdomains (lipid-rafts and tetraspanin webs) and higher-order oligomerization (aggregation of oligomers) at the plasma membrane might be involved in protein sorting to exosomes (de Gassart *et al.*, 2003; Trajkovic *et al.*, 2008; Lakkaraju *et al.*, 2008; Schorey *et al.*, 2008). On the other hand, *N*-glycans have been implicated in protein sorting mechanisms, for example, acting as apical targeting signals for secretory proteins in epithelial cells (Scheiffele *et al.*, 1995). Moreover, they might interact with galectins at the cell surface

leading to their enrichment in membrane lipid domains (Garner and Baum, 2008) and have been described to mediate oligomerization via interaction with lectins (Vidal *et al*., 1997). Therefore, it is possible that glycans could also play a role on protein sorting to exosomes and consequently the presence of specific glycoproteins and/or glycoforms in secreted vesicles could be the result of more complex type glycoforms being preferentially sorted to the multivesicular bodies and/or to the exosomes. A glycan-dependent protein sorting mechanism that targets proteins to microdomains from where both microvesicles and HIV particles emerge has already been proposed in T-cells (Krishnamoorthy *et al*., 2009). Further studies are still required to understand if glycosylated proteins have specific mechanisms of sorting to exosomes and if glycans play any role in this sorting process. It is also feasible that different protein glycoforms are sorted to exosomes through different mechanisms.

The enrichment of specific *N*-glycans in exosomes could also result from the fact that more processed glycoforms are less susceptible to proteolysis. Thus *N*-glycans could have a role in the protection of proteins present in secreted vesicles. The role of *N*-glycans in protein stability and steric protection of susceptible sites from attack by proteases is well known (Varki, 1993; Opdenakker *et al*., 1993). This protection by *N*-glycans has been observed for several proteins, including ADAM10, where the removal of N439 glycosylation site exposed a particular region susceptible to protease degradation (Chapter 2). Supporting the hypothesis that exosomes are enriched in proteolytic activity are the observations that active metalloproteases, such as the membrane type 1 matrix metalloproteinase (Hakulinen *et al*., 2008) and ADAM10 (Stoeck *et al*., 2006), are present in exosomes and are capable of cleaving protein substrates. Accordingly, in SKOV3 exosomes, an ADAM10 proteolytic product resulting from metalloprotease cleavage was found in exosomes and not in cellular extracts (Chapter 2).

More studies are still necessary to fully elucidate the mechanisms underlying the enrichment of specific glycoproteins/glycoforms in exosomes.

5.1.2. Internalization of exosomes by target cells

Exosomes can interact and be internalized by target cells. They can deliver cytokines, growth factors, receptors and genetic material, thus conferring new functional properties to the recipient cells. The process of internalization can occur through direct fusion of the exosomes with the plasma membrane or alternatively, exosomes can enter the cells via clathrin-mediated endocytosis, phagocytosis or macropinocitosys (Morelli, *et al*., 2004; Feng *et al*., 2010; Fitzner *et al*., 2011). In Chapter 3, SKOV3 cell-derived exosomes were found to be internalized by SKOV3 cells in an energy-dependent process, via various endocytic pathways. Incubation with different endocytic inhibitors showed that a clathrin-mediated endocytosis pathway, macropinocytosis and a cholesterol associated pathway independent of caveolae were associated with the uptake.

The initial recognition events that precede uptake may involve several molecules such as proteins (Chapter 3) (Simons and Raposo, 2009), lipids (Keller *et al*., 2009) or glycans (Hao *et al*., 2007) present at the cell surface or in the exosomes membrane. Glycans have been shown to bind specifically carbohydrate receptors (lectins) on other cell surfaces and mediate several biological interactions such as cell-cell adhesion and host-pathogen recognition (reviewed in Brooks, 2009). Many pathogens, such as HIV and the influenza virus, are dependent on the recognition of specific glycan epitopes for the process of infection to occur. Since virus and exosomes might share similar biogenesis and internalization pathways (Izquierdo-Useros *et al*., 2011), it is plausible that glycans could also have a

role in exosomes uptake by target cells. Accordingly, studies have shown that in dendritic cells exosome uptake was at least in part mediated by a C-type lectin and was specifically inhibited by mannose and *N*-acetylglucosamine (Hao *et al*., 2007). In macrophages, lactose was found to reduce exosomes uptake probably through its action on galectin-5 (Barres *et al*., 2010).

In SKOV3 cells, NeuAc removal from exosomes caused a trend towards an increase of uptake but sugar inhibition assays with fucose, mannose, galactose, *N*-acetylglucosamine or lactose reduced exosomes uptake to the same extent as the control glucose (Chapter 3). Overall these results suggested that *N*-glycans did not play a major role in exosomes uptake by ovarian tumour SKOV3 cells.

The observation that *N*-glycans are important for exosomes uptake in antigen presenting cells such as dendritic cells or macrophages but not in tumour cells, like SKOV3 cells, might be explained by the fact that different cell types have different internalization mechanisms depending on their function. Antigen presenting cells were shown to recognize pathogens through specific carbohydrate-binding proteins, especially C-type lectins, galectins and sialic acid-specific lectins of the Siglec family that recognize specific glycan structures such as Lewis[x], Lewis[y], GlcNAc, high mannose structures and sialic acid (reviewed in van Kooyk and Rabinovich, 2008; Davicino *et al*., 2011). This interaction leads to antigen presentation and signalling in antigen presenting cells, thus modulating immune responses. Similarly dendritic cells were shown to internalize exosomes that can also mediate immune responses either as activators or as inhibitors depending on their source (Théry *et al*., 2009). It would be interesting to investigate the role of *N*-glycans in the uptake of SKOV3 cell-derived exosomes by dendritic cells and explore the potential differences between the internalization mechanisms of antigen-presenting and tumour cells.

The interaction and internalization of tumour cell-derived exosomes by the same tumour cells that produced them raises several questions, namely the *in vivo* role of this phenomenon. Microvesicles secreted from tumour cells can be internalized by normal cells and transfer RNA and proteins that promote tumour growth (Skog *et al*., 2008). Similarly, tumour cell-derived exosomes could also be internalized by the same tumour cells to transfer information and facilitate tumour progression and dissemination. For example, glioblastoma secreted vesicles were shown to transfer the oncogenic form of the epidermal growth factor receptor, known as EGFRvIII, between cells with an aggressive phenotype and glioblastoma cells lacking EGFRvIII (Al-Nedawi *et al*., 2008) and exosomes from melanoma cells were found to transfer the tumour-associated protein caveolin-1 to melanoma cells that do not express this protein (Parolini *et al*., 2009). Further investigation is required to clarify all the biological roles of tumour exosomes uptake by the same cells that produce them. This knowledge could help to unveil the role of secreted vesicles in tumour progression and dissemination.

5.1.3. Exosomes from ovarian tumour cells as biomarkers and potential therapeutic targets

A major goal in the field of ovarian cancer research is to identify biomarkers for the early diagnosis of the disease. The ability to isolate exosomes, in a non-invasive manner, from different physiological sources such as blood, holds significant potential. Several studies have shown that microRNA profile and proteins expressed in exosomes might be used as markers for the early detection and diagnosis of diseases, for determining

prognosis, and for prediction of therapeutic efficacy (Taylor and Gercel-Taylor, 2008; Rabinowits *et al*., 2009; Li *et al*., 2009; Lu *et al*., 2009).

Cell surface glycosylation is one of the major changes that occur in cancer cells. Alterations include the synthesis of highly branched and heavily sialylated glycans, the premature termination of biosynthesis resulting in the expression of uncompleted forms and the re-expression of glycosidic antigens of fetal type (reviewed in Dall'Olio, 1996). As a result, many of the markers used to detect tumours are glycoproteins and glycan epitopes (Peracaula *et al*., 2008).

In this study, the analysis of different human ovarian tumour cell lines and neuroglioma H4 cells revealed that secreted vesicles contained specific glycoproteins, in particular high mannose and sialic acid-containing proteins, which were not found in cellular extracts or other membrane enriched fractions such as plasma membrane or microsomal fractions (Chapter 3 and Chapter 4). In the future, the purification of these specific glycoproteins, by lectin affinity chromatography, and their characterization might help to establish if they constitute exosome markers. Additionally, antibodies raised against these glycoproteins could be used to screen for the presence of exosome markers in other cell lines.

Studies are still required to determine if the glycoproteins, detected by lectin blot in secreted vesicles, are specific or enriched in tumour cell-derived vesicles. If confirmed, their use as cancer markers could be explored. Furthermore, given that the rate of exosomes release has been shown to correlate with tumour invasiveness (Ginestra *et al*., 1999), it would be interesting to explore the possibility of using these glycoproteins to monitor disease progression.

The structural analysis of the glycan epitopes of ovarian tumour cells by HPAEC-PAD and MALDI-TOF-MS (Chapter 4) suggested the presence of the LacdiNAc motif in SKOV3 cells secreted vesicles (Chapter 4). The LacdiNAc motif has already been described in endogenous cellular

and secreted glycoproteins from SKOV3 cells (Machado *et al.*, 2010) and it has previously been reported in glycoproteins associated to tumour cells, such as, ribonuclease I found in pancreatic tumour cells (Peracaula *et al.*, 2003), plasminogen activator from Bowes melanoma cells (Chan *et al.*, 1991) and glycodelin-A that is increased in many gynecological tumours (Horowitz *et al.*, 2001). Since exosomes can be collected from biological fluids, the presence of the LacdiNac motif could be investigated in exosomes from the blood or ascitic fluid of ovarian cancer patients to determine the potential use of this motif as a diagnosis and/or prognosis marker.

The use of exosomes in immunotherapy has also become a promising area of research. Exosomes are good candidates for the selective delivery of drugs, small molecules or agents for gene therapy mainly due to their ability to evade immune recognition, cell-specificity, efficient cargo delivery and low immunogenicity (reviewed in Tan *et al.*, 2010). Using nanotechnology, exosomes can also be engineered to carry cytokines, DNA, RNA, adjuvants, labels, costimulatory signals, and gene therapy vectors (reviewed in Tan *et al.*, 2010).

Several studies have already shown the potential of exosomes to carry and transfer information. Exosomes derived from murine mast cells were found to deliver functional mRNAs to human mast cells (Valadi *et al.*, 2007) and the delivery of curcumin by exosomes was found to be more effective in preventing septic shock than the delivery using liposomes (Sun *et al.*, 2010). Recently, purified exosomes, loaded with exogenous siRNA and targeted to neurons, were shown to deliver siRNA specifically to mouse brain, suggesting that exosomes might cross the blood-brain barrier (Alvarez-Erviti *et al.*, 2011).

The observation that B-cell derived exosomes could bear functional MHC class II complexes leading to antigen specific T-cell activation *in vitro* (Raposo *et al.*, 1996) and the capacity of exosomes released from dendritic

cells, pulsed with tumor antigens, to stimulate T-cells and to promote anti-tumour immune responses *in vivo* (Zitvogel *et al*., 1998) has lead to clinical studies exploiting the application of exosomes as therapeutic vaccines. To date, three Phase I clinical trials have been conducted involving the application of dendritic cell derived exosomes to elicit immune responses against established tumours of colorectal, melanoma and non-small cell lung carcinoma (Dai *et al*., 2008; Escudier *et al*., 2005; Morse *et al*., 2005). In all studies, exosomes were proven to be safely administered but the immune responses were very limited. In the future immune responses will need to be enhanced by using proper adjuvants or by engineering exosomes with tumour antigens to make them more recognizable to the immune system (Tan *et al*., 2010). A Phase II clinical trial using dendritic cell-derived exosomes, with enhanced bioactivity, in inoperable non small cell lung cancer is currently in progress (ClinicalTrials.gov identifier: NCT01159288).

The identification of glycoproteins and/or glycans enriched in vesicles secreted by tumour cells may provide with specific and more efficient targets for the development of future cancer vaccines. Several carbohydrate-based vaccines have already been developed and some have proceeded into clinical trials (reviewed in Vliegenthart, 2006; Astronomo and Burton, 2010). As an example, the LacdiNAc motif that is uncommon in mammals but that is frequently expressed by helminth parasites was found to induce an immune response mediated by galectin-3 (van den Berg *et al*., 2004). Since the LacdiNAc is found in SKOV3 secreted vesicles, the use of this motif in the development of a vaccine against ovarian cancer could be explored.

In a different approach, exosomes immune properties could be influenced by changing their glycoprotein and/or glycan composition. Exosomes could be modified to carry or overexpress specific glycoproteins or glycan epitopes in order to increase their immunogenicity and enhance

possible immune responses against the tumour from where they originated. This could be achieved with the genetic engineering of the corresponding cell lines (overexpression of the target glycoprotein and/or engineering of the glycosylation pathway) or with the modulation of exosome glycosylation using glycosyltransferases *in vitro*. Additional studies are required to understand the potential of the glycoproteins and glycans, identified in secreted vesicles, in the induction of immune responses against tumour cells.

The study performed in this Thesis used vesicles secreted from ovarian tumour cells in culture; however, this approach has some obvious limitations. Cells in culture have been selected through successive passages and their exosomes may display a molecular composition distinct from patient exosomes. Moreover, most human tumours are a heterogeneous mixture of different cells that potentially release exosomes as well as other vesicles. It would be interesting to perform a detailed *N*-glycosylation analysis of exosomes derived from blood and malignant ascites of patients with ovarian carcinoma to confirm and possibly identify new glycoproteins and/or *N*-glycans that could be used as biomarkers and/or therapeutic targets in ovarian cancer.

5.2. General conclusions

The work described in this Thesis allowed a better understanding of the protein glycosylation of vesicles secreted by ovarian tumour cells.

N-glycosylation was shown to have important functions in ADAM10 processing, protection from proteolysis, and full-enzyme activity.

Exosomes from SKOV3 ovarian tumour cells were shown to be internalized by the same cell line that produced them via several endocytic pathways but *N*-glycans had no major role in the internalization process.

SKOV3 secreted vesicles were found to be enriched in specific mannose- and sialic acid-containing glycoproteins that were not present in cellular extracts, plasma membrane or microsomal fractions.

The *N*-glycan profiles of cellular fractions and vesicles of SKOV3 and OVM cells showed some distinguishing features: the microsomal fractions were abundant in high mannose glycans; the profiles of secreted vesicles were more heterogeneous than those of plasma membrane or microsomal fractions and contained complex type glycans, which for SKOV3 cells were partially truncated; the LacdiNAc motif was found enriched in SKOV3 vesicles.

In summary, this work contributed to a better knowledge of the protein glycosylation of vesicles secreted by tumour cells and opens new perspectives in the use of specific glycoproteins and/or *N*-glycans as potential biomarkers and therapeutic targets.

Supplementary material

Supplementary Figure 1

SKOV3 cells
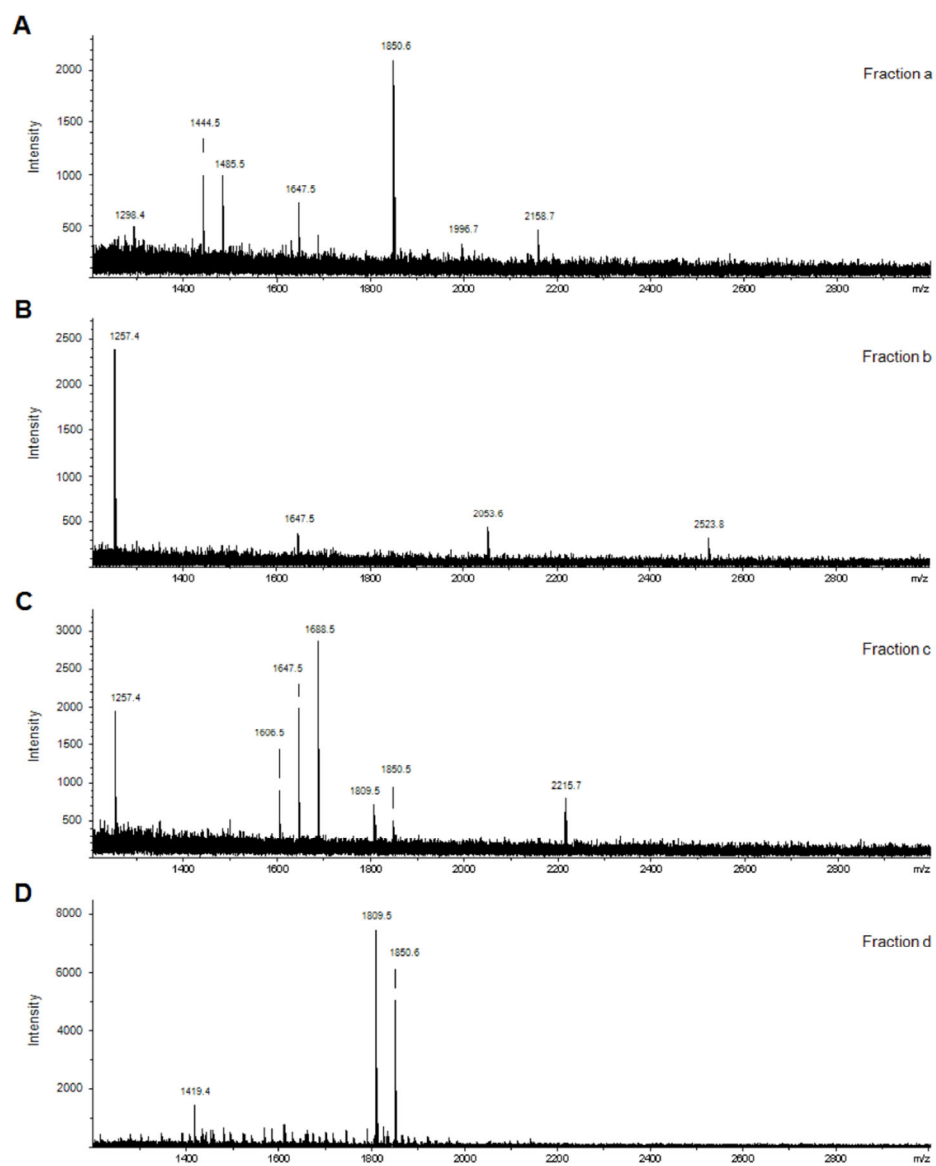
Supplementary Figure 1 (continued)
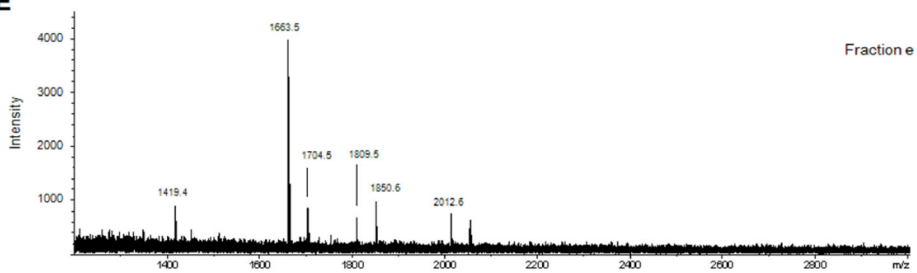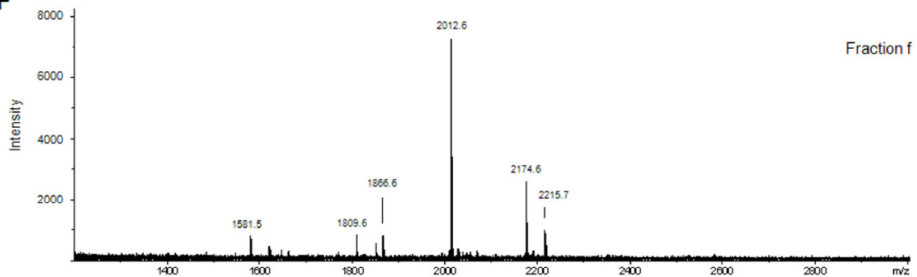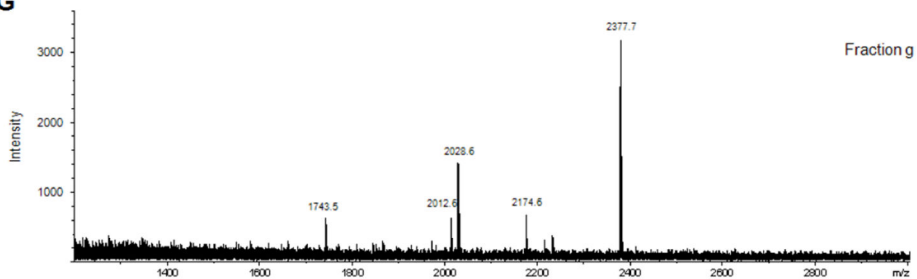
Supplementary Figure 1 (continued)
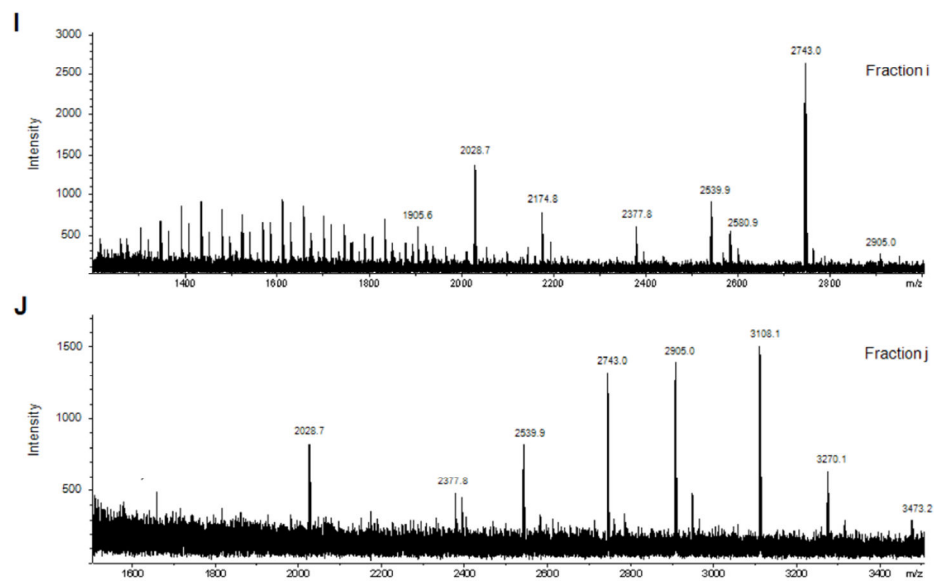
Supplementary Figure 2
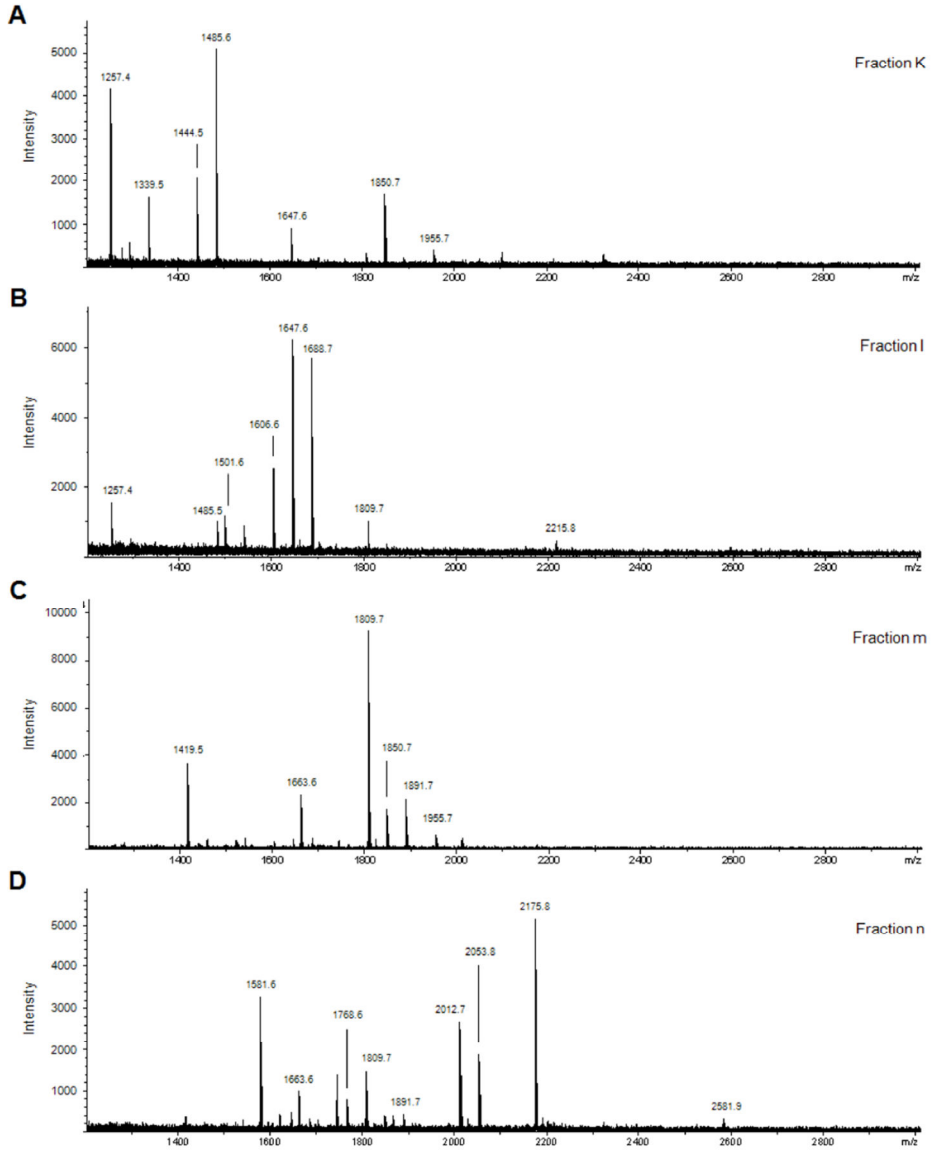
Supplementary Figure 2 (continued)

OVM cells
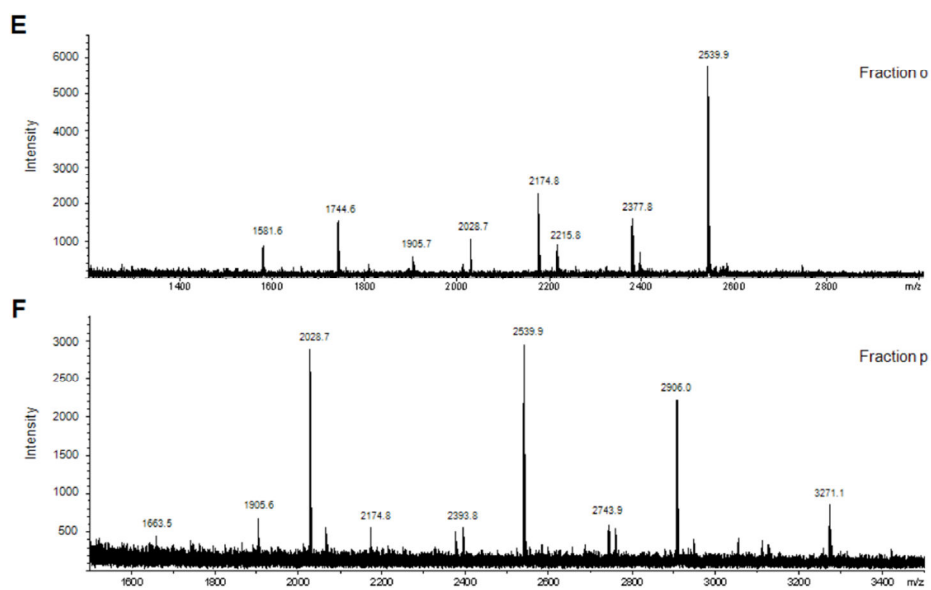
Supplementary Figure 1. MALDI/TOF-MS analysis of desialylated *N*-linked oligosaccharides from SKOV3 secreted vesicles, obtained from fractions a-j (Figure 22).

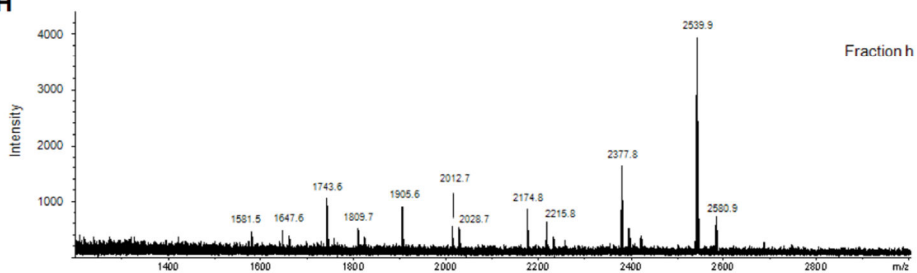**Supplementary Figure 2.** MALDI/TOF-MS analysis of desialylated *N*-linked oligosaccharides from OVM secreted vesicles, obtained from fractions k-p (Figure 23).

References

References

Abbott KL, Nairn AV, Hall EM, Horton MB, McDonald JF, Moremen KW, Dinulescu DM, and Pierce M (2008). Focused glycomic analysis of the N-linked glycan biosynthetic pathway in ovarian cancer. *Proteomics*. 8: 3210-3220.

Abrahams VM, Straszewski SL, Kamsteeg M, Hanczaruk B, Schwartz PE, Rutherford TJ, and Mor G (2003). Epithelial Ovarian Cancer Cells Secrete Functional Fas Ligand. *Cancer Res*. 63: 5573-5581.

Admyre C, Johansson SM, Qazi KR, Filen JJ, Lahesmaa R, Norman M, Neve EP, Scheynius A, and Gabrielsson S (2007). Exosomes with immune modulatory features are present in human breast milk. *J Immunol*. 179: 1969-1978.

Al-Nedawi K, Meehan B, Micallef J, Lhotak V, May L, Guha A, and Rak J (2008). Intercellular transfer of the oncogenic receptor EGFRvIII by microvesicles derived from tumour cells. *Nat Cell Biol*. 10: 619-624.

Alvarez-Erviti L, Seow Y, Yin H, Betts C, Lakhal S, and Wood MJ (2011). Delivery of siRNA to the mouse brain by systemic injection of targeted exosomes. *Nat Biotechnol*. 29: 341-345.

Amour A, Knight CG, Webster A, Slocombe PM, Stephens PE, Knauper V, Docherty AJ, and Murphy G (2000). The in vitro activity of ADAM-10 is inhibited by TIMP-1 and TIMP-3. *FEBS Lett*. 473: 275-279.

Anders A, Gilbert S, Garten W, Postina R, and Fahrenholz F (2001). Regulation of the {alpha}-secretase ADAM10 by its prodomain and proprotein convertases. *FASEB J.* 15: 1837-1839.

Andre F, Schartz NE, Chaput N, Flament C, Raposo G, Amigorena S, Angevin E, and Zitvogel L (2002). Tumor-derived exosomes: a new source of tumor rejection antigens. *Vaccine*. 20 Suppl 4: A28-31.

Aranganathan S, Senthil K, and Nalini N (2005). A case control study of glycoprotein status in ovarian carcinoma. *Clin Biochem*. 38: 535-539.

References

Arribas, J., and S. Ruiz-Paz. (2005). ADAM 17: Regulation of Ectodomain Shedding. Springer, Netherlands.

Astronomo RD, and Burton DR (2010). Carbohydrate vaccines: developing sweet solutions to sticky situations? *Nat Rev Drug Discov*. 9: 308-324.

Badgwell D, and Bast RC, Jr. (2007). Early detection of ovarian cancer. *Dis Markers*. 23: 397-410.

Bard MP, Hegmans JP, Hemmes A, Luider TM, Willemsen R, Severijnen LA, van Meerbeeck JP, Burgers SA, Hoogsteden HC, and Lambrecht BN (2004). Proteomic analysis of exosomes isolated from human malignant pleural effusions. *Am J Respir Cell Mol Biol*. 31: 114-121.

Barres C, Blanc L, Bette-Bobillo P, Andre S, Mamoun R, Gabius H-J, and Vidal M (2010). Galectin-5 is bound onto the surface of rat reticulocyte exosomes and modulates vesicle uptake by macrophages. *Blood*. 115: 696-705.

Bast RC, Hennessy B, and Mills GB (2009). The biology of ovarian cancer: new opportunities for translation. *Nat Rev Cancer*. 9: 415-428.

Beauvillain C, Juste MO, Dion S, Pierre J, and Dimier-Poisson I (2009). Exosomes are an effective vaccine against congenital toxoplasmosis in mice. *Vaccine*. 27: 1750-1757.

Bhattacharyya L, Khan MI, and Brewer CF (1988). Interactions of concanavalin A with asparagine-linked glycopeptides: formation of homogeneous cross-linked lattices in mixed precipitation systems. *Biochemistry*. 27: 8762-8767.

Blanchard N, Lankar D, Faure F, Regnault A, Dumont C, Raposo G, and Hivroz C (2002). TCR activation of human T cells induces the production of exosomes bearing the TCR/CD3/zeta complex. *J Immunol*. 168: 3235-3241.

Brooks NL, Corey MJ, and Schwalbe RA (2006). Characterization of N-glycosylation consensus sequences in the Kv3.1 channel. *FEBS J*. 273: 3287-3300.

Brooks S (2009). Strategies for Analysis of the Glycosylation of Proteins: Current Status and Future Perspectives. *Molecular Biotechnology*. 43: 76-88.

Brown MS, Ye J, Rawson RB, and Goldstein JL (2000). Regulated intramembrane proteolysis: a control mechanism conserved from bacteria to humans. *Cell*. 100: 391-398.

Caby M-P, Lankar D, Vincendeau-Scherrer C, Raposo G, and Bonnerot C (2005). Exosomal-like vesicles are present in human blood plasma. *Int. Immunol.* 17: 879-887.

Caescu CI, Jeschke GR, and Turk BE (2009). Active-site determinants of substrate recognition by the metalloproteinases TACE and ADAM10. *Biochem J*. 424: 79-88.

Cai, G., P.S. Salonikidis, J. Fei, W. Schwarz, R. Schulein, W. Reutter, and H. Fan. (2005). The role of N-glycosylation in the stability, trafficking and GABA-uptake of GABA-transporter 1. Terminal N-glycans facilitate efficientGABA-uptake activity of theGABA transporter. *FEBS J.* 272:1625-1638.

Castellana D, Zobairi F, Martinez MC, Panaro MA, Mitolo V, Freyssinet JM, and Kunzelmann C (2009). Membrane microvesicles as actors in the establishment of a favorable prostatic tumoral niche: a role for activated fibroblasts and CX3CL1-CX3CR1 axis. *Cancer Res*. 69: 785-793.

Ceroni A, Maass K, Geyer H, Geyer R, Dell A, and Haslam SM (2008). GlycoWorkbench: a tool for the computer-assisted annotation of mass spectra of glycans. *J Proteome Res*. 7: 1650-1659.

Chan AL, Morris HR, Panico M, Etienne AT, Rogers ME, Gaffney P, Creighton-Kempsford L, and Dell A (1991). A novel sialylated N-acetylgalactosamine-containing oligosaccharide is the major complex-type structure present in Bowes melanoma tissue plasminogen activator. *Glycobiology*. 1: 173-185.

Chandrasekaran EV, Jain RK, and Matta KL (1992). Ovarian cancer alpha 1,3-L-fucosyltransferase. Differentiation of distinct catalytic species with the unique substrate, 3'-sulfo-N-acetyllactosamine in conjunction with other synthetic acceptors. *J Biol Chem*. 267: 23806-23814.

References

Chantry A, Gregson NA, and Glynn P (1989). A novel metalloproteinase associated with brain myelin membranes. Isolation and characterization. *J Biol Chem*. 264: 21603-21607.

Clayton A, Court J, Navabi H, Adams M, Mason MD, Hobot JA, Newman GR, and Jasani B (2001). Analysis of antigen presenting cell derived exosomes, based on immuno-magnetic isolation and flow cytometry. *J Immunol Methods*. 247: 163-174.

Clayton A, Mitchell JP, Court J, Mason MD, and Tabi Z (2007). Human tumor-derived exosomes selectively impair lymphocyte responses to interleukin-2. *Cancer Res*. 67: 7458-7466.

Cocucci E, Racchetti G, and Meldolesi J (2009). Shedding microvesicles: artefacts no more. *Trends in Cell Biology*. 19: 43-51.

Cvetkovic D (2003). Early events in ovarian oncogenesis. *Reproductive Biology and Endocrinology*. 1: 68-74.

Dabelsteen E (1996). Cell surface carbohydrates as prognostic markers in human carcinomas. *J Pathol*. 179: 358-369.

Dai S, Wei D, Wu Z, Zhou X, Wei X, Huang H, and Li G (2008). Phase I clinical trial of autologous ascites-derived exosomes combined with GM-CSF for colorectal cancer. *Mol Ther*. 16: 782-790.

Dall'olio F (1996). Protein glycosylation in cancer biology: an overview. *Clin Mol Pathol*. 49: M126-135.

Dallas DJ, Genever PG, Patton AJ, Millichip MI, McKie N, and Skerry TM (1999). Localization of ADAM10 and notch receptors in bone. *Bone*. 25: 9-15.

Davicino RC, Elicabe RJ, Di Genaro MS, and Rabinovich GA (2011). Coupling pathogen recognition to innate immunity through glycan-dependent mechanisms. *Int Immunopharmacol*.

Davidson B, Berner A, Nesland JM, Risberg B, Kristensen GB, Trope CG, and Bryne M (2000). Carbohydrate antigen expression in primary tumors, metastatic lesions, and serous effusions from patients diagnosed with

epithelial ovarian carcinoma: evidence of up-regulated Tn and Sialyl Tn antigen expression in effusions. *Hum Pathol*. 31: 1081-1087.

de Gassart A, Geminard C, Fevrier B, Raposo G, and Vidal M (2003). Lipid raft-associated protein sorting in exosomes. *Blood*. 102: 4336-4344.

DeFife KM, Jenney CR, Colton E, and Anderson JM (1999). Disruption of filamentous actin inhibits human macrophage fusion. *FASEB J*. 13: 823-832.

DeLano, W.L. (2002). The PyMOL Molecular Graphics System. DeLano Scientific, Palo Alto.

Denzer K, Kleijmeer MJ, Heijnen HF, Stoorvogel W, and Geuze HJ (2000). Exosome: from internal vesicle of the multivesicular body to intercellular signaling device. *J Cell Sci*. 113: 3365-3374.

Edwards DR, Handsley MM, and Pennington CJ (2008). The ADAM metalloproteinases. *Mol Aspects Med*. 29: 258-289.

Escrevente C, Machado E, Brito C, Reis CA, Stoeck A, Runz S, Marme A, Altevogt P, and Costa J (2006). Different expression levels of alpha3/4 fucosyltransferases and Lewis determinants in ovarian carcinoma tissues and cell lines. *Int J Oncol*. 29: 557-566.

Escudier B, Dorval T, Chaput N, Andre F, Caby MP, Novault S, Flament C, Leboulaire C, Borg C, Amigorena S, Boccaccio C, Bonnerot C, Dhellin O, Movassagh M, Piperno S, Robert C, Serra V, Valente N, Le Pecq JB, Spatz A, Lantz O, Tursz T, Angevin E, and Zitvogel L (2005). Vaccination of metastatic melanoma patients with autologous dendritic cell (DC) derived-exosomes: results of thefirst phase I clinical trial. *J Transl Med*. 3: 10.

Fahrenholz F, Gilbert S, Kojro E, Lammich S, and Postina R (2000). Alpha-secretase activity of the disintegrin metalloprotease ADAM 10. Influences of domain structure. *Ann N Y Acad Sci*. 920: 215-222.

References

Faure J, Lachenal G, Court M, Hirrlinger J, Chatellard-Causse C, Blot B, Grange J, Schoehn G, Goldberg Y, and Boyer V (2006). Exosomes are released by cultured cortical neurones. *Molecular and Cellular Neuroscience*. 31: 642-648.

Federici MF, Kudryashov V, Saigo PE, Finstad CL, and Lloyd KO (1999). Selection of carbohydrate antigens in human epithelial ovarian cancers as targets for immunotherapy: serous and mucinous tumors exhibit distinctive patterns of expression. *Int J Cancer*. 81: 193-198.

Feng D, Zhao W-L, Ye Y-Y, Bai X-C, Liu R-Q, Chang L-F, Zhou Q, and Sui S-F (2010). Cellular Internalization of Exosomes Occurs Through Phagocytosis. *Traffic*. 11: 675-687.

Fevrier B, Vilette D, Laude H, and Raposo G (2005). Exosomes: a bubble ride for prions? *Traffic*. 6: 10-17.

Février B, and Raposo G (2004). Exosomes: endosomal-derived vesicles shipping extracellular messages. *Current Opinion in Cell Biology*. 16: 415-421.

Fitzner D, Schnaars M, van Rossum D, Krishnamoorthy G, Dibaj P, Bakhti M, Regen T, Hanisch UK, and Simons M (2011). Selective transfer of exosomes from oligodendrocytes to microglia by macropinocytosis. *J Cell Sci*. 124: 447-458.

Fogel M, Gutwein P, Mechtersheimer S, Riedle S, Stoeck A, Smirnov A, Edler L, Ben-Arie A, Huszar M, and Altevogt P (2003). L1 expression as a predictor of progression and survival in patients with uterine and ovarian carcinomas. *The Lancet*. 362: 869-875.

Fogel M, Mechtersheimer S, Huszar M, Smirnov A, Abu-Dahi A, Tilgen W, Reichrath J, Georg T, Altevogt P, and Gutwein P (2003). L1 adhesion molecule (CD 171) in development and progression of human malignant melanoma. *Cancer Letters*. 189: 237-247.

Fu D, Chen L, and O'Neill RA (1994). A detailed structural characterization of ribonuclease B oligosaccharides by 1H NMR spectroscopy and mass spectrometry. *Carbohydrate Research*. 261: 173-186.

Gao Y, and Pimplikar SW (2001). The gamma -secretase-cleaved C-terminal fragment of amyloid precursor protein mediates signaling to the nucleus. *PNAS*. 98: 14979-14984.

Garner OB, and Baum LG (2008). Galectin-glycan lattices regulate cell-surface glycoprotein organization and signalling. *Biochem Soc Trans*. 36: 1472-1477.

Gavel Y, and von Heijne G (1990). Sequence differences between glycosylated and non-glycosylated Asn-X-Thr/Ser acceptor sites: implications for protein engineering. *Protein Eng*. 3: 433-442.

Gavert N, Conacci-Sorrell M, Gast D, Schneider A, Altevogt P, Brabletz T, and Ben-Ze'ev A (2005). L1, a novel target of {beta}-catenin signaling, transforms cells and is expressed at the invasive front of colon cancers. *J. Cell Biol.* 168: 633-642.

Ginestra A, Miceli D, Dolo V, Romano FM, and Vittorelli ML (1999). Membrane vesicles in ovarian cancer fluids: a new potential marker. *Anticancer Res*. 19: 3439-3445.

Gould SJ, Booth AM, and Hildreth JE (2003). The Trojan exosome hypothesis. *Proc Natl Acad Sci U S A*. 100: 10592-10597.

Gupta D, and Lis CG (2009). Role of CA125 in predicting ovarian cancer survival - a review of the epidemiological literature. *J Ovarian Res*. 2: 13.

Gutwein P, Mechtersheimer S, Riedle S, Stoeck A, Gast D, Joumaa S, Zentgraf H, Fogel M, and Altevogt DP (2003). ADAM10-mediated cleavage of L1 adhesion molecule at the cell surface and in released membrane vesicles. *FASEB J*. 17: 292-294.

Gutwein P, Stoeck A, Riedle S, Gast D, Runz S, Condon TP, Marme A, Phong M-C, Linderkamp O, Skorokhod A, and Altevogt P (2005). Cleavage of L1 in Exosomes and Apoptotic Membrane Vesicles Released from Ovarian Carcinoma Cells. *Clin Cancer Res*. 11: 2492-2501.

References

Hakomori S (2004). Carbohydrate-to-carbohydrate interaction, through glycosynapse, as a basis of cell recognition and membrane organization. *Glycoconjugate Journal*. 21: 125-137.

Hakulinen J, Sankkila L, Sugiyama N, Lehti K, and Keski-Oja J (2008). Secretion of active membrane type 1 matrix metalloproteinase (MMP-14) into extracellular space in microvesicular exosomes. *J Cell Biochem*. 105: 1211-1218.

Hao S, Bai O, Li F, Yuan J, Laferte S, and Xiang J (2007). Mature dendritic cells pulsed with exosomes stimulate efficient cytotoxic T-lymphocyte responses and antitumour immunity. *Immunology*. 120: 90-102.

Hartmann D, de Strooper B, Serneels L, Craessaerts K, Herreman A, Annaert W, Umans L, Lubke T, Lena Illert A, von Figura K, and Saftig P (2002). The disintegrin/metalloprotease ADAM 10 is essential for Notch signalling but not for {alpha}-secretase activity in fibroblasts. *Hum. Mol. Genet.* 11: 2615-2624.

Hattori M, Osterfield M, and Flanagan JG (2000). Regulated Cleavage of a Contact-Mediated Axon Repellent. *Science*. 289: 1360-1365.

Hauri, H., C. Appenzeller, F. Kuhn, and O. Nufer. (2000). Lectins and traffic in the secretory pathway. *FEBS Lett.* 476:32-37.

Helenius A, and Aebi M (2001). Intracellular functions of N-linked glycans. *Science*. 291: 2364-2369.

Helenius A, and Aebi M (2004). Roles of N-Linked Glycans in the Endoplasmic Reticulum. *Annual Review of Biochemistry*. 73: 1019-1049.

Holschneider CH, and Berek JS (2000). Ovarian cancer: Epidemiology, biology, and prognostic factors. *Seminars in Surgical Oncology*. 19: 3-10.

Hoorn EJ, Pisitkun T, Zietse R, Gross P, Frokiaer J, Wang NS, Gonzales PA, Star RA, and Knepper MA (2005). Prospects for urinary proteomics: exosomes as a source of urinary biomarkers. *Nephrology (Carlton)*. 10: 283-290.

Horowitz IR, Cho C, Song M, Flowers LC, Santanam N, Parthasarathy S, and Ramachandran S (2001). Increased glycodelin levels in gynecological malignancies. *Int J Gynecol Cancer*. 11: 173-179.

Hundhausen C, Misztela D, Berkhout TA, Broadway N, Saftig P, Reiss K, Hartmann D, Fahrenholz F, Postina R, Matthews V, Kallen K-J, Rose-John S, and Ludwig A (2003). The disintegrin-like metalloproteinase ADAM10 is involved in constitutive cleavage of CX3CL1 (fractalkine) and regulates CX3CL1-mediated cell-cell adhesion. *Blood*. 102: 1186-1195.

Huovila AP, Turner AJ, Pelto-Huikko M, Karkkainen I, and Ortiz RM (2005). Shedding light on ADAM metalloproteinases. *Trends Biochem Sci*. 30: 413-422.

Iero M, Valenti R, Huber V, Filipazzi P, Parmiani G, Fais S, and Rivoltini L (2008). Tumour-released exosomes and their implications in cancer immunity. *Cell Death Differ*. 15: 80-88.

Imre T, Kremmer T, Heberger K, Molnar-Szollosi E, Ludanyi K, Pocsfalvi G, Malorni A, Drahos L, and Vekey K (2008). Mass spectrometric and linear discriminant analysis of N-glycans of human serum alpha-1-acid glycoprotein in cancer patients and healthy individuals. *J Proteomics*. 71: 186-197.

Izquierdo-Useros N, Naranjo-Gomez M, Archer J, Hatch SC, Erkizia I, Blanco J, Borras FE, Puertas MC, Connor JH, Fernandez-Figueras MT, Moore L, Clotet B, Gummuluru S, and Martinez-Picado J (2009). Capture and transfer of HIV-1 particles by mature dendritic cells converges with the exosome-dissemination pathway. *Blood*. 113: 2732-2741.

Izquierdo-Useros N, Puertas MC, Borras FE, Blanco J, and Martinez-Picado J (2011). Exosomes and retroviruses: the chicken or the egg? *Cell Microbiol*. 13: 10-17.

Janes PW, Saha N, Barton WA, Kolev MV, Wimmer-Kleikamp SH, Nievergall E, Blobel CP, Himanen J-P, Lackmann M, and Nikolov DB (2005). Adam

Meets Eph: An ADAM Substrate Recognition Module Acts as a Molecular Switch for Ephrin Cleavage In trans. *Cell*. 123: 291-304.

Jankovic MM, and Milutinovic BS (2008). Glycoforms of CA125 antigen as a possible cancer marker. *Cancer Biomark*. 4: 35-42.

Jelovac D, and Armstrong DK (2011). Recent progress in the diagnosis and treatment of ovarian cancer. *CA Cancer J Clin*. 61: 183-203.

Johnstone RM, Adam M, Hammond JR, Orr L, and Turbide C (1987). Vesicle formation during reticulocyte maturation. Association of plasma membrane activities with released vesicles (exosomes). *Journal of Biological Chemistry*. 262: 9412-9420.

Kaku T, Ogawa S, Kawano Y, Ohishi Y, Kobayashi H, Hirakawa T, and Nakano H (2003). Histological classification of ovarian cancer. *Medical Electron Microscopy*. 36: 9-17.

Katzmann DJ, Babst M, and Emr SD (2001). Ubiquitin-Dependent Sorting into the Multivesicular Body Pathway Requires the Function of a Conserved Endosomal Protein Sorting Complex, ESCRT-I. *Cell*. 106: 145-155.

Keller S, Sanderson MP, Stoeck A, and Altevogt P (2006). Exosomes: From biogenesis and secretion to biological function. *Immunology Letters*. 107: 102-108.

Keller S, König A-K, Marmé F, Runz S, Wolterink S, Koensgen D, Mustea A, Sehouli J, and Altevogt P (2009). Systemic presence and tumor-growth promoting effect of ovarian carcinoma released exosomes. *Cancer Letters*. 278: 73-81.

Kim SH, Lechman ER, Bianco N, Menon R, Keravala A, Nash J, Mi Z, Watkins SC, Gambotto A, and Robbins PD (2005). Exosomes derived from IL-10-treated dendritic cells can suppress inflammation and collagen-induced arthritis. *J Immunol*. 174: 6440-6448.

Knibbs RN, Goldstein IJ, Ratcliffe RM, and Shibuya N (1991). Characterization of the carbohydrate binding specificity of the leukoagglutinating lectin from

Maackia amurensis. Comparison with other sialic acid-specific lectins. *Journal of Biological Chemistry*. 266: 83-88.

Ko SY, Lin SC, Wong YK, Liu CJ, Chang KW, and Liu TY (2007). Increase of disintergin metalloprotease 10 (ADAM10) expression in oral squamous cell carcinoma. *Cancer Lett*. 245: 33-43.

Krishnamoorthy L, Bess JW, Preston AB, Nagashima K, and Mahal LK (2009). HIV-1 and microvesicles from T cells share a common glycome, arguing for a common origin. *Nat Chem Biol*. 5: 244-250.

Lakkaraju A, and Rodriguez-Boulan E (2008). Itinerant exosomes: emerging roles in cell and tissue polarity. *Trends in Cell Biology*. 18: 199-209.

Lammich S, Kojro E, Postina R, Gilbert S, Pfeiffer R, Jasionowski M, Haass C, and Fahrenholz F (1999). Constitutive and regulated alpha-secretase cleavage of Alzheimer's amyloid precursor protein by a disintegrin metalloprotease. *Proc Natl Acad Sci U S A*. 96: 3922-3927.

Lamparski HG, Metha-Damani A, Yao J-Y, Patel S, Hsu D-H, Ruegg C, and Le Pecq J-B (2002). Production and characterization of clinical grade exosomes derived from dendritic cells. *Journal of Immunological Methods*. 270: 211-226.

Laskowski, R.A., M.W. MacArthur, D.S. Moss, and J.M. Thornton. (1993). PROCHECK: a program to check the stereochemical quality of protein structures. *J. Appl. Crystallogr.* 26:283-291.

Lemjabbar H, and Basbaum C (2002). Platelet-activating factor receptor and ADAM10 mediate responses to Staphylococcus aureus in epithelial cells. *Nat. Med.* 8: 41-46.

Lewandrowski, U., J. Moebius, U. Walter, and A. Sickmann. (2006). Elucidation of N-glycosylation sites on human platelet proteins: a glycoproteomic approach. *Mol. Cell. Proteomics*. 5:226-233.

References

Li J, Sherman-Baust CA, Tsai-Turton M, Bristow RE, Roden RB, and Morin PJ (2009). Claudin-containing exosomes in the peripheral circulation of women with ovarian cancer. *BMC Cancer*. 9: 244.

Li M, Song L, and Qin X (2010). Glycan changes: cancer metastasis and anti-cancer vaccines. *J Biosci*. 35: 665-673.

Lu Q, Zhang J, Allison R, Gay H, Yang WX, Bhowmick NA, Frelix G, Shappell S, and Chen YH (2009). Identification of extracellular delta-catenin accumulation for prostate cancer detection. *Prostate*. 69: 411-418.

Lunn CA, Fan X, Dalie B, Miller K, Zavodny PJ, Narula SK, and Lundell D (1997). Purification of ADAM 10 from bovine spleen as a TNF[alpha] convertase. *FEBS Letters*. 400: 333-335.

Machado E, Kandzia S, Carilho R, Altevogt P, Conradt HS, and Costa J (2011). N-Glycosylation of total cellular glycoproteins from the human ovarian carcinoma SKOV3 cell line and of recombinantly expressed human erythropoietin. *Glycobiology*. 21: 376-386.

Marcello E, Gardoni F, Mauceri D, Romorini S, Jeromin A, Epis R, Borroni B, Cattabeni F, Sala C, Padovani A, and Di Luca M (2007). Synapse-associated protein-97 mediates alpha-secretase ADAM10 trafficking and promotes its activity. *J Neurosci*. 27: 1682-1691.

Marek KW, Vijay IK, and Marth JD (1999). A recessive deletion in the GlcNAc-1-phosphotransferase gene results in peri-implantation embryonic lethality. *Glycobiology*. 9: 1263-1271.

Maretzky T, Schulte M, Ludwig A, Rose-John S, Blobel C, Hartmann D, Altevogt P, Saftig P, and Reiss K (2005). L1 Is Sequentially Processed by Two Differently Activated Metalloproteases and Presenilin/{gamma}-Secretase and Regulates Neural Cell Adhesion, Cell Migration, and Neurite Outgrowth. *Mol. Cell. Biol.* 25: 9040-9053.

Martin L, Fluhrer R, Reiss K, Kremmer E, Saftig P, and Haass C (2008). Regulated intramembrane proteolysis of Bri2 (Itm2b) by ADAM10 and SPPL2a/SPPL2b. *J Biol Chem*. 283: 1644-1652.

Martina, J.A., J.L. Daniotti, and H.J. Maccioni. (1998). Influence of N-glycosylation and N-glycan trimming on the activity and intracellular traffic of GD3 synthase. *J. Biol. Chem.* 273:3725-3731.

Maskos, K., C. Fernandez-Catalan, R. Huber, G.P. Bourenkov, H. Bartunik, G.A. Ellestad, P. Reddy, M.F. Wolfson, C.T. Rauch, B.J. Castner, R. Davis, H.R. Clarke, M. Petersen, J.N. Fitzner, D.P. Cerretti, C.J. March, R.J. Paxton, R.A. Black, and W. Bode. (1998). Crystal structure of the catalytic domain of human tumor necrosis factor-alphaconverting enzyme. *Proc. Natl. Acad. Sci. U. S. A.* 95:3408-3412.

Mathivanan S, Ji H, and Simpson RJ (2010). Exosomes: extracellular organelles important in intercellular communication. *J Proteomics*. 73: 1907-1920.

McCulloch DR, Akl P, Samaratunga H, Herington AC, and Odorico DM (2004). Expression of the Disintegrin Metalloprotease, ADAM-10, in Prostate Cancer and Its Regulation by Dihydrotestosterone, Insulin-Like Growth Factor I, and Epidermal Growth Factor in the Prostate Cancer Cell Model LNCaP. *Clin Cancer Res*. 10: 314-323.

Mechtersheimer S, Gutwein P, Agmon-Levin N, Stoeck A, Oleszewski M, Riedle S, Postina R, Fahrenholz F, Fogel M, Lemmon V, and Altevogt P (2001). Ectodomain shedding of L1 adhesion molecule promotes cell migration by autocrine binding to integrins. *J. Cell Biol.* 155: 661-674.

Michelsen U, and von Hagen J (2009). Chapter 19 Isolation of Subcellular Organelles and Structures. in Methods in Enzymology. (Richard, R. B., and Murray, P. D. eds.). *Academic Press*. pp 305-328.

Millichip MI, Dallas DJ, Wu E, Dale S, and McKie N (1998). The Metallo-Disintegrin ADAM10 (MADM) from Bovine Kidney Has Type IV Collagenase Activityin Vitro. *Biochemical and Biophysical Research Communications*. 245: 594-598.

Mohler KM, Sleath PR, Fitzner JN, Cerretti DP, Alderson M, Kerwar SS, Torrance DS, Otten-Evans C, Greenstreet T, Weerawarna K, and et al. (1994).

Protection against a lethal dose of endotoxin by an inhibitor of tumour necrosis factor processing. *Nature*. 370: 218-220.

Morais, V.A., M.T. Costa, and J. Costa. (2003). N-glycosylation of recombinant human fucosyltransferase III is required for its in vivo folding in mammalian and insect cells. *Biochim. Biophys. Acta.* 1619:133-138.

Morais, V.A., C. Brito, D.S.C. Pijak, A.S, R.R. Fortna, T. Li, P.C. Wong, R.W. Doms, and J. Costa. (2006). N-glycosylation of human nicastrin is required for interaction with the lectins from the secretory pathway calnexin and ERGIC-53. *Biochim. Biophys. Acta.* 1762:802-810.

Morelli AE, Larregina AT, Shufesky WJ, Sullivan MLG, Stolz DB, Papworth GD, Zahorchak AF, Logar AJ, Wang Z, Watkins SC, Falo LD, Jr., and Thomson AW (2004). Endocytosis, intracellular sorting, and processing of exosomes by dendritic cells. *Blood*. 104: 3257-3266.

Morse MA, Garst J, Osada T, Khan S, Hobeika A, Clay TM, Valente N, Shreeniwas R, Sutton MA, Delcayre A, Hsu DH, Le Pecq JB, and Lyerly HK (2005). A phase I study of dexosome immunotherapy in patients with advanced non-small cell lung cancer. *J Transl Med*. 3: 9.

Moss ML, Bomar M, Liu Q, Sage H, Dempsey P, Lenhart PM, Gillispie PA, Stoeck A, Wildeboer D, Bartsch JW, Palmisano R, and Zhou P (2007). The ADAM10 prodomain is a specific inhibitor of ADAM10 proteolytic activity and inhibits cellular shedding events. *J Biol Chem*. 282: 35712-35721.

Moss ML, Stoeck A, Yan W, and Dempsey PJ (2008). ADAM10 as a target for anti-cancer therapy. *Curr Pharm Biotechnol*. 9: 2-8.

Muralidharan-Chari V, Clancy JW, Sedgwick A, and D'Souza-Schorey C (2010). Microvesicles: mediators of extracellular communication during cancer progression. *J Cell Sci*. 123: 1603-1611.

Nagano O, Murakami D, Hartmann D, de Strooper B, Saftig P, Iwatsubo T, Nakajima M, Shinohara M, and Saya H (2004). Cell-matrix interaction via CD44 is independently regulated by different metalloproteinases activated

in response to extracellular Ca2+ influx and PKC activation. *J. Cell Biol.* 165: 893-902.

Nilsson J, Skog J, Nordstrand A, Baranov V, Mincheva-Nilsson L, Breakefield XO, and Widmark A (2009). Prostate cancer-derived urine exosomes: a novel approach to biomarkers for prostate cancer. *Br J Cancer*. 100: 1603-1607.

Obregon C, Rothen-Rutishauser B, Gerber P, Gehr P, and Nicod LP (2009). Active Uptake of Dendritic Cell-Derived Exovesicles by Epithelial Cells Induces the Release of Inflammatory Mediators through a TNF-{alpha}-Mediated Pathway. *Am J Pathol*. 175: 696-705.

Ogawa Y, Kanai-Azuma M, Akimoto Y, Kawakami H, and Yanoshita R (2008). Exosome-like vesicles with dipeptidyl peptidase IV in human saliva. *Biol Pharm Bull*. 31: 1059-1062.

Ohtsubo K, and Marth JD (2006). Glycosylation in cellular mechanisms of health and disease. *Cell*. 126: 855-867.

Oka JA, Christensen MD, and Weigel PH (1989). Hyperosmolarity inhibits galactosyl receptor-mediated but not fluid phase endocytosis in isolated rat hepatocytes. *J Biol Chem*. 264: 12016-12024.

Opdenakker G, Rudd PM, Ponting CP, and Dwek RA (1993). Concepts and principles of glycobiology. *FASEB J*. 7: 1330-1337.

Ostrowski M, Carmo NB, Krumeich S, Fanget I, Raposo G, Savina A, Moita CF, Schauer K, Hume AN, Freitas RP, Goud B, Benaroch P, Hacohen N, Fukuda M, Desnos C, Seabra MC, Darchen F, Amigorena S, Moita LF, and Thery C (2010). Rab27a and Rab27b control different steps of the exosome secretion pathway. *Nat Cell Biol*. 12: 19-30.

Pandiella A, and Massague J (1991). Multiple signals activate cleavage of the membrane transforming growth factor-alpha precursor. *J Biol Chem*. 266: 5769-5773.

Parish CR (1999). Fluorescent dyes for lymphocyte migration and proliferation studies. *Immunol Cell Biol*. 77: 499-508.

References

Parkin E, and Harris B (2009). A disintegrin and metalloproteinase (ADAM)-mediated ectodomain shedding of ADAM10. *J Neurochem*. 108: 1464-1479.

Parolini I, Federici C, Raggi C, Lugini L, Palleschi S, De Milito A, Coscia C, Iessi E, Logozzi M, Molinari A, Colone M, Tatti M, Sargiacomo M, and Fais S (2009). Microenvironmental pH Is a Key Factor for Exosome Traffic in Tumor Cells. *Journal of Biological Chemistry*. 284: 34211-34222.

Peng P, Yan Y, and Keng S (2011). Exosomes in the ascites of ovarian cancer patients: origin and effects on anti-tumor immunity. *Oncol Rep*. 25: 749-762.

Peracaula R, Royle L, Tabares G, Mallorqui-Fernandez G, Barrabes S, Harvey DJ, Dwek RA, Rudd PM, and de Llorens R (2003). Glycosylation of human pancreatic ribonuclease: differences between normal and tumor states. *Glycobiology*. 13: 227-244.

Peracaula R, Barrabes S, Sarrats A, Rudd PM, and de Llorens R (2008). Altered glycosylation in tumours focused to cancer diagnosis. *Dis Markers*. 25: 207-218.

Petrescu, A.J., A.L. Milac, S.M. Petrescu, R.A. Dwek, and M.R. Wormald. (2004). Statistical analysis of the protein environment of N-glycosylation sites: implications for occupancy, structure, and folding. *Glycobiology*. 14:103-114.

Pisitkun T, Shen RF, and Knepper MA (2004). Identification and proteomic profiling of exosomes in human urine. *Proc Natl Acad Sci U S A*. 101: 13368-13373.

Pruessmeyer J, and Ludwig A (2009). The good, the bad and the ugly substrates for ADAM10 and ADAM17 in brain pathology, inflammation and cancer. *Semin Cell Dev Biol*. 20: 164-174.

Rabinowits G, Gercel-Taylor C, Day JM, Taylor DD, and Kloecker GH (2009). Exosomal microRNA: a diagnostic marker for lung cancer. *Clin Lung Cancer*. 10: 42-46.

Raposo G, Nijman HW, Stoorvogel W, Liejendekker R, Harding CV, Melief CJ, and Geuze HJ (1996). B lymphocytes secrete antigen-presenting vesicles. *J Exp Med*. 183: 1161-1172.

Raposo G, Tenza D, Mecheri S, Peronet R, Bonnerot C, and Desaymard C (1997). Accumulation of major histocompatibility complex class II molecules in mast cell secretory granules and their release upon degranulation. *Mol Biol Cell*. 8: 2631-2645.

Reiss K, Maretzky T, Ludwig A, Tousseyn T, de Strooper B, Hartmann D, and Saftig P (2005). ADAM10 cleavage of N-cadherin and regulation of cell-cell adhesion and beta-catenin nuclear signalling. *EMBO J.* 24: 742-752.

Reiss K, Ludwig A, and Saftig P (2006). Breaking up the tie: disintegrin-like metalloproteinases as regulators of cell migration in inflammation and invasion. *Pharmacol Ther*. 111: 985-1006.

Reiss K, and Saftig P (2009). The "a disintegrin and metalloprotease" (ADAM) family of sheddases: physiological and cellular functions. *Semin Cell Dev Biol*. 20: 126-137.

Ristorcelli E, Beraud E, Verrando P, Villard C, Lafitte D, Sbarra V, Lombardo D, and Verine A (2008). Human tumor nanoparticles induce apoptosis of pancreatic cancer cells. *FASEB J.* 22: 3358-3369.

Rodal SK, Skretting G, Garred O, Vilhardt F, van Deurs B, and Sandvig K (1999). Extraction of cholesterol with methyl-beta-cyclodextrin perturbs formation of clathrin-coated endocytic vesicles. *Mol Biol Cell*. 10: 961-974.

Runz S, Keller S, Rupp C, Stoeck A, Issa Y, Koensgen D, Mustea A, Sehouli J, Kristiansen G, and Altevogt P (2007). Malignant ascites-derived exosomes of ovarian carcinoma patients contain CD24 and EpCAM. *Gynecol Oncol*. 107: 563-571.

Safaei R, Larson BJ, Cheng TC, Gibson MA, Otani S, Naerdemann W, and Howell SB (2005). Abnormal lysosomal trafficking and enhanced exosomal export of cisplatin in drug-resistant human ovarian carcinoma cells. *Mol Cancer Ther*. 4: 1595-1604.

References

Saldova R, Royle L, Radcliffe CM, Abd Hamid UM, Evans R, Arnold JN, Banks RE, Hutson R, Harvey DJ, Antrobus R, Petrescu SM, Dwek RA, and Rudd PM (2007). Ovarian cancer is associated with changes in glycosylation in both acute-phase proteins and IgG. *Glycobiology*. 17: 1344-1356.

Sanchez, R., and A. Sali. (1997). Advances in comparative protein-structure modelling. *Curr. Opin. Struct. Biol.* 7:206-214.

Sanderson MP, Erickson SN, Gough PJ, Garton KJ, Wille PT, Raines EW, Dunbar AJ, and Dempsey PJ (2005). ADAM10 Mediates Ectodomain Shedding of the Betacellulin Precursor Activated by p-Aminophenylmercuric Acetate and Extracellular Calcium Influx. *J. Biol. Chem.* 280: 1826-1837.

Sasaki H, Ochi N, Dell A, and Fukuda M (1988). Site-specific glycosylation of human recombinant erythropoietin: analysis of glycopeptides or peptides at each glycosylation site by fast atom bombardment mass spectrometry. *Biochemistry*. 27: 8618-8626.

Schauer R (2009). Sialic acids as regulators of molecular and cellular interactions. *Current Opinion in Structural Biology*. 19: 507-514.

Scheiffele P, Peranen J, and Simons K (1995). N-glycans as apical sorting signals in epithelial cells. *Nature*. 378: 96-98.

Schlondorff J, and Blobel CP (1999). Metalloprotease-disintegrins: modular proteins capable of promoting cell-cell interactions and triggering signals by protein-ectodomain shedding. *J Cell Sci*. 112 (Pt 21): 3603-3617.

Schorey JS, and Bhatnagar S (2008). Exosome Function: From Tumor Immunology to Pathogen Biology. *Traffic*. 9: 871-881.

Scully RE (1987). Classification of human ovarian tumors. *Environ Health Perspect*. 73: 15-25.

Seals DF, and Courtneidge SA (2003). The ADAMs family of metalloproteases: multidomain proteins with multiple functions. *Genes Dev*. 17: 7-30.

Shedden K, Xie XT, Chandaroy P, Chang YT, and Rosania GR (2003). Expulsion of small molecules in vesicles shed by cancer cells: association with gene expression and chemosensitivity profiles. *Cancer Res*. 63: 4331-4337.

Simons M, and Raposo G (2009). Exosomes--vesicular carriers for intercellular communication. *Curr Opin Cell Biol*. 21: 575-581.

Simpson RJ, Jensen SS, and Lim JW (2008). Proteomic profiling of exosomes: current perspectives. *Proteomics*. 8: 4083-4099.

Simpson RJ, Lim JWE, Moritz RL, and Mathivanan S (2009). Exosomes: proteomic insights and diagnostic potential. *Expert Review of Proteomics*. 6: 267-283.

Skog J, Wurdinger T, van Rijn S, Meijer DH, Gainche L, Curry WT, Carter BS, Krichevsky AM, and Breakefield XO (2008). Glioblastoma microvesicles transport RNA and proteins that promote tumour growth and provide diagnostic biomarkers. *Nat Cell Biol*. 10: 1470-1476.

Skropeta D (2009). The effect of individual N-glycans on enzyme activity. *Bioorg Med Chem*. 17: 2645-2653.

Sousa VL, Brito C, Costa T, Lanoix J, Nilsson T, and Costa J (2003). Importance of Cys, Gln, and Tyr from the Transmembrane Domain of Human alpha 3/4 Fucosyltransferase III for Its Localization and Sorting in the Golgi of Baby Hamster Kidney Cells. *J. Biol. Chem.* 278: 7624-7629.

Spik G, Bayard B, Fournet B, Strecker G, Bouquelet S, and Montreuil J (1975). Studies on glycoconjugates. LXIV. Complete structure of two carbohydrate units of human serotransferrin. *FEBS Letters*. 50: 296-299.

Stoeck A, Keller S, Riedle S, Sanderson MP, Runz S, Le Naour F, Gutwein P, Ludwig A, Rubinstein E, and Altevogt P (2006). A role for exosomes in the constitutive and stimulus-induced ectodomain cleavage of L1 and CD44. *Biochem J*. 393: 609-618.

Stoorvogel W, Kleijmeer MJ, Geuze HJ, and Raposo G (2002). The Biogenesis and Functions of Exosomes. *Traffic*. 3: 321-330.

References

Subra C, Laulagnier K, Perret B, and Record M (2007). Exosome lipidomics unravels lipid sorting at the level of multivesicular bodies. *Biochimie*. 89: 205-212.

Sun D, Zhuang X, Xiang X, Liu Y, Zhang S, Liu C, Barnes S, Grizzle W, Miller D, and Zhang HG (2010). A novel nanoparticle drug delivery system: the anti-inflammatory activity of curcumin is enhanced when encapsulated in exosomes. *Mol Ther*. 18: 1606-1614.

Takahashi N, Yamamoto E, Ino K, Miyoshi E, Nagasaka T, Kajiyama H, Shibata K, Nawa A, and Kikkawa F (2009). High expression of N-acetylglucosaminyltransferase V in mucinous tumors of the ovary. *Oncol Rep*. 22: 1027-1032.

Takahashi T, Ikeda Y, Miyoshi E, Yaginuma Y, Ishikawa M, and Taniguchi N (2000). alpha1,6fucosyltransferase is highly and specifically expressed in human ovarian serous adenocarcinomas. *Int J Cancer*. 88: 914-919.

Tan A, De La Pena H, and Seifalian AM (2010). The application of exosomes as a nanoscale cancer vaccine. *Int J Nanomedicine*. 5: 889-900.

Tanida S, Joh T, Itoh K, Kataoka H, Sasaki M, Ohara H, Nakazawa T, Nomura T, Kinugasa Y, and Ohmoto H (2004). The mechanism of cleavage of EGFR ligands induced by inflammatory cytokines in gastric cancer cells. *Gastroenterology*. 127: 559-569.

Tanious FA, Veal JM, Buczak H, Ratmeyer LS, and Wilson WD (1992). DAPI (4',6-diamidino-2-phenylindole) binds differently to DNA and RNA: minor-groove binding at AT sites and intercalation at AU sites. *Biochemistry*. 31: 3103-3112.

Taylor DD, and Gercel-Taylor C (2008). MicroRNA signatures of tumor-derived exosomes as diagnostic biomarkers of ovarian cancer. *Gynecol Oncol*. 110: 13-21.

Taylor ME, and Drickamer K (2006). Introduction to Glycobiology. Second ed. *Oxford University Press*, New York.

Tellier E, Canault M, Rebsomen L, Bonardo B, Juhan-Vague I, Nalbone G, and Peiretti F (2006). The shedding activity of ADAM17 is sequestered in lipid rafts. *Exp Cell Res*. 312: 3969-3980.

Thery C, Regnault A, Garin J, Wolfers J, Zitvogel L, Ricciardi-Castagnoli P, Raposo G, and Amigorena S (1999). Molecular characterization of dendritic cell-derived exosomes. Selective accumulation of the heat shock protein hsc73. *J Cell Biol*. 147: 599-610.

Thery C, Amigorena S, Raposo G, and Clayton A (2006). Isolation and characterization of exosomes from cell culture supernatants and biological fluids. *Curr Protoc Cell Biol*. Chapter 3: Unit 3 22.

Thery C, Ostrowski M, and Segura E (2009). Membrane vesicles as conveyors of immune responses. *Nat Rev Immunol*. 9: 581-593.

Tousseyn T, Thathiah A, Jorissen E, Raemaekers T, Konietzko U, Reiss K, Maes E, Snellinx A, Serneels L, Nyabi O, Annaert W, Saftig P, Hartmann D, and De Strooper B (2009). ADAM10, the rate-limiting protease of regulated intramembrane proteolysis of Notch and other proteins, is processed by ADAMS-9, ADAMS-15, and the gamma-secretase. *J Biol Chem*. 284: 11738-11747.

Trajkovic K, Hsu C, Chiantia S, Rajendran L, Wenzel D, Wieland F, Schwille P, Brugger B, and Simons M (2008). Ceramide Triggers Budding of Exosome Vesicles into Multivesicular Endosomes. *Science*. 319: 1244-1247.

Trombetta, E.S., and A.J. Parodi. (2003). Quality control and protein folding in the secretory pathway. *Annu. Rev. Cell Dev. Biol.* . 19:649-676.

Turner GA, Goodarzi MT, and Thompson S (1995). Glycosylation of alpha-1-proteinase inhibitor and haptoglobin in ovarian cancer: evidence for two different mechanisms. *Glycoconj J*. 12: 211-218.

Ungar D (2009). Golgi linked protein glycosylation and associated diseases. *Semin Cell Dev Biol*. 20: 762-769.

References

Valadi H, Ekstrom K, Bossios A, Sjostrand M, Lee JJ, and Lotvall JO (2007). Exosome-mediated transfer of mRNAs and microRNAs is a novel mechanism of genetic exchange between cells. *Nat Cell Biol*. 9: 654-659.

Valenti R, Huber V, Iero M, Filipazzi P, Parmiani G, and Rivoltini L (2007). Tumor-Released Microvesicles as Vehicles of Immunosuppression. *Cancer Res*. 67: 2912-2915.

van den Berg TK, Honing H, Franke N, van Remoortere A, Schiphorst WE, Liu FT, Deelder AM, Cummings RD, Hokke CH, and van Die I (2004). LacdiNAc-glycans constitute a parasite pattern for galectin-3-mediated immune recognition. *J Immunol*. 173: 1902-1907.

van Kooyk Y, and Rabinovich GA (2008). Protein-glycan interactions in the control of innate and adaptive immune responses. *Nat Immunol*. 9: 593-601.

van Niel G, Raposo G, Candalh C, Boussac M, Hershberg R, Cerf-Bensussan N, and Heyman M (2001). Intestinal epithelial cells secrete exosome-like vesicles. *Gastroenterology*. 121: 337-349.

van Niel G, Porto-Carreiro I, Simoes S, and Raposo G (2006). Exosomes: A Common Pathway for a Specialized Function. *J Biochem*. 140: 13-21.

Varki A (1993). Biological roles of oligosaccharides: all of the theories are correct. *Glycobiology*. 3: 97-130.

Varki A, Cummings RD, Esko JD, Freeze HH, Stanley P, Bertozzi CR, Hart GW, and Etzler ME (2009). Essentials of Glycobiology. Second ed. *Cold Spring Harbor Laboratory Press*, Cold Spring Harbor, (NY).

Vella LJ, Sharples RA, Lawson VA, Masters CL, Cappai R, and Hill AF (2007). Packaging of prions into exosomes is associated with a novel pathway of PrP processing. *The Journal of Pathology*. 211: 582-590.

Vidal M, Mangeat P, and Hoekstra D (1997). Aggregation reroutes molecules from a recycling to a vesicle-mediated secretion pathway during reticulocyte maturation. *J Cell Sci*. 110 (Pt 16): 1867-1877.

Vigerust DJ, and Shepherd VL (2007). Virus glycosylation: role in virulence and immune interactions. *Trends in Microbiology*. 15: 211-218.

Vliegenthart JF (2006). Carbohydrate based vaccines. *FEBS Lett*. 580: 2945-2950.

Wang PH, Lee WL, Juang CM, Yang YH, Lo WH, Lai CR, Hsieh SL, and Yuan CC (2005). Altered mRNA expressions of sialyltransferases in ovarian cancers. *Gynecol Oncol*. 99: 631-639.

Welton JL, Khanna S, Giles PJ, Brennan P, Brewis IA, Staffurth J, Mason MD, and Clayton A (2010). Proteomics analysis of bladder cancer exosomes. *Mol Cell Proteomics*. 9: 1324-1338.

Weskamp G, Ford JW, Sturgill J, Martin S, Docherty AJP, Swendeman S, Broadway N, Hartmann D, Saftig P, Umland S, Sehara-Fujisawa A, Black RA, Ludwig A, Becherer JD, Conrad DH, and Blobel CP (2006). ADAM10 is a principal 'sheddase' of the low-affinity immunoglobulin E receptor CD23. *Nat Immunol*. 7: 1293-1298.

West MA, Bretscher MS, and Watts C (1989). Distinct endocytotic pathways in epidermal growth factor-stimulated human carcinoma A431 cells. *J Cell Biol*. 109: 2731-2739.

White JM (2003). ADAMs: modulators of cell-cell and cell-matrix interactions. *Curr Opin Cell Biol*. 15: 598-606.

Wild-Bode C, Fellerer K, Kugler J, Haass C, and Capell A (2006). A Basolateral Sorting Signal Directs ADAM10 to Adherens Junctions and Is Required for Its Function in Cell Migration. *Journal of Biological Chemistry*. 281: 23824-23829.

Wiley RD, and Gummuluru S (2006). Immature dendritic cell-derived exosomes can mediate HIV-1 trans infection. *Proc Natl Acad Sci U S A*. 103: 738-743.

Wolfers J, Lozier A, Raposo G, Regnault A, Thery C, Masurier C, Flament C, Pouzieux S, Faure F, Tursz T, Angevin E, Amigorena S, and Zitvogel L

(2001). Tumor-derived exosomes are a source of shared tumor rejection antigens for CTL cross-priming. *Nat Med*. 7: 297-303.

Wolfsberg TG, Primakoff P, Myles DG, and White JM (1995). ADAM, a novel family of membrane proteins containing A Disintegrin And Metalloprotease domain: multipotential functions in cell-cell and cell- matrix interactions. *J. Cell Biol.* 131: 275-278.

Wu E, Croucher PI, and McKie N (1997). Expression of Members of the Novel Membrane Linked Metalloproteinase Family ADAM in Cells Derived from a Range of Haematological Malignancies. *Biochemical and Biophysical Research Communications*. 235: 437-442.

Yamazaki K, Mizui Y, Sagane K, and Tanaka I (1997). Assignment of a disintegrin and metalloproteinase domain 10 (Adam10) gene to mouse chromosome 9. *Genomics*. 46: 528-529.

Yan Y, Shirakabe K, and Werb Z (2002). The metalloprotease Kuzbanian (ADAM10) mediates the transactivation of EGF receptor by G protein-coupled receptors. *J. Cell Biol.* 158: 221-226.

Yavari R, Adida C, Bray-Ward P, Brines M, and Xu T (1998). Human metalloprotease-disintegrin Kuzbanian regulates sympathoadrenal cell fate in development and neoplasia. *Hum. Mol. Genet.* 7: 1161-1167.

Yu S, Liu C, Su K, Wang J, Liu Y, Zhang L, Li C, Cong Y, Kimberly R, Grizzle WE, Falkson C, and Zhang HG (2007). Tumor exosomes inhibit differentiation of bone marrow dendritic cells. *J Immunol*. 178: 6867-6875.

Zhang HG, and Grizzle WE (2011). Exosomes and cancer: a newly described pathway of immune suppression. *Clin Cancer Res*. 17: 959-964.

Zitvogel L, Regnault A, Lozier A, Wolfers J, Flament C, Tenza D, Ricciardi-Castagnoli P, Raposo G, and Amigorena S (1998). Eradication of established murine tumors using a novel cell-free vaccine: dendritic cell-derived exosomes. *Nat Med*. 4: 594-600.